

STUDIES ON SEDIMENT TRANSPORT
IN THE SURF ZONE
ALONG CERTAIN BEACHES OF KERALA

THESIS SUBMITTED TO THE UNIVERSITY OF COCHIN
IN PARTIAL FULFILMENT OF THE REQUIREMENT
FOR THE DEGREE OF

DOCTOR OF PHILOSOPHY
IN
PHYSICAL OCEANOGRAPHY

By

S. PRASANNAKUMAR, M.Sc.

SCHOOL OF MARINE SCIENCES, UNIVERSITY OF COCHIN
COCHIN-682 016

APRIL, 1985

CONTENTS

Page No.

LIST OF FIGURES		
LIST OF TABLES		
CERTIFICATE		
DECLARATION		
ACKNOWLEDGEMENT		
1. CHAPTER 1	: INTRODUCTION	1
2. CHAPTER 2	: BEACH MORPHOLOGICAL CHANGES	17
3. CHAPTER 3	: BEACH SEDIMENTS	36
4. CHAPTER 4	: WAVE REFRACTION	46
5. CHAPTER 5	: NEARSHORE CIRCULATION	62
6. CHAPTER 6	: SEDIMENT TRANSPORT	73
7. CHAPTER 7	: SYNTHESIS	81
REFERENCES		95
APPENDIX		106

LIST OF FIGURES

- 1.1. Physiography of the west coast of India.
- 1.2. Distribution of the average rainfall over Kerala during southwest and northeast monsoon seasons.
- 1.3. Monthly distribution of winds over Arabian sea.
- 1.4. Shore protective structures along Vypeen and Chellanam islands.
- 1.5. Map showing bathymetry and zones under study.
- 2.1. Schematic diagram showing beach terminology along a barrier beach system and beach profiling.
- 2.2. Spatial and temporal distribution of the empirical eigen function at location N1.
- 2.3a. Beach profiles at Narakkal zone.
- 2.3b. Beach profiles at Malipuram zone.
- 2.3c. Beach profiles at Fort Cochin zone.
- 2.3d. Beach profiles at Anthakaranazhi zone.
- 2.4a. Spatial and temporal distribution of the empirical eigen function at Narakkal zone.
- 2.4b. Spatial and temporal distribution of the empirical eigen function at Malipuram zone.
- 2.4c. Spatial and temporal distribution of the empirical eigen function at Fort Cochin zone.
- 2.4d. Spatial and temporal distribution of the empirical eigen function at Anthakaranazhi zone.
- 2.5a. Monthly changes of beach volumes at Narakkal zone.
- 2.5b. Monthly changes of beach volumes at Malipuram zone.
- 2.5c. Monthly changes of beach volumes at Fort Cochin zone.
- 2.5d. Monthly changes of beach volumes at Anthakaranazhi zone.

- 3.1a. Monthly variation of mean grain size distribution along profiles at Narakkal zone.
- 3.1b. Monthly variation of mean grain size distribution along profiles at Malipuram zone.
- 3.1c. Monthly variation of mean grain size distribution along profiles at Fort Cochin zone.
- 3.1d. Monthly variation of mean grain size distribution along profiles at Anthakaranazhi zone.
- 3.2a. Monthly variation of standard deviation of grain size along profiles at Narakkal zone.
- 3.2b. Monthly variation of standard deviation of grain size along profiles at Malipuram zone.
- 3.2c. Monthly variation of standard deviation of grain size along profiles at Fort Cochin zone.
- 3.2d. Monthly variation of standard deviation of grain size along profiles at Anthakaranazhi zone.
- 4.1. Monthly wave roses showing height and direction of wave approach off Cochin.
- 4.2a. Variation of refraction function along locations A - T for waves approaching from 220°TN .
- 4.2b. Variation of refraction function along locations A - T for waves approaching from 240°TN .
- 4.2c. Variation of refraction function along locations A - T for waves approaching from 260°TN .
- 4.2d. Variation of refraction function along locations A - T for waves approaching from 280°TN .
- 4.2e. Variation of refraction function along locations A - T for waves approaching from 300°TN .
- 5.1.a. Cellular circulation associated with wave convergence and divergence for waves approaching from 220°TN .
- 5.1b. Cellular circulation associated with wave convergence and divergence for waves approaching from 240°TN .

- 5.1c. Cellular circulation associated with wave convergence and divergence for waves approaching from 260°TN .
- 5.1d. Cellular circulation associated with wave convergence and divergence for waves approaching from 280°TN .
- 5.1e. Cellular circulation associated with wave convergence and divergence for waves approaching from 300°TN .
- 5.2a. Distribution of bottom orbital velocities in the near-shore zone for waves approaching from 240°TN .
- 5.2b. Distribution of bottom orbital velocities in the near-shore zone for waves approaching from 260°TN .
- 5.2c. Distribution of bottom orbital velocities in the near-shore zone for waves approaching from 280°TN .
- 5.2d. Distribution of bottom orbital velocities in the near-shore zone for waves approaching from 300°TN .

LIST OF TABLES

	<u>Page No.</u>
2.1. Details of beach profile locations.	18
2.2. Percentage of mean square value of the data as explained by the first three eigen values.	22
4.1. Monthly percentage frequency of swell periods off Cochin.	50
4.2. Values of H/H_0 at 2 m isobath for waves of different periods and directions of approach.	53
4.3. Direction function (θ) for different periods and directions of approach along locations A-T.	56
4.4a. Observed breaker characteristics at Narakkal zone.	57
4.4b. Observed breaker characteristics at Malipuram zone.	58
4.4c. Observed breaker characteristics at Fort Cochin zone.	59
4.4d. Observed breaker characteristics at Anthakaranazhi zone.	60
5.1. Observed longshore current speed and direction.	71
6.1. Alongshore component of wave energy.	77
6.2. Computed littoral drift during rough and fair weather seasons.	79
7.1. Thickness of bottom boundary-layer for different wave periods and kinematic viscosities.	88

CERTIFICATE

This is to certify that this thesis bound herewith is an authentic record of the research carried out by Shri S.Prasanna Kumar, M.Sc., under my supervision and guidance in the School of Marine Sciences, in partial fulfilment of the requirement for the Ph.D. Degree of the University of Cochin and that no part thereof has been presented before for any other degree in any University.

School of Marine Sciences
University of Cochin
Cochin - 682 016
April, 1985.

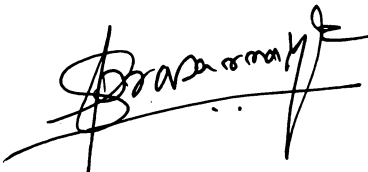


Dr.P.G.Kurup
(Supervising Teacher)
Professor in Physical Oceanography

DECLARATION

I hereby declare that the thesis entitled, 'STUDIES ON SEDIMENT TRANSPORT IN THE SURF ZONE ALONG CERTAIN BEACHES OF KERALA', is an authentic record of research carried out by me under the supervision and guidance of Dr.P.G.Kurup, Professor, School of Marine Sciences, University of Cochin, in partial fulfilment of the requirement for the Ph.D. Degree of the University of Cochin and that no part of it has previously formed the basis for the award of any degree, diploma or associateship in any University.

Physical Oceanography Division
National Institute of Oceanography
Dona Paula, Goa.



(S. Prasanna Kumar)

ACKNOWLEDGEMENTS

I wish to record my deep sense of gratitude to Dr.P.G.Kurup, Professor and Head, Physical Oceanography and Meteorology Division, School of Marine Sciences, University of Cochin, for suggesting the research problem and for guidance and constant encouragement. I am also grateful for his valuable advice and help in preparation of the manuscript and for suggesting improvements.

I am grateful to Dr.C.S.Murty, Scientist, National Institute of Oceanography, Goa, for help in the preparation of the thesis. I am also thankful to Dr.Ramana Murty and Shri A.A.Fernandez for their help in carrying out the computations. I wish to record my thanks to Dr.J.S. Sastry, Head, Physical Oceanography Division, National Institute of Oceanography, Goa and to the Director, School of Marine Sciences, University of Cochin, for encouragement.

The help and co-operation rendered by Dr.S.Sateesh Chandra Shenoi, Scientist, National Institute of Oceanography, Goa, in the collection of field data and Shri K.V.Chandran, University of Cochin, for secretarial assistance, are gratefully acknowledged.

CHAPTER 1 : INTRODUCTION

	<u>Page</u>
1.1. Geomorphology of west coast of India	2
1.2. Shelf sediments	3
1.3. Mud banks	4
1.4. Rainfall	5
1.5. Winds	5
1.6. Waves	7
1.7. Tides	8
1.8. Currents	9
1.9. Shore environment	9
1.10. Previous study	10
1.11. Present study	12
1.12. Area of investigation	13
1.13. Scheme of thesis	16

The general configuration of sandy beaches along most of the shorelines of the world appears to be one of a permanent nature to a casual observer at any given time. Studies on the morphological aspects of beaches reveal a variety of changes occurring in this environment over varying time and length scales. These changes are principally the responses of the beach geometric form to the prevailing dynamic forces.

Of the many forms of beaches bordering and/or sheltering the coasts, barrier beaches form one such depository system. These beaches bordering barrier islands are considered as a special type of shores along the world's coastline. The beaches, along the coast of Kerala, belong to this category. They are backed by an extensive system of lagoons. The changes occurring in their geometric form can be understood from a detailed knowledge of the physical processes of turbulence, diffusion and advection that govern the movement of sedimentary material. These processes are controlled by (1) winds, waves, tides and associated currents, (2) indirect effects due to man-made structures, (3) nearshore

bathymetry, (4) weather disturbances giving rise to storm surges and tidal waves, and (5) beach slope and nature of constituent sediments. The beach profile gets altered depending on the balance between the above physical agencies and the supply of material. Large scale irreversible transformations, however, would lead to deformations in the shoreline configuration.

The environmental parameters that constitute the various physical process variables and contribute to the changes in beach morphology along the coast of Kerala are briefly summarised below.

1.1. Geomorphology of west coast of India

West coast of India, the origin of which is attributed to faulting and uplifting during the late Pliocene (Krishnan, 1968), is bordered by the Western Ghats extending to heights of about 1.8 km. These ghats, composed of rocks of Pre-Cambrian gneissic complex with thick laterite capping, fringe the coast from Cape Comorin in the south and extend as a range of hills, 24 to 28 km in width, over a distance of nearly 720 km in a NNW-SSE direction (Fig.1.1) and provide the most important orographic feature of peninsular India. They are cut into a steep scarp on the west by faulting and denudation. The distance between the scarp and seashore

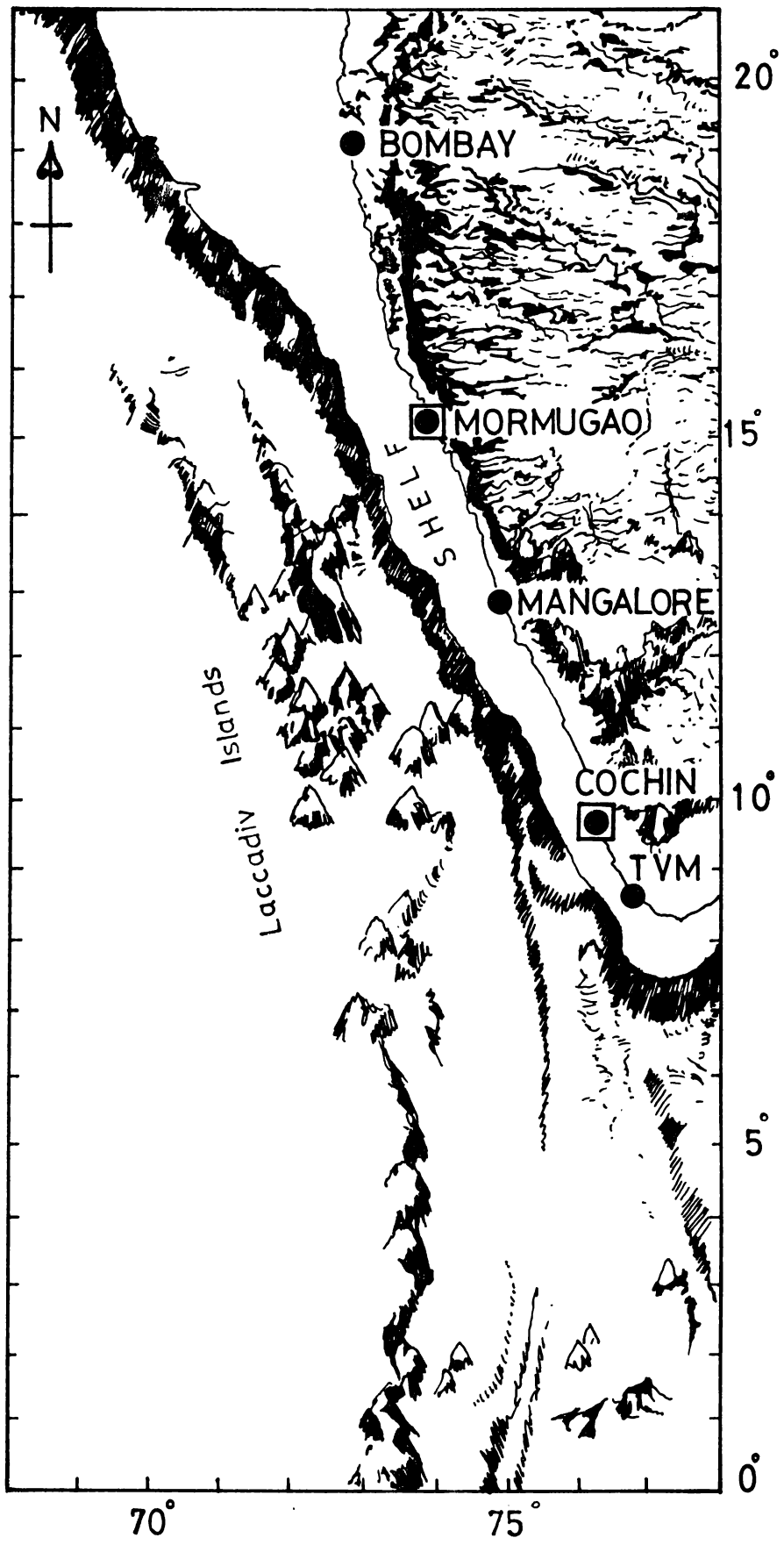


Fig.1.1. PHYSIOGRAPHY OF THE WEST COAST OF INDIA.

varies from 8 to 40 km resulting in a narrow coastal strip of alluvial deposits.

The coastal area of Kerala - the emergence of which is legendarily ascribed to Lord Parasurama - is characterised by a strip of barrier land between Quilon and Cannanore which separates the Arabian sea from a chain of long irregular lagoons and estuaries. This barrier has a remarkably straight outer shoreline of emergent nature and a highly irregular inner shoreline of submergent nature representing the eastern margin of the lakes and lagoons. The entire coastal belt is backed by coconut plantation and holds a dense population (550 per km² according to 1971 census, Kerala Government).

1.2. Shelf sediments

Along the west coast of India, the continental shelf has a straight course and a gentle slope. It has a maximum width of 160 km off Bombay and narrows down to about 48 km off Cranganore, north of Cochin (Fig.1.1).

The surface sediments of the shelf show well defined zonation in the offshore direction. Broadly, seven zones - nearshore sand, grey to olive brown mud, calcareous sand, foraminiferal sand, olive grey mud, grey mud and globigerina ooze - have been identified by Schott (1968). In general,

the distribution of clastic and non-clastic sediments (Nair and Pylee, 1968; Kurian, 1967; Mattiat et al., 1973) over this shelf from the shore could be visualized as:

<u>Water depth (m)</u>		<u>Nature of sediment</u>
0	- 3/6	Sands
3/6	- 18	Muds
18	- 108/144	Sands
108/144	- 270	Grey/black and white sand

1.3. Mud banks

Mud banks are regions of calm water appearing close to the shore at certain locations along the Kerala coast during southwest monsoon season. They act as natural littoral barriers, influencing the sedimentation processes along the coast of Kerala and directly affect the dynamics of the adjoining shore. The occurrence of these mud banks at few locations between Quilon and Cannanore is an annual phenomenon (Bristow, 1938). The available historical records on the occurrence of these mud banks (dating back to 17th century) indicate their migratory nature (Moni, 1970). The sediments constituting these banks have been reported to be essentially clays or silty clays and less commonly sand-silt clays or sandy silts (Dora et al., 1968). They are not charted on bathymetric maps.

1.4. Rainfall

During southwest monsoon season, Western Ghats receive enormous rainfall forming the water-shed of Peninsular India and play an important role in the climate of this region. Under the influence of the southwest monsoon, which prevails for 3 to 4 months commencing from May/June, the whole of the western region receives heavy rainfall. The distribution of average rainfall over the state of Kerala during the southwest monsoon (principal rainy season) and the northeast monsoon (retreating phase of the southwest monsoon) season (figure 1.2) indicates that the coastal belt from Cochin to Calicut receives an annual rainfall of about 300 cm (Ananthakrishnan et al., 1979). As a result, the catchment area receives $\sim 113.4 \times 10^9 \text{ m}^3$ of precipitable water. Approximately 60% of this quantity is estimated to flow down as surface drainage (Prabhakar Rao, 1968) directly or indirectly through the backwater systems to the sea. Of the six major rivers - Periyar, Muvattupuzha, Pamba, Manimala, Achankoil and Meenachil - Periyar opens out directly into the Arabian sea while other rivers debouch into the backwater system.

1.5. Winds

Monthly distribution of winds over the Arabian sea, obtained by streamlining of the data presented in KNMI

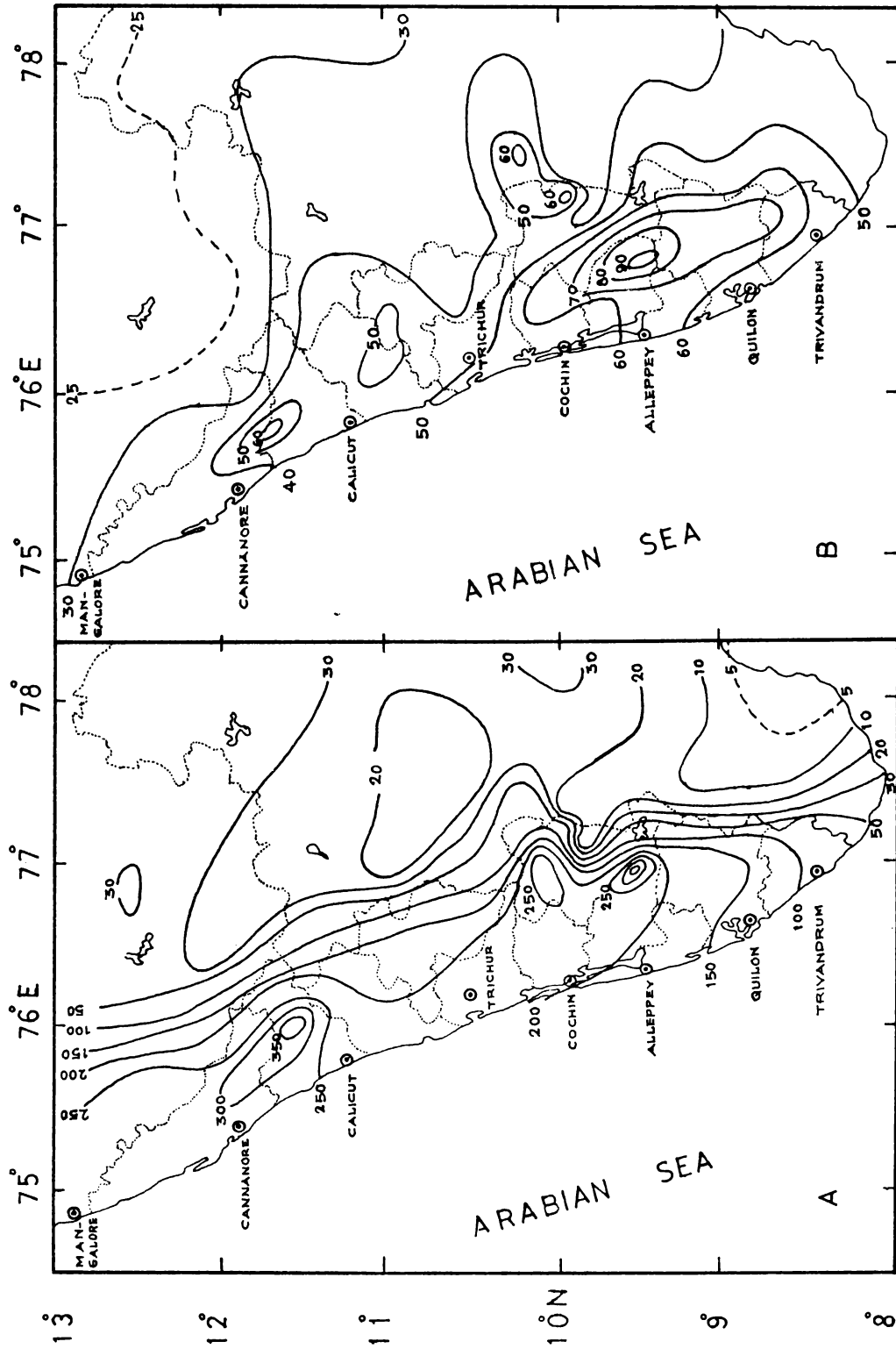


Fig.1.2 DISTRIBUTION OF AVERAGE RAIN FALL (cm) OVER KERALA DURING (A) SOUTH-WEST MONSOON AND (B) NORTH-EAST MONSOON SEASONS (AFTER ANANTHAKRISHNAN *et al.*, 1979)

Atlas (1952) is presented in Fig.1.3. The characteristic feature of the winds over this area is the reversal of the wind system over an year known as the monsoons. This reversal occurs from south-westerly direction during May - September, to north-westerly direction during December - March with transition periods in between.

During December and January, the winds are generally north-northeasterly in the northern parts and north-easterly in the southern parts and blow with speeds of about 3 m s^{-1} . During February, they are mainly north-northwesterly and vary in speeds between $3 - 4 \text{ m s}^{-1}$. Conditions are similar during March but with a slight increase in magnitude and decrease in stability than during February. Westerly winds with magnitude of $3 - 5 \text{ m s}^{-1}$ prevail during April. During May, the winds are mostly from southwest and west, and have speeds from $4 - 10 \text{ m s}^{-1}$. During June, July and August the winds blow from southwest with increased constancy and magnitude. West-northwesterly winds prevail in September. October presents highly variable winds, while north-easterly winds approximately 5 m s^{-1} in magnitude prevail during November.

In the coastal areas, land and sea breezes are experienced almost throughout the year except during the southwest monsoon season. The land breeze is well developed and forms a part of the northeast monsoonal winds during

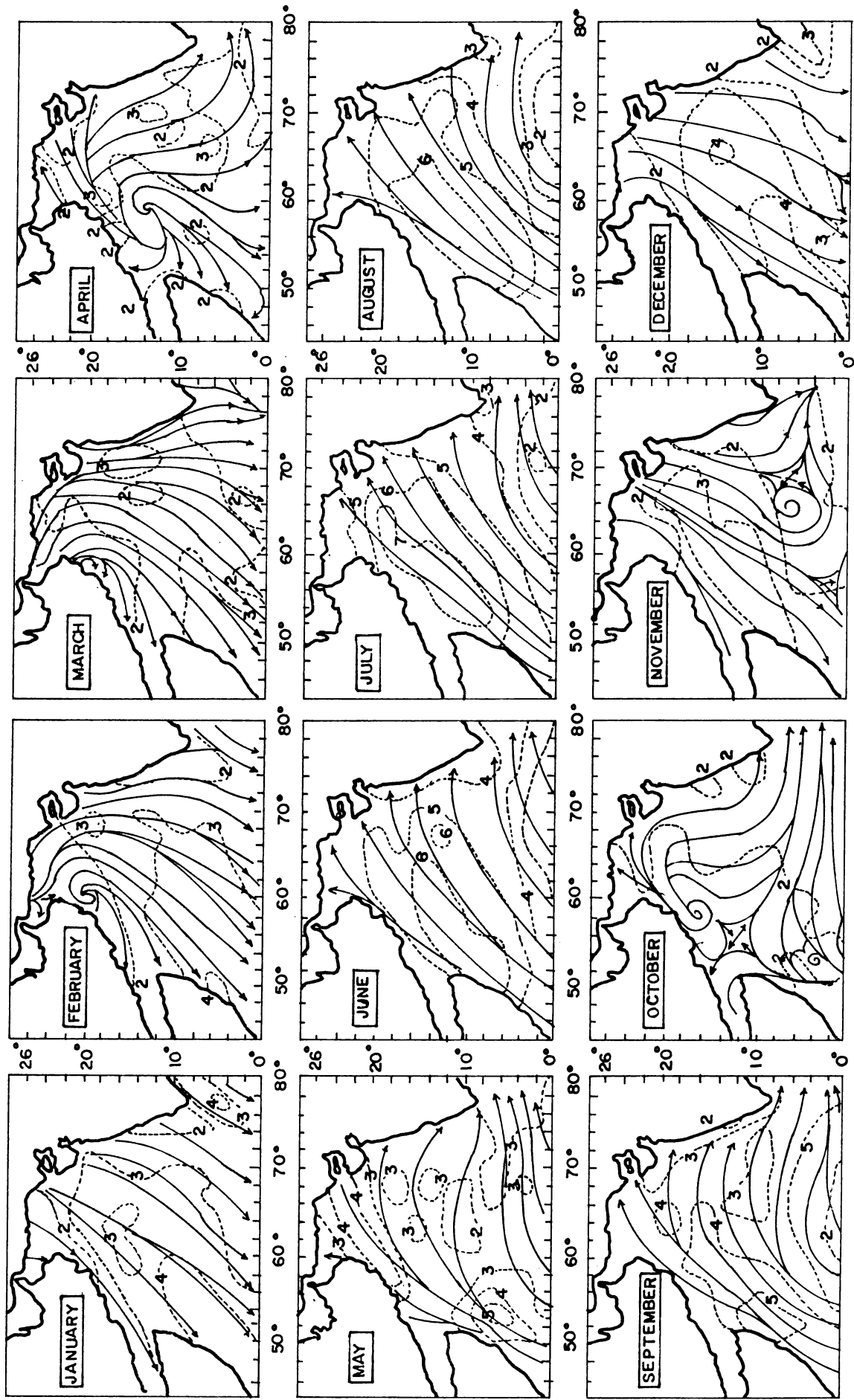


FIG. 1.3 MONTHLY DISTRIBUTION OF WINDS OVER ARABIAN SEA (KNMI, 1952)

December and January. In general, the daily onshore winds exceed offshore winds. The maximum onshore wind speeds occur just after the mid-day.

1.6. Waves

Observations on waves published in the Indian Daily Weather Reports (IDWR) of India Meteorological Department have been compiled by Srivastava et al. (1968) and Varkey et al. (1982). The wave characteristics as seen from these studies indicate greater dependency on the prevailing winds over the Arabian sea. Owing to the reversing wind systems, variable fetches occur from time to time with almost unlimited fetches on the southwest and west of this area and limited fetches on the northern side. These fetches contribute significantly to the generation of waves that affect the shoreline bordering this coast. Keeping in view the orientation of this coast (NNE-SSW), waves originating and propagating towards the coast from 180° to 340° IN can be considered significant. The waves generated in the south Indian Ocean associated with cyclonic storms are also likely to propagate towards this coast as long period swells.

In general, the seas present comparatively calm conditions for nearly eight months in a year and rough or confused seas prevail during the rest of the year. One finds

a general increase in wave activity subsequent to increase in winds over this area. The waves during this phase present higher inconsistencies in their direction of approach.

Data collected at Mangalore with the help of wave recorders during 1968, '69 provide corroborative observations. The wave occurrence presents two peaks at 7 sec and 12 sec during December - February, sharp peaks at 7 sec and 13 sec during March to April, and almost a uniform curve with mode around 10 sec during May through August. The significant heights of these waves are conspicuously high during June through August. The significant period also shows an increase during this period (Sundararamam et al., 1974).

The data based on visual observation in the area between $8^{\circ}30'N$ and $11^{\circ}30'N$ Lat. and between $73^{\circ}30'E$ Long. and the coast for the years 1974 - 1980 have been compiled from IDWR and presented in the form of rose diagrams in Chapter 4.

1.7. Tides

The tides in this area are of mixed semi-diurnal nature and fall within the micro-tidal range. They vary in range from mean neap tides of 0.3 m to mean spring tides of 1.2 m. Noticeable variation in tidal range may occur by the combination of surge and wave activity during rough weather

on the shelf. The current associated with these tides attain speeds of about $1.0 - 1.5 \text{ m s}^{-1}$ in the vicinity of inlets. The fluctuations in water level associated with these tides affect the beach processes through (1) ground water and swash water interactions on the beach face, and (2) nearshore water circulation and morphology.

1.8. Currents

The coastal currents have been reported to be northerly during northeast monsoon months with speeds of 0.5 m s^{-1} . These currents, show a reversal in their direction during southwest monsoon and present greater variability with mean speeds of 1 m s^{-1} (HMSO, 1975).

1.9. Shore environment

The shores of Kerala are in general sandy. At places they are backed by sand dunes and vary in their width from 30 to 100 m. Based on available revenue records for over 100 years, these beaches have been found to experience erosion of varying magnitudes at few locations (eg., Punthura, Thottapally, Purakad, Thumboli, Chellanam, Cheriakadavu, Manasserrey, Saudi, Fort Cochin, Malipuram, Azhikode, Crangannore, Chetwai, Cherai, Calicut and Bakal) resulting in recession of the shoreline and loss of valuable property. The problem has become acute during the last two

decades. The average rate of recession of shoreline has been shown to be about 2 m per year at Purakad and 5 m per year at Chellanam (Moni, 1980). As recession of shoreline takes place at few locations, progression of the shore can be seen, particularly north of Cochin harbour (Vypeen), from available hydrographic charts.

In order to prevent erosion, shore protection works such as sea-walls have been constructed along certain parts of this coastline. More systematic efforts were made since early fifties in this regard as could be seen from the first experimental sea-wall and groin assembly at Manassery near Cochin (Fig.1.4). The design of the sea-wall has been modified from time to time and as of today nearly 70% of the shoreline of the coast has been padded up by artificial shore protection structures.

1.10. Previous studies

Earlier studies on beach and nearshore environment along the west coast of India can be divided into three main types. They are (a) studies to identify areas of erosion and accretion through construction of wave refraction diagrams (Reddy, 1970; Reddy and Varadachari, 1972; Sastry and D'Souza, 1973; Gouveia et al., 1976; Antony, 1976 and Veerayya et al., 1981), (b) studies on morphological changes at selected places in relation to the available wave energies (Veerayya, 1972;

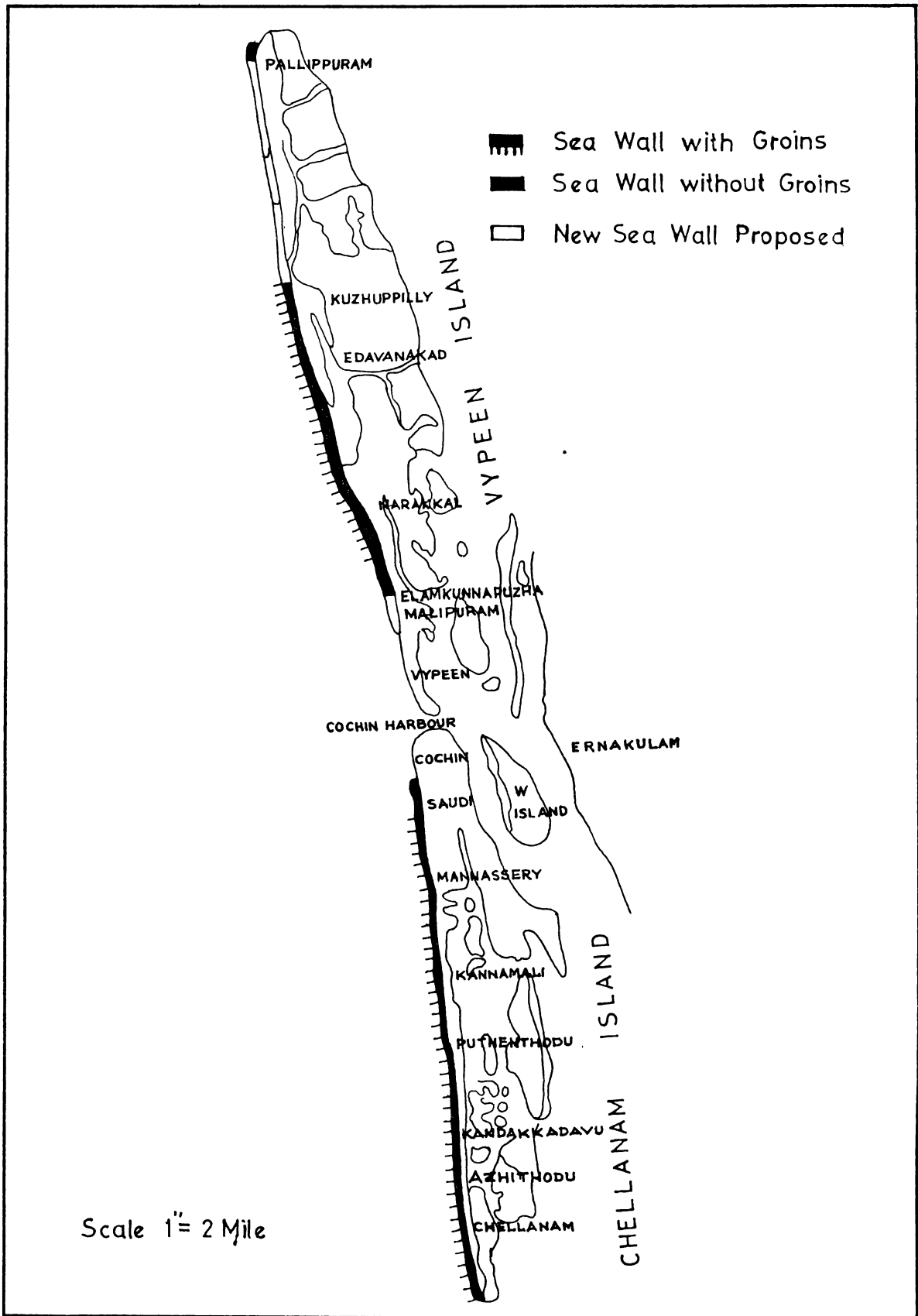


Fig.1.4 SHORE PROTECTION STRUCTURES ALONG VYPEEN AND CHELLANAM ISLANDS. (AFTER ACHUTHAPANICKER, 1971)

Veerayya and Varadachari, 1975; Murty, 1977 and Murty et al., 1982) and (c) studies on the movement of sediments using radioactive/fluorescent tracers (Manohar, 1960; Gole and Tarapore, 1966 and Nair et al., 1972 etc.).

Along the coast of Kerala, studies on wave refraction in relation to beach erosion have been carried out by Das et al. (1966), Varma and Varadachari (1977), Shenoi and Prasanna Kumar (1982) and Prasanna Kumar et al. (1983). Shoreline changes based on available historical records have been investigated by Ravindran et al. (1971). A review of erosion and shore protection works along the Kerala coast has been provided by Achuthapanicker (1971) and Moni (1972). The morphological changes of the beaches at various locations along the Kerala coast have been examined for their stability (Murty and Varadachari, 1980), and for the efficacy of the existing shoreline structures by Murty et al. (1980). Shenoi (1984) has carried out a study on the littoral processes along the beaches around Cochin.

The physical aspects of mud banks including the sediments of the nearshore environs, particularly from regions where the mud banks are reported to be active, have been studied by Dora et al. (1968), Nair and Murty (1968), Varma and Kurup (1969), Moni (1971), Kurup (1972,1977), Jacob and Qasim (1974), Gopinathan and Qasim (1974), Kurup and Varadachari (1975) and Mac Pherson and Kurup (1981).

The above studies have indicated the susceptibility of certain beaches of this coast to severe erosion during some years though they have been observed to recover during subsequent years. Further, erosion is not confined to any singular locality. The zone of erosion and deposition have been found to shift from one location to another over the years. The shore protection structure appear to have some stabilizing effect on the beaches at few localities while detrimental effects on beaches adjoining such structures have been reported at many places (Moni, 1972; Murty, 1980).

1.11. Present study

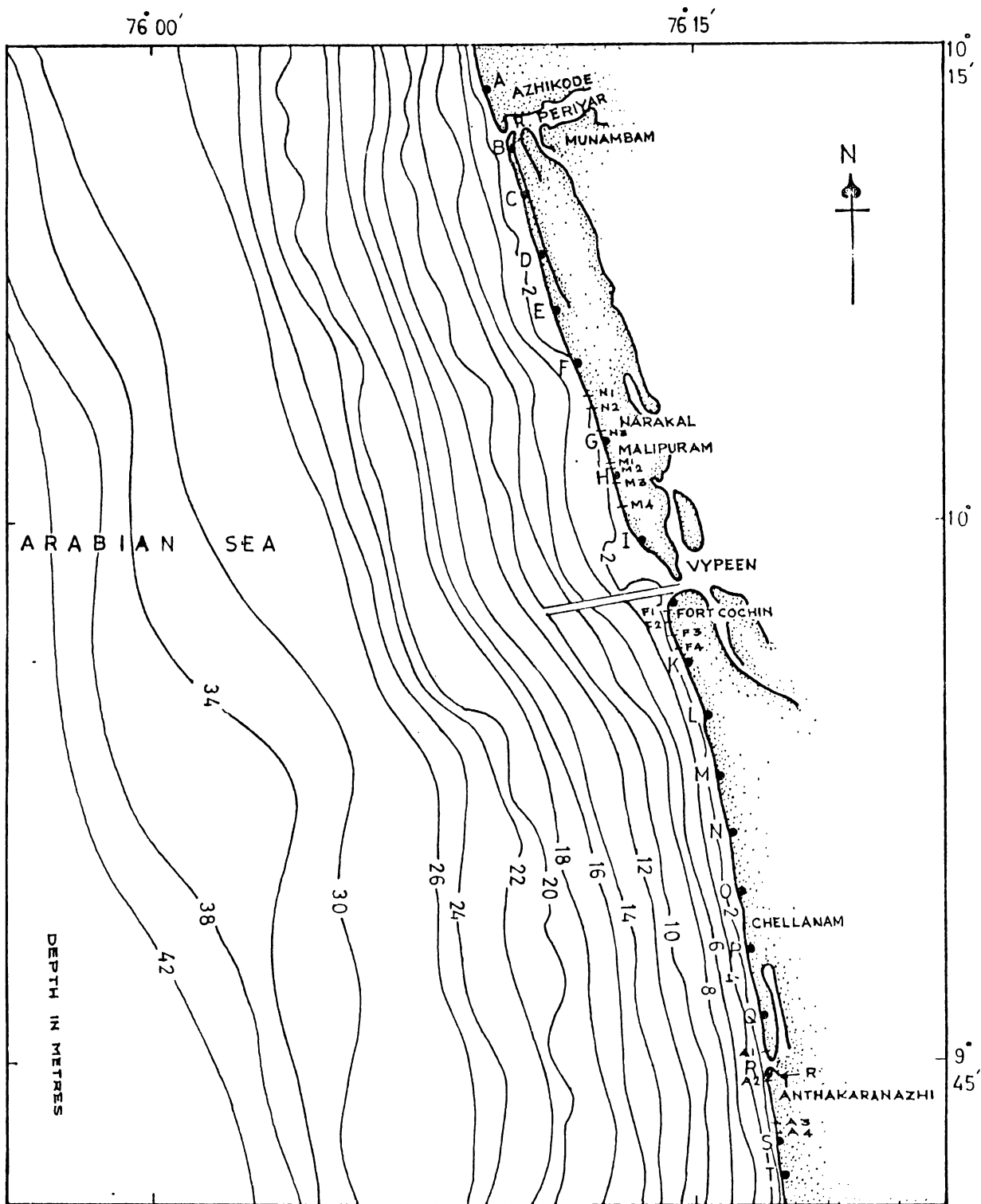
Sediment transport in the nearshore areas is an important process in deciding the coastline stability. The design and effective maintenance of navigable waterways, harbours and marine structures depend on the stability of the sediment substrate and the nature of sedimentation in the nearshore zone. The nearshore zone is a complex environment and the exact relationships existing between water motions and the resulting sediment transports are not well understood. During the rough weather season, when the sediment movement is considerable, processes occurring in the nearshore area are much less understood. Moreover, there is a general lack of field measurements, especially during the time of severe storm conditions.

The increasing pressures and the concern on the preservation of the valuable coastal environment have led to the development of shore protection programmes. Conservation not only demands knowledge of what needs to be done, but also requires the basic processes to be fully understood. Considering the fragile nature of barrier beaches and intense occupancy of these areas by man, these coastal features have long been a subject of study by coastal oceanographers, geomorphologists and engineers.

The present study is an attempt to understand the sediment movement in relation to beach dynamics, especially in the surf zone, along some part of Kerala coast and the response of the beaches to various forcing functions over different seasons.

1.12. Area of investigation

The area under study is a stretch of about 57 km of shoreline from Azhikode to Anthakaranazhi (Fig.1.5). Azhikode, where river Periyar opens out into the Arabian sea, is located on the northern side. The Cochin harbour entrance channel is located mid-way between Azhikode and Anthakaranazhi. The navigation channel of Cochin harbour consists of 6 km long approach channel, oriented along an eastwest direction and two inner channels - 3 km long Ernakulam channel and 4 km long Mattancheri channel - inside the backwater system. The



A,B-S,T- Locations for Refraction function estimations.
 N1-N3; M1-M4; F1-F4; A1-A4- Locations for field observations.

FIG.1.5 MAP SHOWING BATHYMETRY AND ZONES UNDER STUDY.

approach channel was constructed in 1928 by cutting the offshore sand bar about 1.6 km west of the coast. Silting is a severe problem in the outer channel which is being dredged every year to maintain the required depth. At Anthakaranazhi on the south - a seasonal opening exists which remains open throughout the southwest monsoon season. The strip of the coast from Azhikode to Vypeen (26.5 km) and Cochin to Anthakaranazhi (30 km) form two barrier islands, known as Vypeen island and Chellanam island, lying on the northern and southern sides of the Cochin harbour entrance channel. The width of these islands varies from 1.6 - 2.4 km. There are large stretches of paddy fields along the eastern shores of these islands backed by backwaters. The land is low lying with a number of cross canals serving as navigational and drainage channels. The coastal belt is congested with houses and hutments in close proximities and coconut plantations extending right upto the beach face.

The bottom topography on the northern side of the Cochin harbour channel (Fig.1.5).presents gentle offshore slopes and waves generally break well offshore. South of the channel, bottom slopes are relatively steep and enable the waves to break very close to the shore.

At Narakkal and Malipuram, during southwest monsoon season the shore is usually protected by the presence of mud bank. Considerable stretches of the shore between Fort Cochin

and Anthakaranazhi are subjected to seasonal erosion.

In order to understand the sediment movement within the surf zone in relation to beach dynamics, four zones - Narakkal and Malipuram along the Vypeen island and Fort Cochin and Anthakaranazhi along Challanam island - were selected. The beaches at Narakkal and Anthakaranazhi were protected by seawall-groin assemblies. In recent years, the groins have collapsed and are out of function. At Malipuram and Fort Cochin, the beaches are backed by seawalls. At each of the four zones a number of locations have been selected for detailed field observations. These are shown in Fig.1.5.

The parameters monitored are: (1) beach morphology at low tide time, (2) sediment characteristics along the profile section from backshore, berm, foreshore and breaker zone, (3) breaker height and period, orientation to the shoreline and direction of approach of breakers, and (4) speed of littoral current and its direction. The observations were carried out by undertaking fortnightly/monthly field surveys to 15 locations, spread over the four zones under study, during the period from October 1980 to January 1982, as a part of the coastal zone management programme.

1.13. Scheme of the thesis

The observations on beach morphology and analysis of the data using Empirical Eigen Function (EEF) techniques are presented in Chapter 2. The spatial and seasonal variations of grain size parameters of the beaches are discussed in Chapter 3. Chapter 4 deals with wave climate as obtained from analysis of six years' visual observations reported by ships of opportunity and published in the daily weather reports. Refraction of waves and the nearshore wave characteristics are also included in this Chapter. Chapter 5 deals with the wave-induced currents as deduced from wave refraction studies and the bottom velocity distribution. The longshore component of wave energy has been computed and the probable sediment transport has been assessed and presented in Chapter 6. In the light of the environmental process variables operating in this nearshore zone, the changes in the geometric form of the beaches and the probable sediment transport within the stretch of the coast investigated have been synthesised in Chapter 7.

CHAPTER 2 : BEACH MORPHOLOGICAL CHANGES

	<u>Page</u>
2.1. Data collection and analysis	19
2.1.1. Beach profiles	19
2.1.2. Analysis of data	19
2.2. Results	20

The interdependence of sediment movement, the prevailing dynamic forces due to waves, winds and currents, and the resulting changes in geometric form of beaches were indicated in the previous Chapter. In order to examine these changes, results of studies carried out on morphology of the beaches at selected locations with differing environmental set-up are presented in this chapter. Beaches, in all 57 km in length, from Azhikode to Anthakaranazhi along the coast of Kerala have been chosen for this study. These beaches, composed of sediments in the fine sand-size limits and of a low profile, are exposed to seasonally changing wind and wave climates. The stretch of the shore has been divided into four zones considering the environmental setting as indicated in Table 2.1. This shore is characterised by the opening of river Periyar at Azhikode on the north, the entrance channel of harbour at Cochin and a seasonal opening at Anthakaranazhi on the south, all of which influence the sedimentation regime of this environment.

The method of measurement adopted for obtaining beach geometric form at the fifteen locations (Fig.1.5) along the

Table 2.1. Details of beach profile locations

Zone	Number and name of profile locations	Survey interval	Width of the beach from R.P. (m)	Distance between profiles (km)	Remarks
Narakkal	3 (N1, N2, N3)	Monthly	30 - 35	N1 - N2 N2 - N3 0.5 0.3	Low beach composed of fine sand. Seawall-groin assembly present prior to this investigation. In recent years, the groins collapsed. Receives partial protection from the mud bank active during SW monsoon season.
Malipuram	4 (M1, M2, M3, M4)	Fortnightly	55 - 75	M1 - M2 M2 - M3 M3 - M4 0.4 0.9 0.8	Low beach composed of fine sand. Seawall exists well behind the backshore and unaffected by waves. Mud deposits exist on the nearshore bed.
Fort Cochin	4 (F1, F2, F3, F4)	Fortnightly	40 - 90	F1 - F2 F2 - F3 F3 - F4 0.5 0.7 0.5	Relatively high beach composed of medium sand. Locations F2, F3 and F4 are backed by seawall. Partially protected by mud bank.
Anthakaranazhi	4 (A1, A2, A3, A4)	Monthly	30 - 50	A1 - A2 A2 - A3 A3 - A4 0.5 0.3 0.4	Low beach composed of fine sand. Seawall-groin assembly exists but in damaged condition. At present, buried seawall exists at all locations except A3 where seawall is absent and a collapsed groin is present.

shore under study and the analysis carried out are presented in the following sections.

2.1. Data collection and analysis

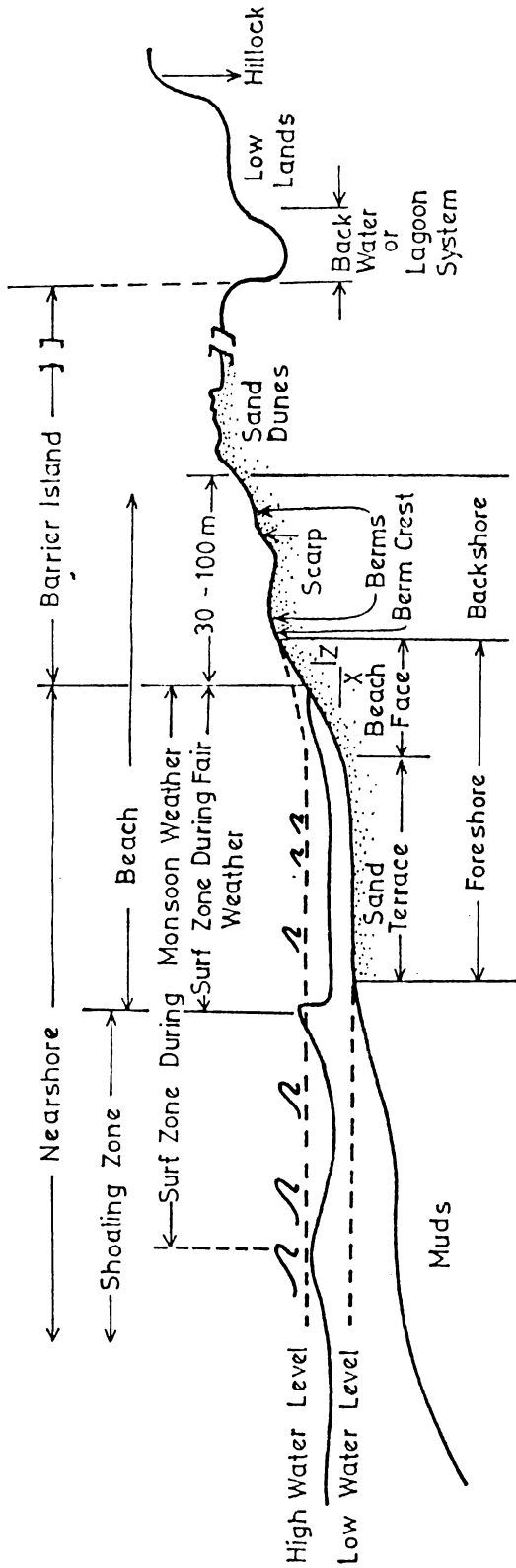
2.1.1. Beach profiles

The beach profiles (geometric form) were measured following the technique of Emery (1961) for a period of 16 months from October, 1980 to January, 1982 at fifteen locations (Fig.1.5). These surveys were carried out at the time of low tide at fortnightly intervals along the Malipuram and Fort Cochin zones and at monthly intervals along Narakkal and Anthakaranazhi zones keeping a constant distance of 5 m between stations (Fig.2.1) along the profile.

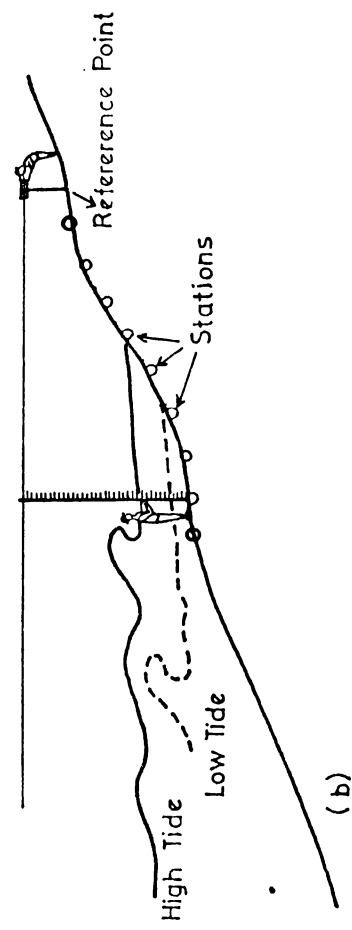
2.1.2. Analysis of data

From the data collected during these surveys, the beach profiles were drawn using a HP 1000 computer. From these plots, changes in the volume of sediments ($\text{m}^3 \text{m}^{-1}$ of the shoreline) were computed to examine the temporal variations

The profile data were further subjected to Empirical Eigen Function (EEF) analysis to examine the time variability of the beach responses. A brief description of the eigenfunction technique is given as Appendix (Page 106).



(a)



(b)

Fig. 2.1 (a) SCHEMATIC DIAGRAM SHOWING BEACH TERMINOLOGY ALONG A BARRIER BEACH SYSTEM.
 (b) DIAGRAM SHOWING METHODOLOGY OF BEACH PROFILING. (NOT TO SCALE)

This technique has been applied to the beach profile data by Winant et al. (1975), Aubrey (1978) and Aranuvachapun and Johnson (1979) and helps in (a) separation of the temporal and spatial dependence of the data set in a way that it can be expressed as a linear combination of corresponding factors of time and space, (b) delineation in space of the spatial location at which greater variability occurs, (c) identification of seasonal or any other periodic variations of specific nature which is otherwise less obvious from conventional graphic analysis, and (d) identification of the processes responsible for the profile changes, i.e., the presence of any specific events and their relative importance. In a way, this analysis would indicate clearly several characteristic patterns of sediment movement on the beach face e.g., the onshore/offshore and alongshore (Aubrey et al., 1976; Aubrey, 1979 and Clarke, 1984). Winant et al. (1975) and Aubrey (1978) have shown that when applied to beach profile data, eigenfunctions have a physical analogue.

2.2. Results

Monthly beach profiles at each location along the four zones (Table 2.1) have been presented in Fig.2.3 a-d while the results of EEF analysis are presented in

Fig.2.4 a-d. The monthly variations in the volume of beach material have been presented in Fig.2.5 a-d.

The eigenfunctions are ranked according to the percentage of mean square value of the data (Table 2.2). The first eigenfunction explains the greatest portion of the mean square value. For example, at location N1, the first function accounts for 96.90% of the mean square value of the data, while the second and third functions account for 2.94% and 0.07% respectively for the residual. This indicates that the contribution from the higher order functions becomes negligible and hence they have not been considered in this study.

In order to elucidate some of the relevant features, distribution of the first three eigenfunctions at location N1 is presented in Fig.2.2. The first spatial eigenfunction (U1) represents the mean beach function, analogues to the arithmetic mean profile of the data. Its distribution indicates the presence of a berm and a moderately sloping foreshore (Fig.2.2). The associated temporal function (V1) shows the general trend and overall stability of the beach over the period of investigation. A constant value here reflects the near-stable nature of the beach under consideration. In the present case, an overall increasing

Table 2.2. Percentage of mean square value of the data as explained by the first three eigen values.

Location	Eigen values		
	First	Second	Third
N1	96.90	2.94	0.07
N2	96.27	3.18	0.37
N3	98.83	0.76	0.33
M1	96.54	2.12	0.87
M2	97.81	1.02	0.72
M3	98.55	1.02	0.23
M4	89.96	9.16	0.50
F1	91.29	6.94	1.64
F2	98.20	1.27	0.23
F3	98.66	1.02	0.19
F4	98.13	1.28	0.38
A1	88.02	11.19	0.36
A2	77.53	20.69	1.30
A3	93.90	5.29	0.52
A4	91.91	7.59	0.82

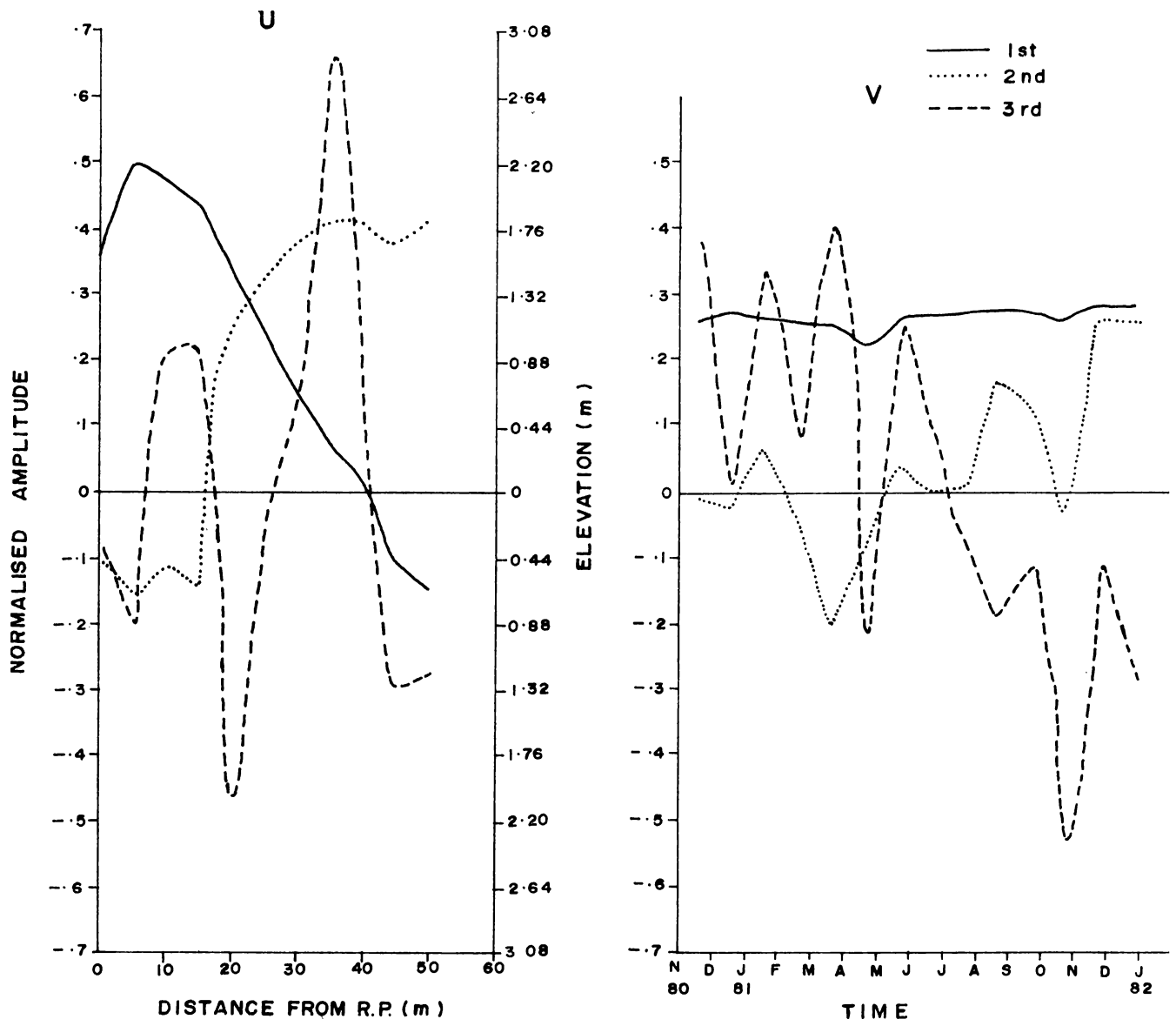


Fig. 2.2 . Spatial and temporal distribution of the empirical eigen function at Location N1

trend in the distribution of V_1 indicates the possible build up of the beach. The second spatial eigenfunction (U_2), represents the berm function, and identifies clearly the spatial location where the beach profile experiences maximum variability. In the present case, U_2 shows maximum spatial variability at the lower foreshore, near the mean low water (MLW 30-40 m) and to a lesser magnitude at the berm (Fig.2.2). The associated temporal function (V_2) is characterised by a strong seasonal temporal dependence. The distribution of V_2 shows the overall depositional feature of the beach achieved through two conspicuous cycles of erosion and accretion. The third spatial eigenfunction (U_3), which is the terrace function, has a broad maximum near the mean low water. The temporal dependence of this function (V_3) shows complicated nature, probably due to changes associated with the differential wave activity coupled with tide. Moreover, it also reflects that the low water itself is variable during the course of an year because of the seasonal changes in sea level and erosion or accretion taking place at the beach under the influence of seasonally reversing wind and wave climates.

In the present study only two eigenfunctions and their distribution in space and time are considered since the profile data did not cover the low tide terrace. The results of the

analysis are presented below to elucidate the intra-variations of the morphological changes along the four zones.

Zone - Narakkal

The observed beach profiles (Fig.2.3a) at the three locations in this zone show the presence of fully grown berm at locations N1 and N2 at distances varying from 5-15 m from the reference point (R.P). At N3 such feature is not observed.

The mean beach function (U1) at the three locations (Fig.2.4a) clearly brings out the presence of berm at N1 and N2. At all the three locations, the beach profiles show steeply sloping foreshore which becomes more flat below the mean low water (MLW). The temporal function associated with the mean beach function (MBF) indicates an overall accretional trend for all the profiles over the period of study. However, the beaches at N1 and N2 present greater temporal fluctuations compared to the beach at N3 (Fig.2.4a).

The distribution of the second spatial eigenfunction (berm function) shows that the variability maximum occurs close to MLW and with a lesser magnitude near the berm crest. At N1 and N2, the maximum variability of the beach profile occurs at the lower foreshore close to MLW, whereas at N3 this featur

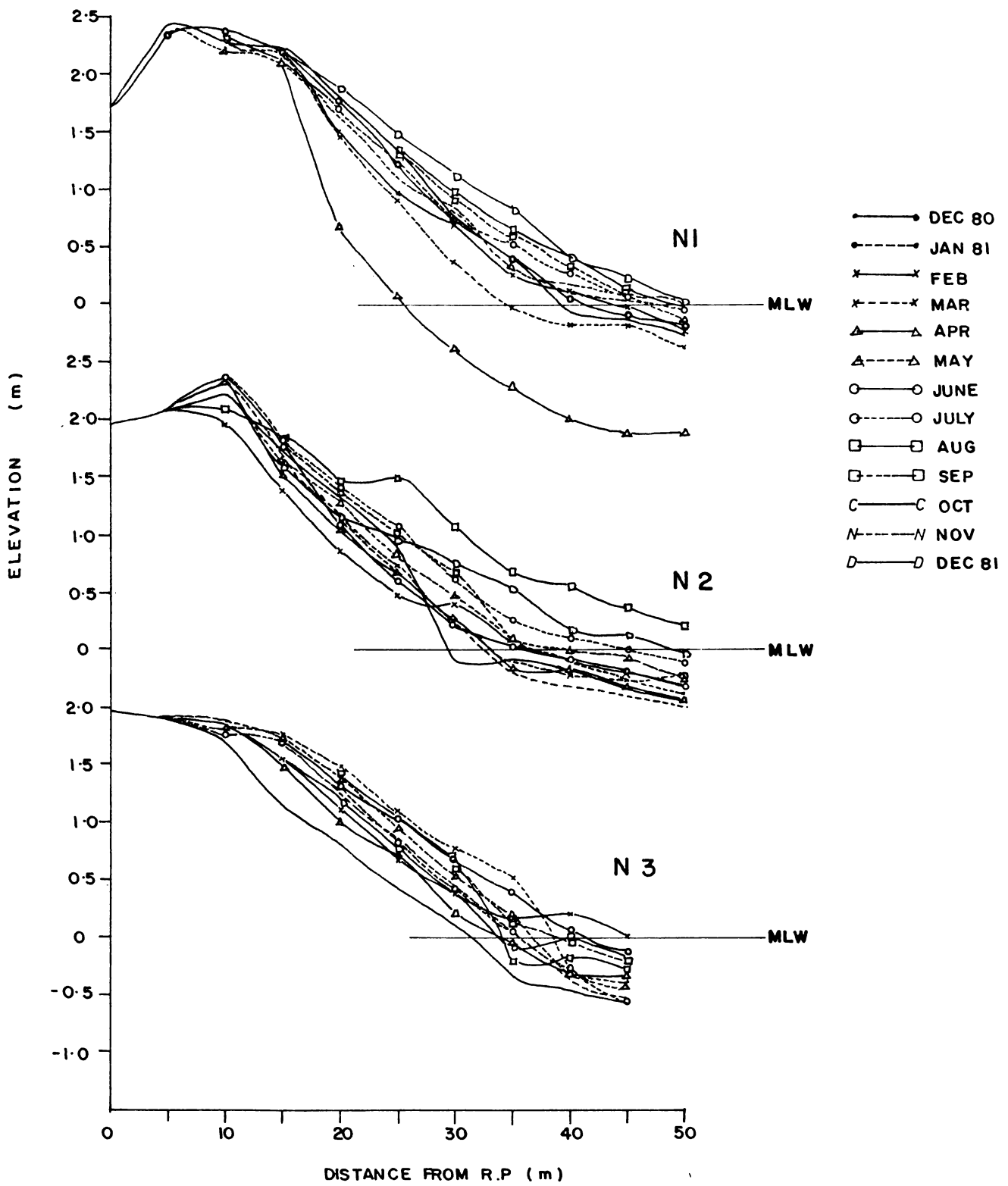


FIG. 2.3a : Beach profiles at Narakkal zone .

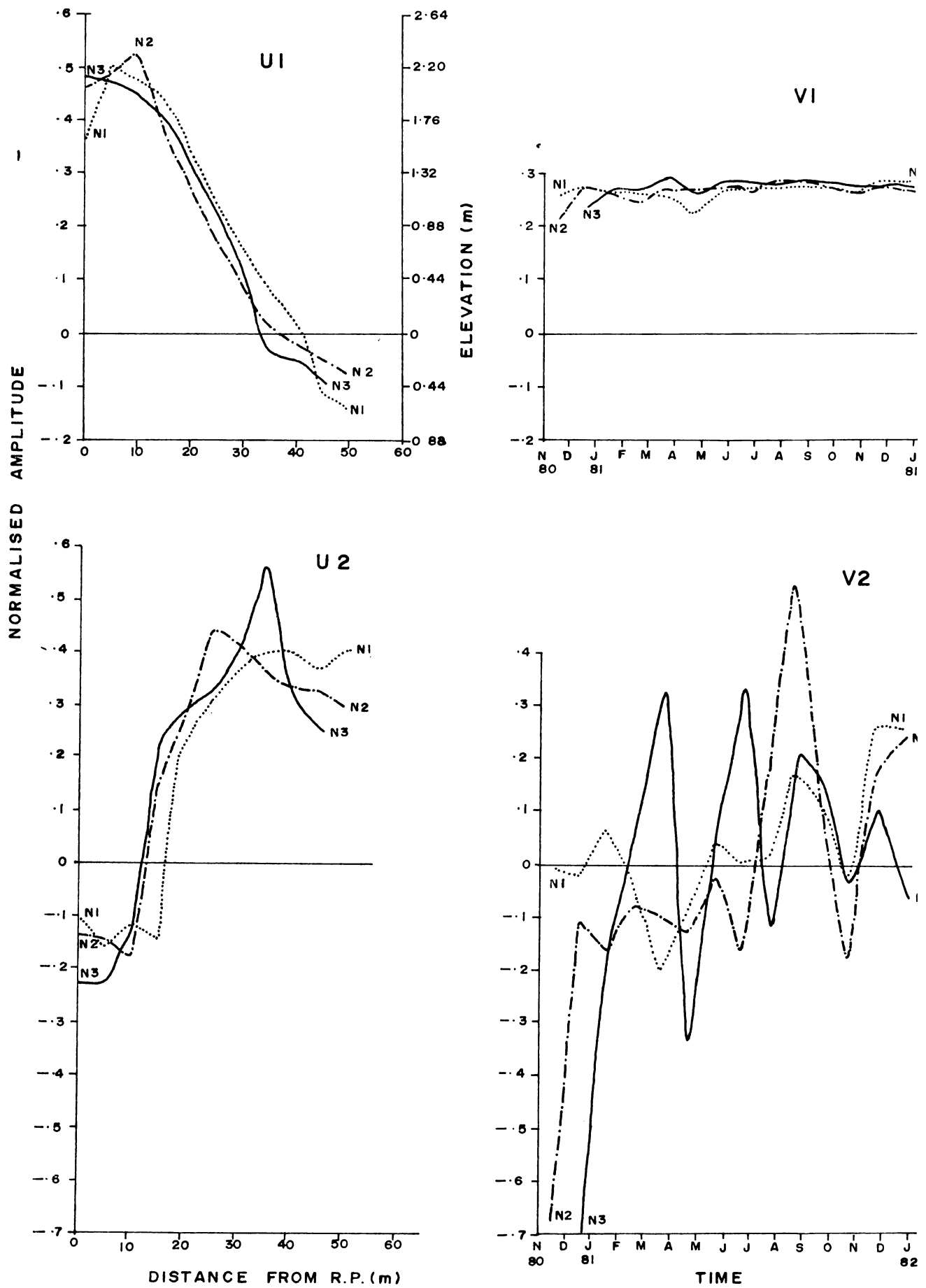


Fig. 2.4 a. Spatial and temporal distribution of the empirical eigen function at Narakkal zone.

occurs below MLW. The second temporal function (V2) indicates the short term cyclicality (of about two to two and half months period) of erosion and accretion to which the beaches are subjected. Eventhough there is some phase difference in the response of the beaches from November (1980) to July (1981) the beaches behave in a similar way from July to November (1981) and pass through a cycle of accretion and erosion.

The volume changes computed from the monthly beach profile data show accretion during November - December (1980) at N1 followed by a period of erosion. This trend continues till the end of April when the beach attains a level of minimum sediment storage of -17 m^3 of material/m of the beach (Fig.2.5a). From April end to mid May the beach experiences rapid accretion and recovers from the losses. Beyond May, once again the beach passes through a state of erosion that lasts till the end of October. During November-December, again the beach passes through accretion and erosion. The overall accretion amounts to $22.90 \text{ m}^3/\text{m}$ of material over the study period.

The beach at N2 also behaves in more or less similar way except during the period from February to end of April when accretion prevails. The beach reaches the minimum storage level of $5.5 \text{ m}^3/\text{m}$ of material during February (1981)

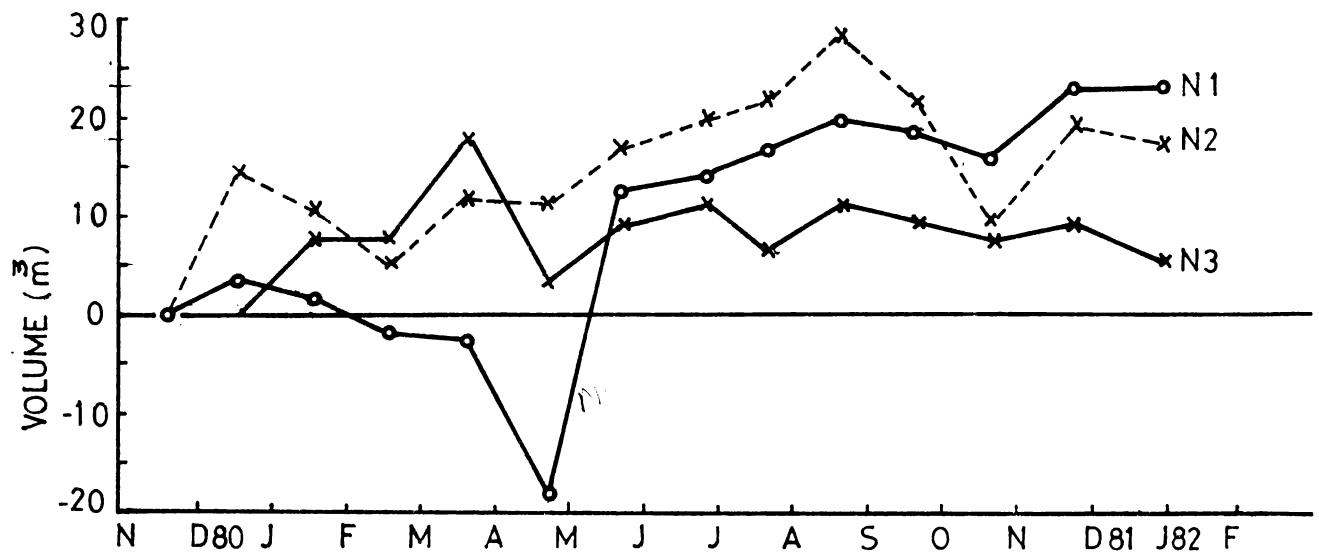


FIG.2.5 a Monthly changes in beach volume at Narakal zone.

but never goes below the initial level. The maximum material storage takes place during August ($28 \text{ m}^3/\text{m}$). The net accretion of beach at N2 amounts to $17 \text{ m}^3/\text{m}$ of material.

At N3, the beach builds up from mid December (1980) till March, when it attains the maximum storage level of $18 \text{ m}^3/\text{m}$. After this the beach loses material at a rapid rate reaching the lowest storage level of $3 \text{ m}^3/\text{m}$ of the material during the end of April. Here again, it never goes below the initial level. The subsequent changes are more or less similar to those along N1 and N2. On the whole the beach gains about $5.3 \text{ m}^3/\text{m}$ of material.

Thus, both the EEF analysis and volume computations indicate the fact that the beaches at Narakkal zone, in general, gain material during the period of study through alternate cycles of accretion and erosion. During the period May to December, the response of the beaches at all the three locations are similar except for minor departures during times of accretion. However, during December (1980) to May (1981), the depositional or erosional trend indicate greater complexity at all the three locations.

Zone - Malipuram

In this zone, the beach profiles at each of the four locations show the presence of a berm and a wider backshore (Fig.2.3b). The location of the berm varies between 5-30 m from the reference point.

The distribution of mean beach function (U1) also indicates the presence of berm (Fig.2.4b) and backshore at all these locations. The width of the backshore, however, decreases progressively from M1 to M4. The beaches in general exhibit moderately sloping foreshore which flattens out below MLW. This is more conspicuous at M1 and M2. The temporal function (V1) associated with MBF shows that the beaches at M1 and M4 undergo greater variability compared to the others. Moreover, the beaches at M1 and M2 show accretional tendency while those at (M2) and M4 show erosional tendency.

The second spatial eigenfunction (U2) shows that at M1 and M3, the maximum variability of profile occurs beyond MLW while at M2 and M4, it occurs at the lower foreshore. A secondary maximum in the variability is clearly noticeable at the berm crest. The distribution of second temporal eigenfunction (V2) shows that the response of the beaches in this zone exhibits considerable temporal variations, specially during January to June. But during June to December,

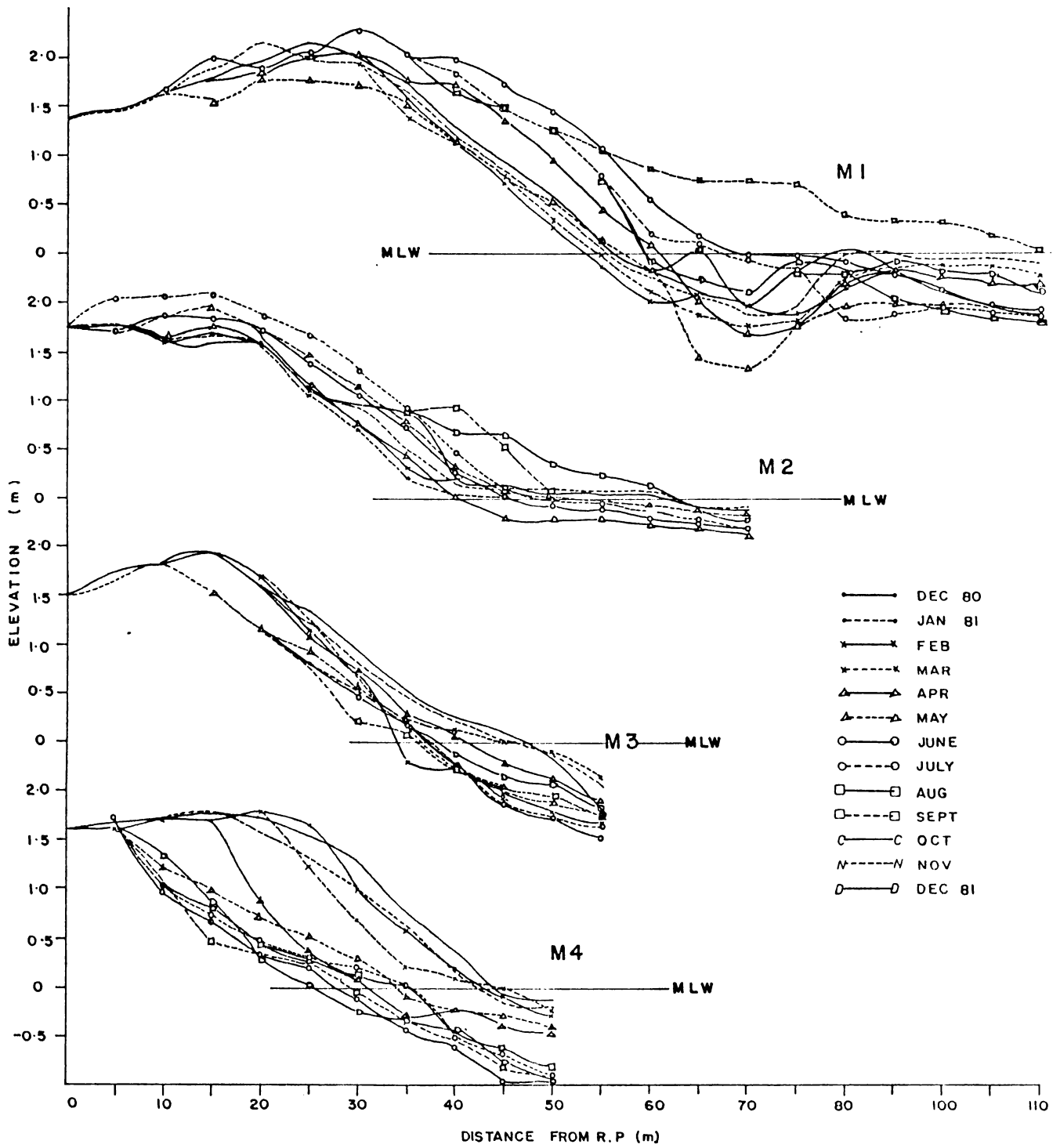


FIG. 2-3b: Beach profiles at Malipuram zone .

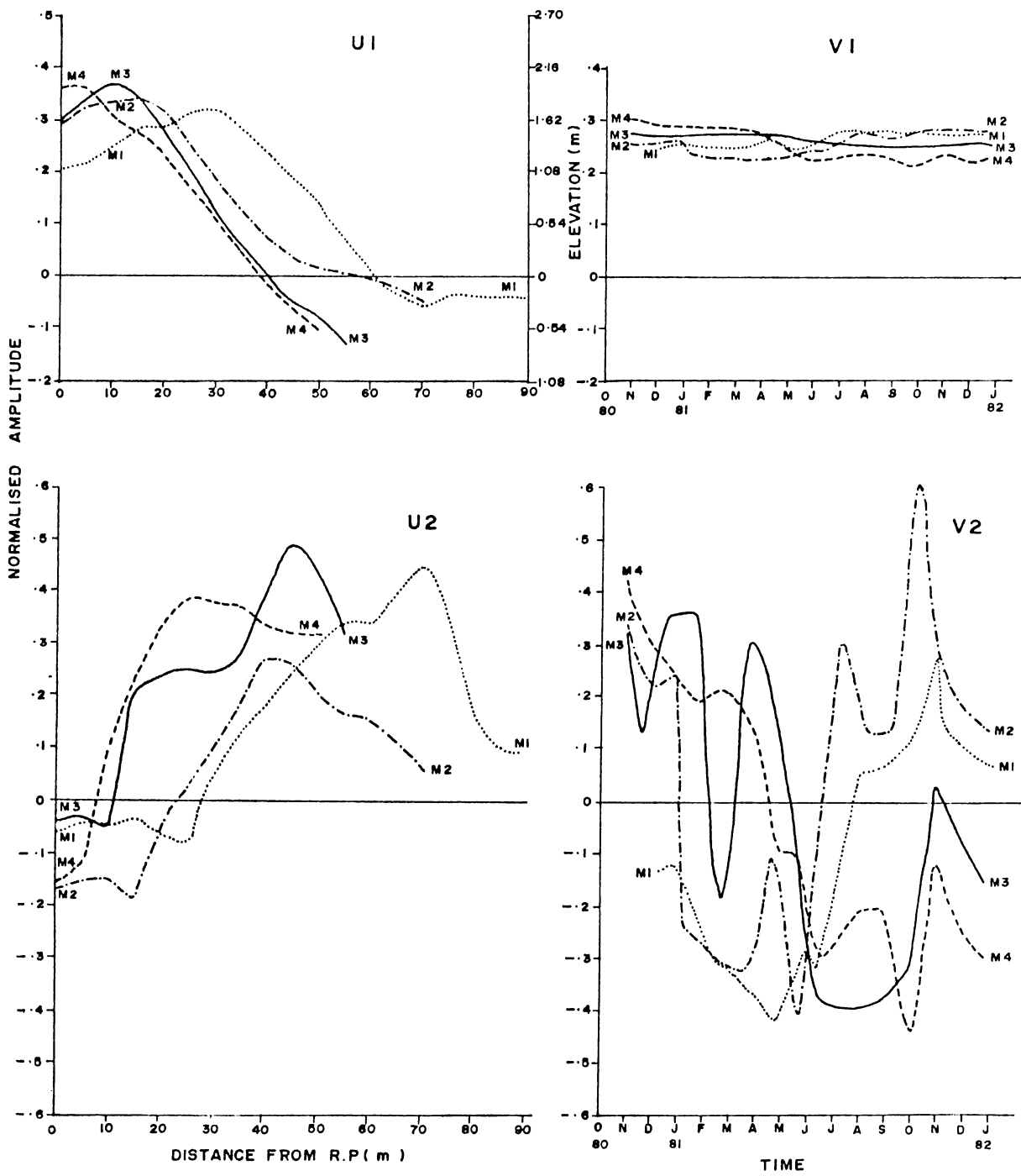


Fig. 2.4 b. Spatial and temporal distribution of the empirical eigen function at Malipuram zone

near systematic accretional and erosional patterns are encountered.

The volume changes show that beach at M1 undergoes (Fig.2.5 gradual erosion till end of April when it reaches the minimum storage volume of -10.5 m^3 of material/m of the beach. From end of April, the beach is subjected to alternate accretions and erosions with about one month periodicity till middle of October, when it reaches the maximum level of storage ($28 \text{ m}^3/\text{m}$ of material). Then onwards the beach loses material. The net volume change shows a decomposition of $14 \text{ m}^3/\text{m}$ of material over the period of study.

At M2 also the beach initially experiences some erosion till January end while during February it builds up considerably. Once again, from March to May it erodes, reaching the level of minimum material storage of $-7 \text{ m}^3/\text{m}$. Then onwards it follows the trends exhibited by M1. The net volume change amounts to a deposition of $15 \text{ m}^3/\text{m}$ of material.

At M3 the beach is subjected to cyclic changes of erosion and accretion with roughly one month periodicity till early April. Then onwards the beach loses material till October when the beach attains the lowest volume of material ($-20 \text{ m}^3/\text{m}$). From October to December, the beach experiences

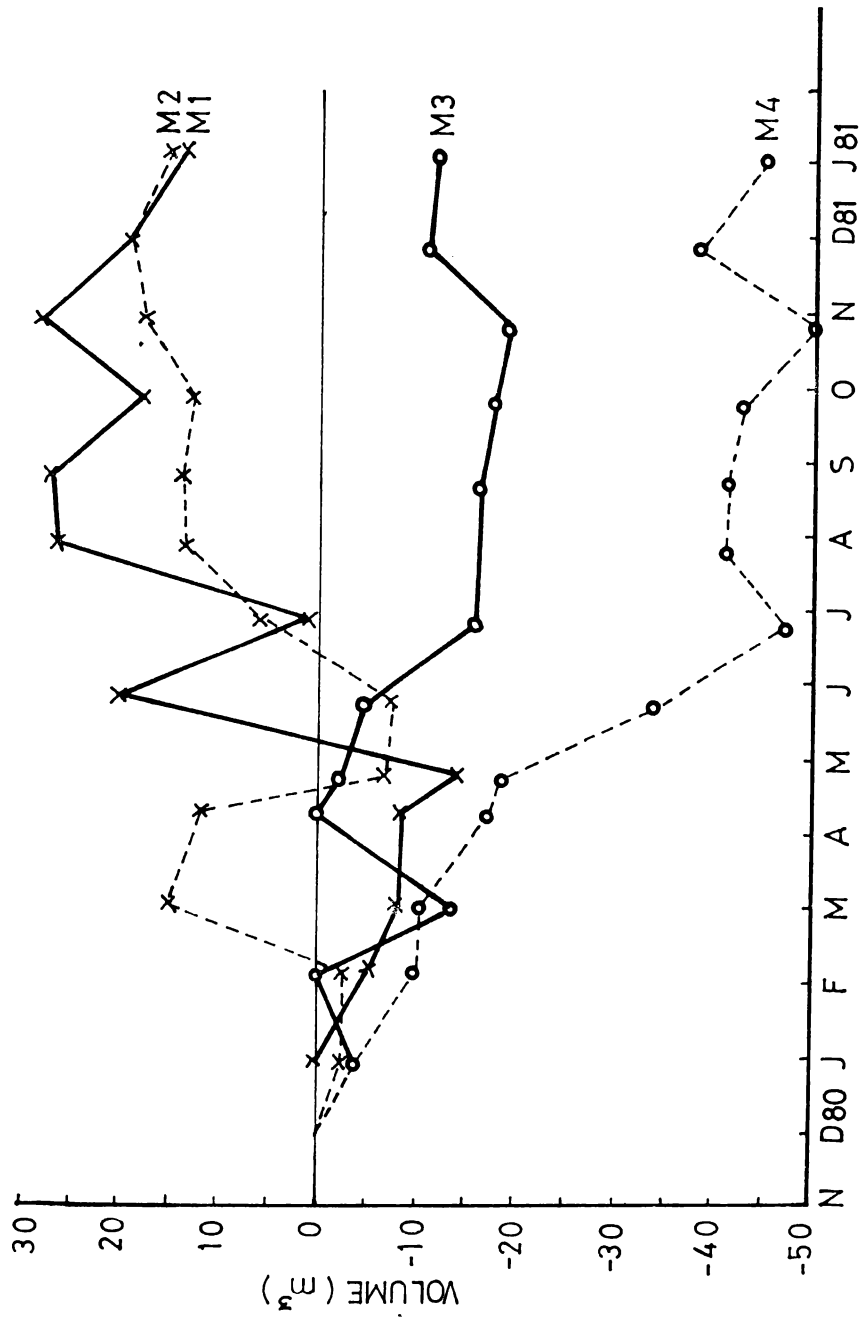


FIG. 2.5 b Monthly changes in beach volume at Malipuram zone.

one cycle of accretion and erosion. This beach reaches its initial volume level twice, initially during February and later during April. Over the study period the beach loses material, amounting to $11.8 \text{ m}^3/\text{m}$.

At M4, however, the beach is subjected to continuous erosion except during June to July and October to November. On the whole the beach loses $44.5 \text{ m}^3/\text{m}$ of material.

In general, the EEF analysis and volume computations highlight the fact that, in the Malipuram zone, though there is a wide variation in the response of beaches during January to June, the beaches on the northern part (M1 and M2) and on the southern part (M3 and M4) behave more or less in a similar pattern during July to December. Even though M1 and M2 are subjected to alternate accretion and erosion, the net change leads to a build up. At M3 and M4, the beaches do not show much of an accretional tendency.

Zone - Fort Cochin

The beach profiles along this zone indicate the presence of wide berm between 5 - 30 m from R.P, except at F4, where no permanent berm exists (Fig.2.3c).

The distribution of MBF (U1) shows that beaches in general have moderately sloping foreshore except at F4, where they are comparatively steeper (Fig.2.4c). It also

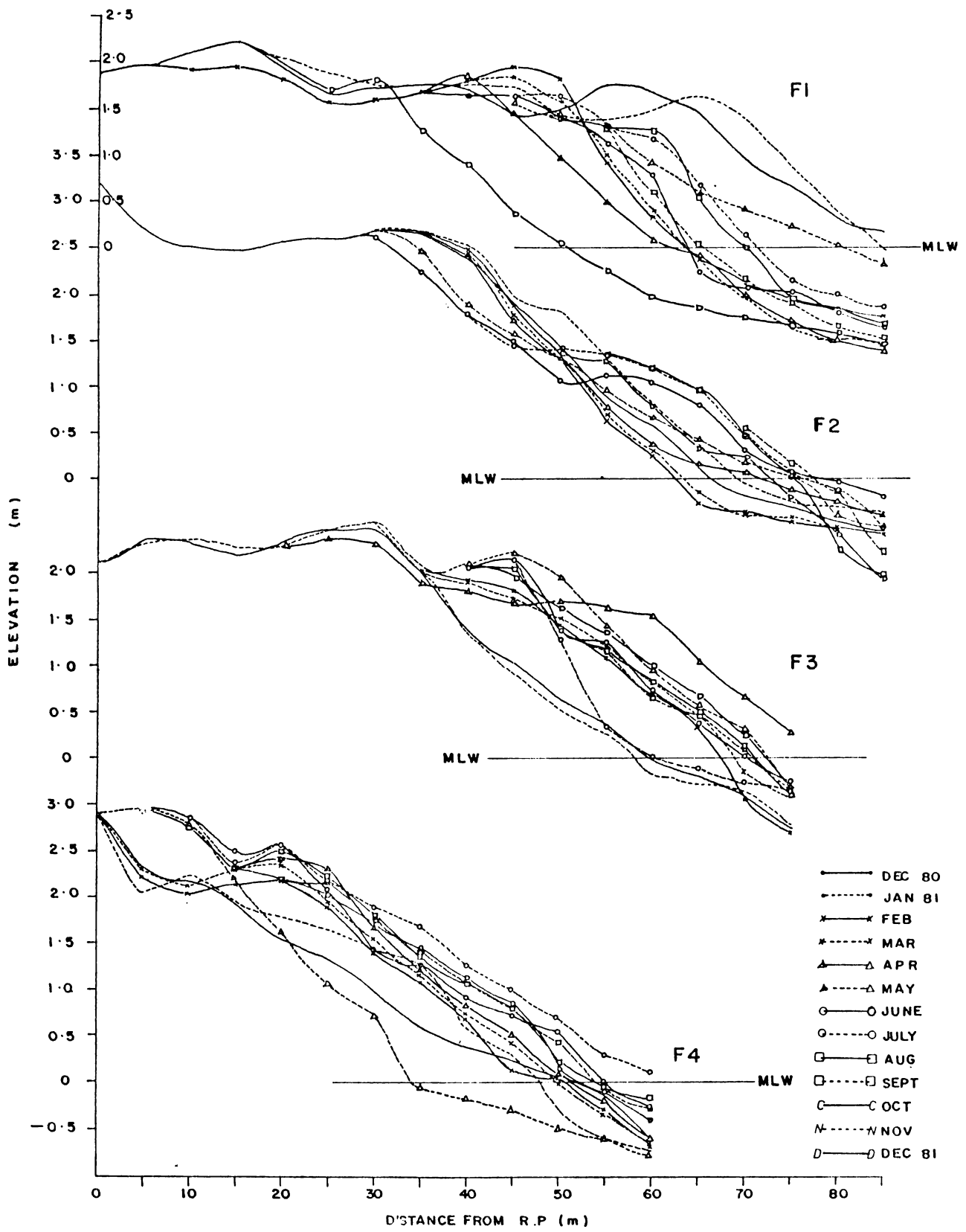


FIG. 2.3c : Beach profiles at Fort Cochin zone .

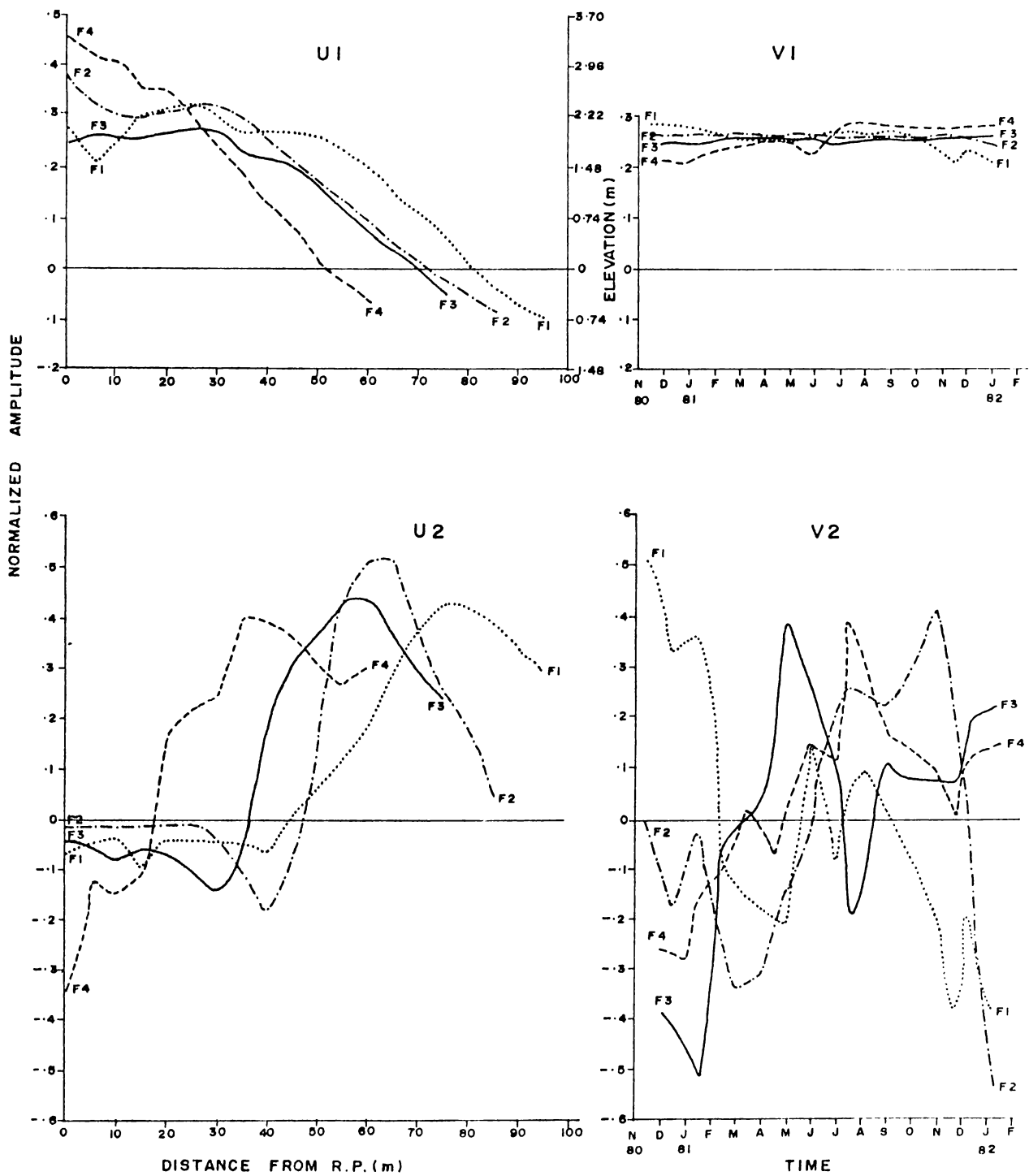


Fig. 2.4 c. Spatial and temporal distribution of the empirical eigen function at Fort Cochin zone

shows a step-like feature at F1, F2 (at 30-40 m from R.P) and F4 (at 15-20 m from R.P). In this zone, the slope of the beach below MLW does not show any change. The temporal function (V1) associated with MBF shows that beaches at F1 and F4 are subjected to greater variability compared to those at F2 and F3. The overall trend of V1 indicates erosional tendency at F1 and F2 and depositional tendency at F3 and F4.

The second eigenfunction (U2) indicates that maximum variability of beaches occurs at the lower foreshore above MLW, while a secondary maximum shows that at F3 the upper foreshore and at F1 and F2 the step undergo variations. The distribution of the second temporal function (V2) shows that the beaches are subjected to accretion and erosion with varying lags and leads.

The volume changes show that at F1, the beach loses material rapidly to the tune of $47 \text{ m}^3/\text{m}$ by the end of February (Fig.2.5c). Thereafter the beach experiences accretion leading to considerable deposition during May. But once again the beach loses material till December except during November when it accretes. The volume change shows a net deficit of $65.6 \text{ m}^3/\text{m}$ of material over the period of study.

At F2 also, the beach loses material till March and then onwards it slowly accretes till end of October. During

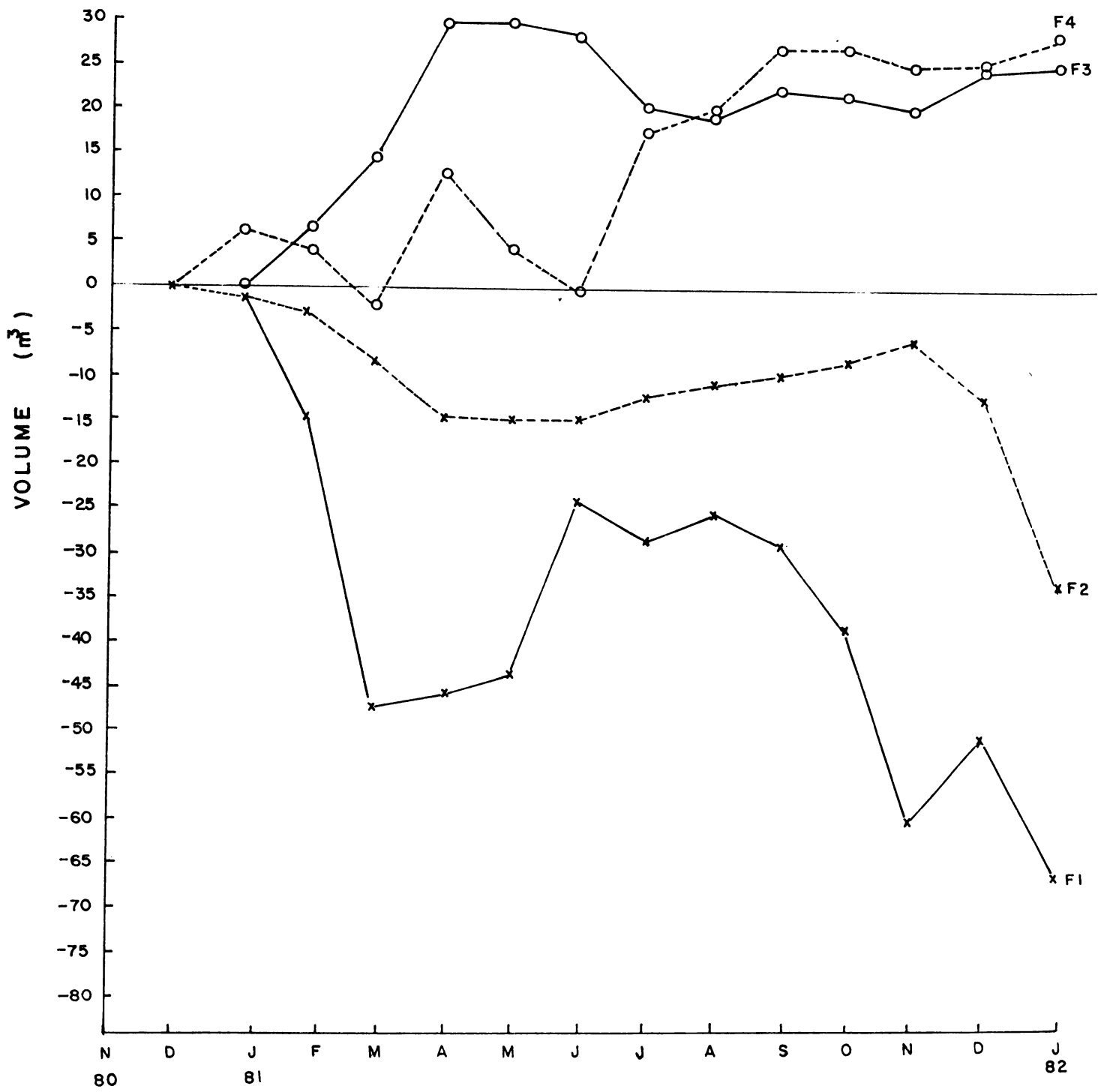


FIG. 2.5 c Monthly changes in beach volume at Fort Cochin zone .

November-December, the beach once again erodes, resulting in a net loss of $33.0 \text{ m}^3/\text{m}$ of material.

At F3, the beach experiences build up till March, resulting in maximum storage of $30 \text{ m}^3/\text{m}$ of material. From April onwards it loses material till July end and passes through a cycle of accretion and erosion resulting in a net gain of $28.5 \text{ m}^3/\text{m}$ of material.

At F4, the beach is subjected to cycles of accretion and erosion with periods of about one and half to two months till May. From June to August, it again accretes and during September-November, it undergoes slight erosion resulting in a net gain of $30.0 \text{ m}^3/\text{m}$ of the material.

Thus the EEF analysis and volume changes show that the beaches at Fort Cochin zone are subjected to accretional and erosional cycles with differential lags and leads.

Zone - Anthakaranazhi

The beaches in this zone exhibit the presence of berm located between 5 - 20 m from R.P (Fig.2.3d).

The distribution of MBF (U1) also indicates the presence of the berm (Fig.2.4d). The beaches at A2 and A3 have moderately sloping foreshore while at A1 and A4 the foreshore is comparatively steeper. The temporal function (V1) associated with MBF shows that beaches at A1 and A3 are

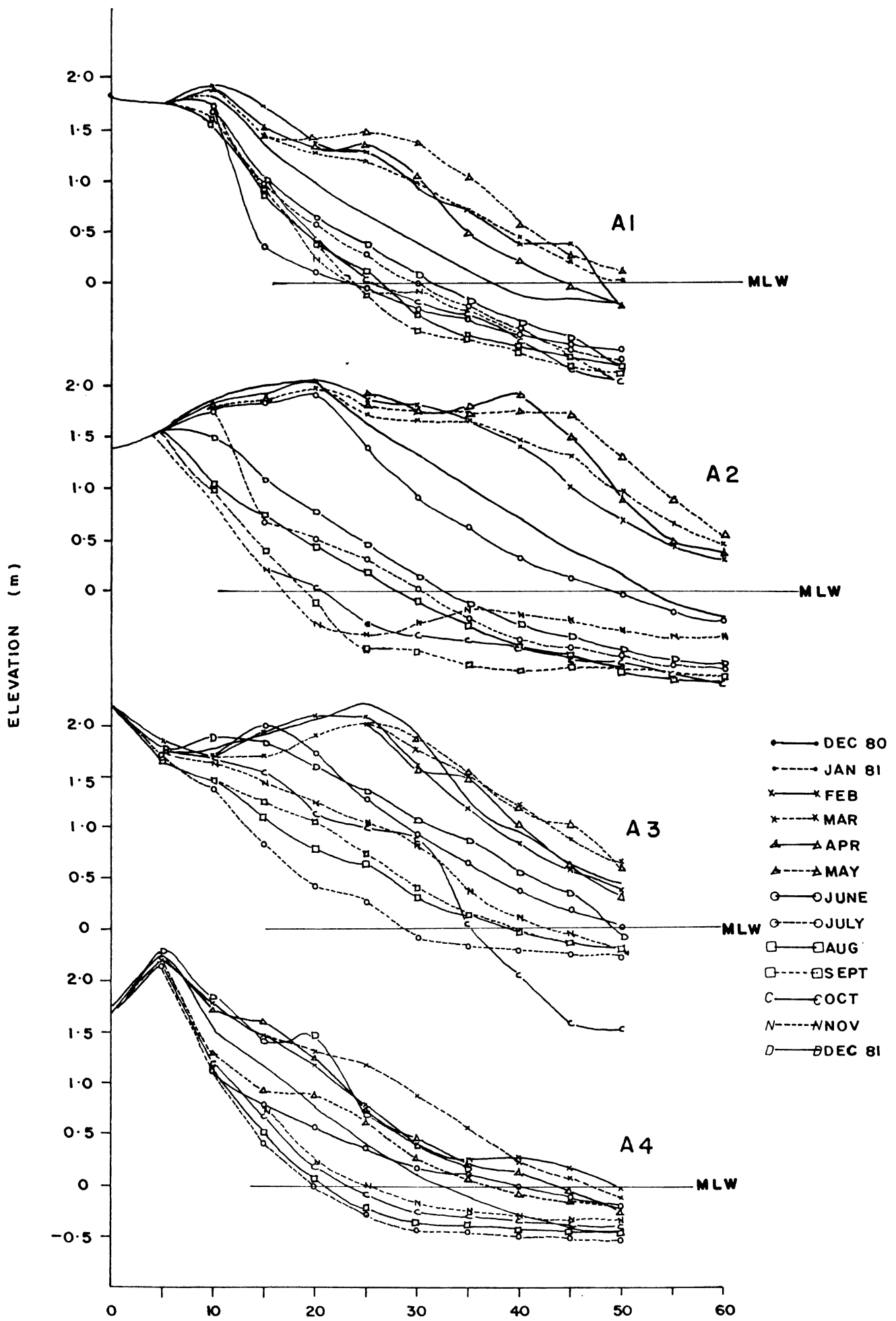


FIG.2.3d: Beach profiles at Anthakaranazi zone .

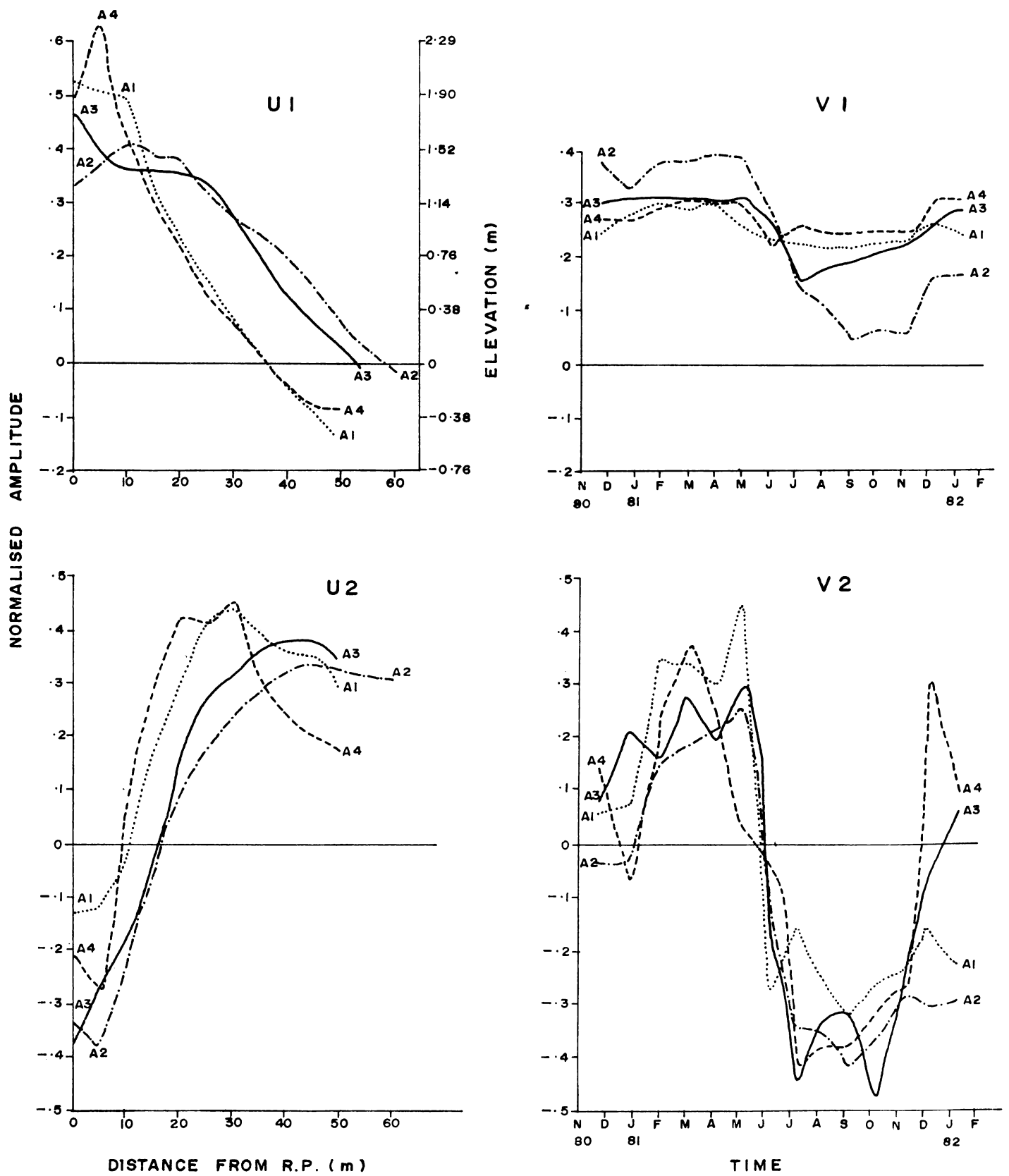


Fig. 2.4 d. Spatial and temporal distribution of the empirical eigen function at Anthakaranazhi zone

subjected to greater temporal variations. During the study period A2 showed maximum material losses.

The distribution of U2 shows that beaches in this zone have maximum variability at the lower foreshore above MLW. At A2 and A4 the berm also shows some amount of variability. The second temporal function (V2) indicates that the beaches in this zone respond in a similar way showing depositional tendency during January to April and rapid erosion during May to July. The beach once again shows recovery trend during the subsequent months.

The volume computations show that at A1, the beach is subjected to alternating accretion and erosion with a periodicity of about one month till April and then suddenly undergoes erosion during May to July (Fig.2.5d). The erosion continues till end of August at a reduced rate. The beach slowly recovers during September to November from the losses. Once again the beach is subjected to erosion during December resulting in a net loss of $9.5 \text{ m}^3/\text{m}$ of beach material.

At A2, the beach accretes till March and shows erosional tendency during April. During May to September, the beach loses material rapidly (about $80.0 \text{ m}^3/\text{m}$). Then onwards it slowly accretes till November. Again during December the beach is eroded resulting in a net loss of about $30.0 \text{ m}^3/\text{m}$ of material.

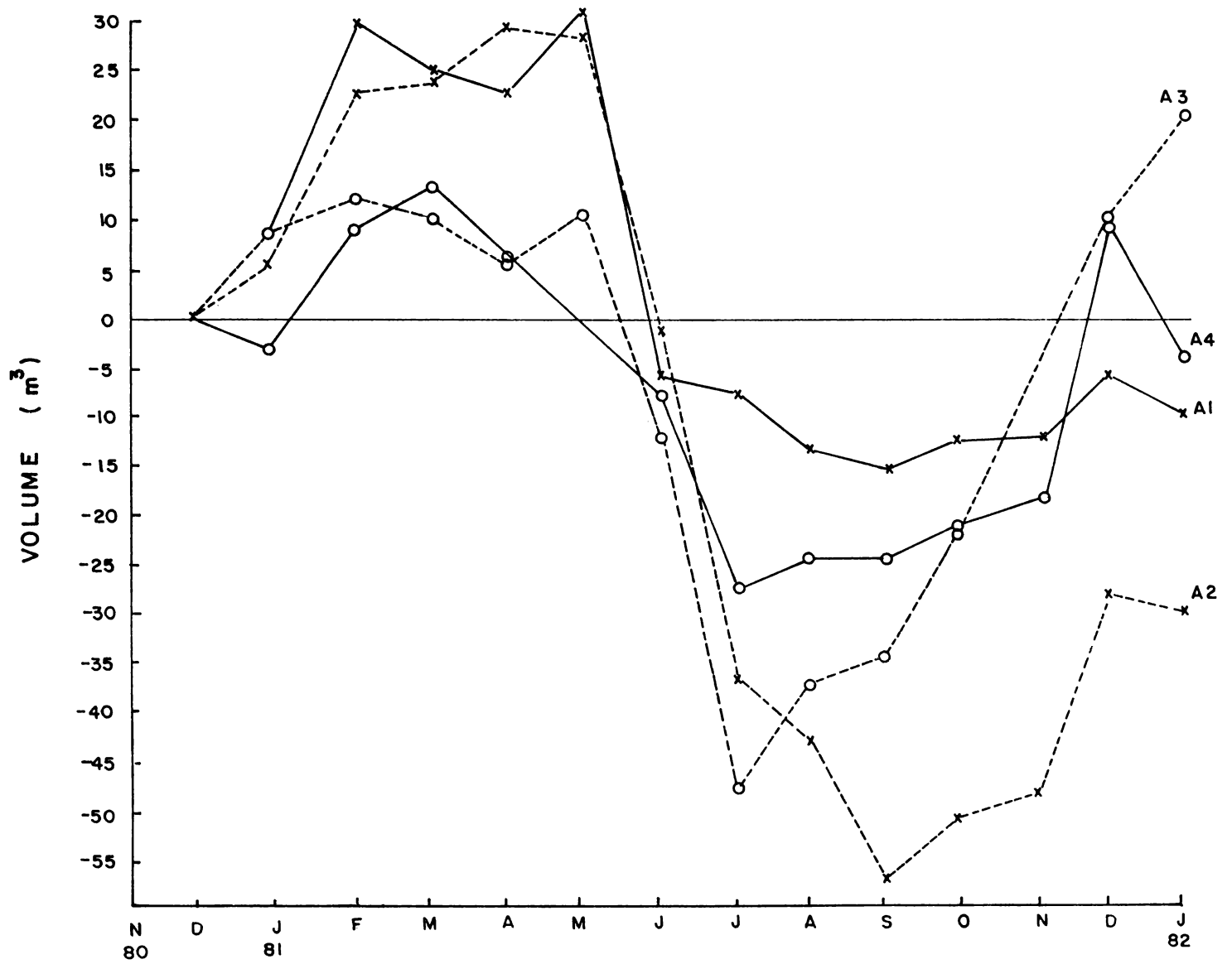


FIG. 2-5 d Monthly changes in beach volume at Anthakaranazhi zone.

At A3, the beach undergoes alternate cycles of accretion and erosion with a periodicity of about two months till the end of April, after which it is subjected to severe erosion till June. From July onwards, the beach accretes and not only recovers from the losses but also shows a net gain of $20.0 \text{ m}^3/\text{m}$ of material.

The beach at A4 builds up, after an initial erosion during December (1980), till February. During March-July, once again the beach gets eroded. It accretes and recovers from the loss during November. The beach is then subjected to erosion resulting in a net loss of about $3.5 \text{ m}^3/\text{m}$ of material.

In general, the EEF analysis as well as volume computations clearly show that the beaches of this zone undergo maximum changes. The beaches show accretional tendency during January to April, and then suddenly experience severe erosion during May to July. Then onwards the beaches show depositional tendency.

These observations can be summed up broadly as under.

- (1) The beach responses are, in general, variable particularly at times of occurrence of accretion or erosion.
- (2) At certain locations, the beaches experience erosion during the southwest and northeast monsoon seasons.

(3) The period of maximum erosion almost coincides with the onset of southwest monsoonal wave climate.

(4) The intra-variability observed clearly points out to the fact that the changes are probably the result of differential wave activity in the dynamic zone and the associated flows that help in transporting the sediments.

CHAPTER 3 : BEACH SEDIMENTS

3.1. Materials and methods

3.2. Results

The observed changes in beach geometric form along the barrier beaches under study have been presented in the preceding Chapter. This, however, provides only a part of the characteristics of the beach changes in this environment. In order to obtain a better understanding of these changes, one need to examine the sediments comprising the beach and the changes they undergo as the geometric form of the beach changes with time. The nature of the beach material in the foreshore and inshore plays an important role in modifying the incoming waves through changes in resistance offered by the sediments.

Beach sediments consist of masses of unconsolidated sedimentary material on which the dynamic forces due to waves, tides, currents, etc. act. Under the influence of these forces, the unconsolidated material gets sorted. The grain size parameters are characteristic of the sediments and are important in the study of movement of nearshore material. The variation of these parameters along the beach profile reflects the energy levels to which the beaches are exposed.

The textural characteristics of the sediments and their variations at various locations on the beaches between

Azhikode to Anthakaranazhi are presented in this Chapter.

3.1. Materials and methods

Beach sediment samples were collected by scoop sampling at different stations along each of the 15 locations at monthly intervals. The sediment samples were washed and oven-dried. A representative portion of each sample was then subjected to size analysis by sieving, using a set of standard Endecott sieves arranged at $1/2 \phi$ intervals. Sieving was done for 15 minutes on a sieve-shaker. The different sieve fractions were then weighed and the weight percentages calculated. When the samples contained material of size less than 0.062 mm, the size analysis was carried out by a combination of sieve and pipette analysis following the method of Krumbein and Pettijohn (1938). In all, 483 samples were analysed from the 15 profile lines. The grain size distributions were estimated by evaluating the descriptive statistical parameters such as graphic mean ($M_z \phi$) and inclusive graphic standard deviation (σ_ϕ), as proposed by Folk and Ward (1957), using TDC - 316 Computer.

3.2. Results

The distribution of mean grain size ($M_z \phi$) along the profiles and their standard deviation (σ_ϕ) in all four zones

are presented in Fig.3.1 a-d and Fig.3.2 a-d respectively.

Zone - Narakkal

The monthly variation of mean grain size ($M_z \phi$) at the beach at location N1 is presented in Fig.3.1a. The mean grain size decreases from berm to upper foreshore (25 m) and then increases towards MLW (40 m). At MLW and beyond, $M_z \phi$ again decreases. During January and May, however, material in the foreshore is within the finer size limits and increases in size beyond MLW. In general, material at the berm shows the highest grain size of 2.1ϕ (fine sand) and its size does not show temporal variations. The finest material of 3.8ϕ (very fine sand) occurs at the upper foreshore. The maximum range of variation of the $M_z \phi$ value occurs at the upper foreshore and near the MLW.

At location N2, the sediments are coarser in the upper foreshore (25 m) and decrease in size towards MLW (35 m) and beyond it. This decrease is very conspicuous during July when the grain size attains the value of 5.5ϕ (silt) beyond MLW. The coarsest material in this location with mean size 1.8ϕ (medium sand) is encountered at the mid-foreshore during March. The maximum temporal variation in $M_z \phi$ occurs along the mid-foreshore.

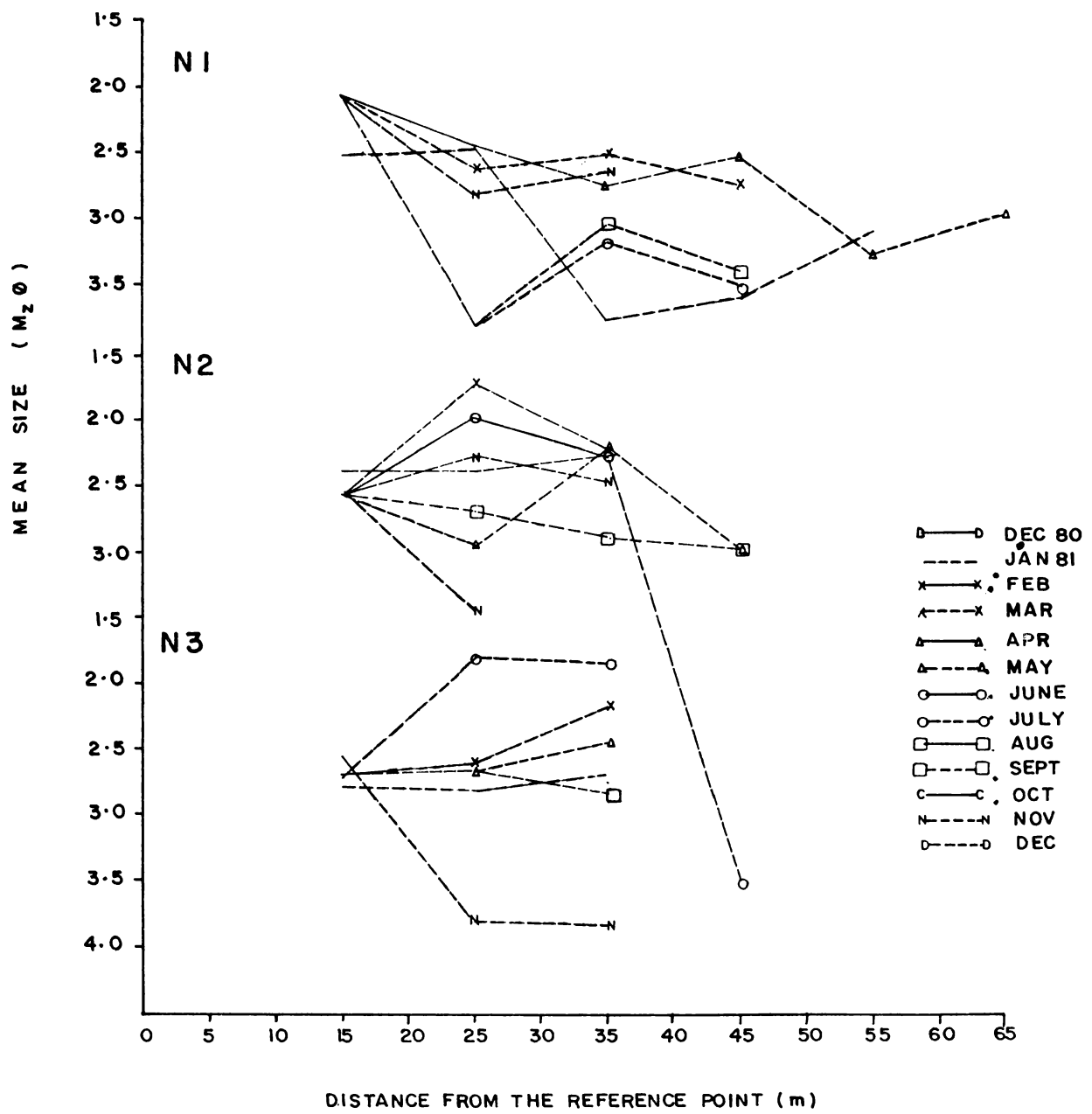


FIG. 3.1a Monthly variation of mean grain size distribution along profiles at Narakkal zone .

At N3, the mean grain size of the sediment does not show appreciable variation from berm crest to mid-foreshore (25 m) except during July and November. Hence the sediments are within the fine sand-size limits. Beyond the mid-foreshore, the grain size shows slight temporal and spatial variations. During July and November, the distribution of $M_z \phi$ shows an entirely different pattern. Between the berm crest and the mid-foreshore, grain size increases to a maximum (1.8 ϕ ; medium sand) during July while it decreases to a minimum (3.8 ϕ ; very fine sand) during November. Beyond this, upto MLW, the mean grain size maintained the same values during these months.

The distribution of standard deviation at N1 (Fig.3.2a) shows that in the upper foreshore the material varies from very well sorted class (<0.35) to moderately sorted class (0.5 - 1.0). Beyond MLW, the material gets moderately sorted during January and very well sorted during July. Except during May (at MLW) and July (20 m beyond MLW), the sediments belong mostly to the moderately sorted class. At N2, along the upper foreshore, the sediment varies from very well sorted to poorly sorted class. In the lower foreshore region, sediment shows moderate to poor sorting. Beyond MLW (35 m), standard deviation again shows wide range of variation from very well sorted to poorly sorted. At N3, material on the berm belongs to the well sorted class. The material becomes moderately sorted towards MLW.

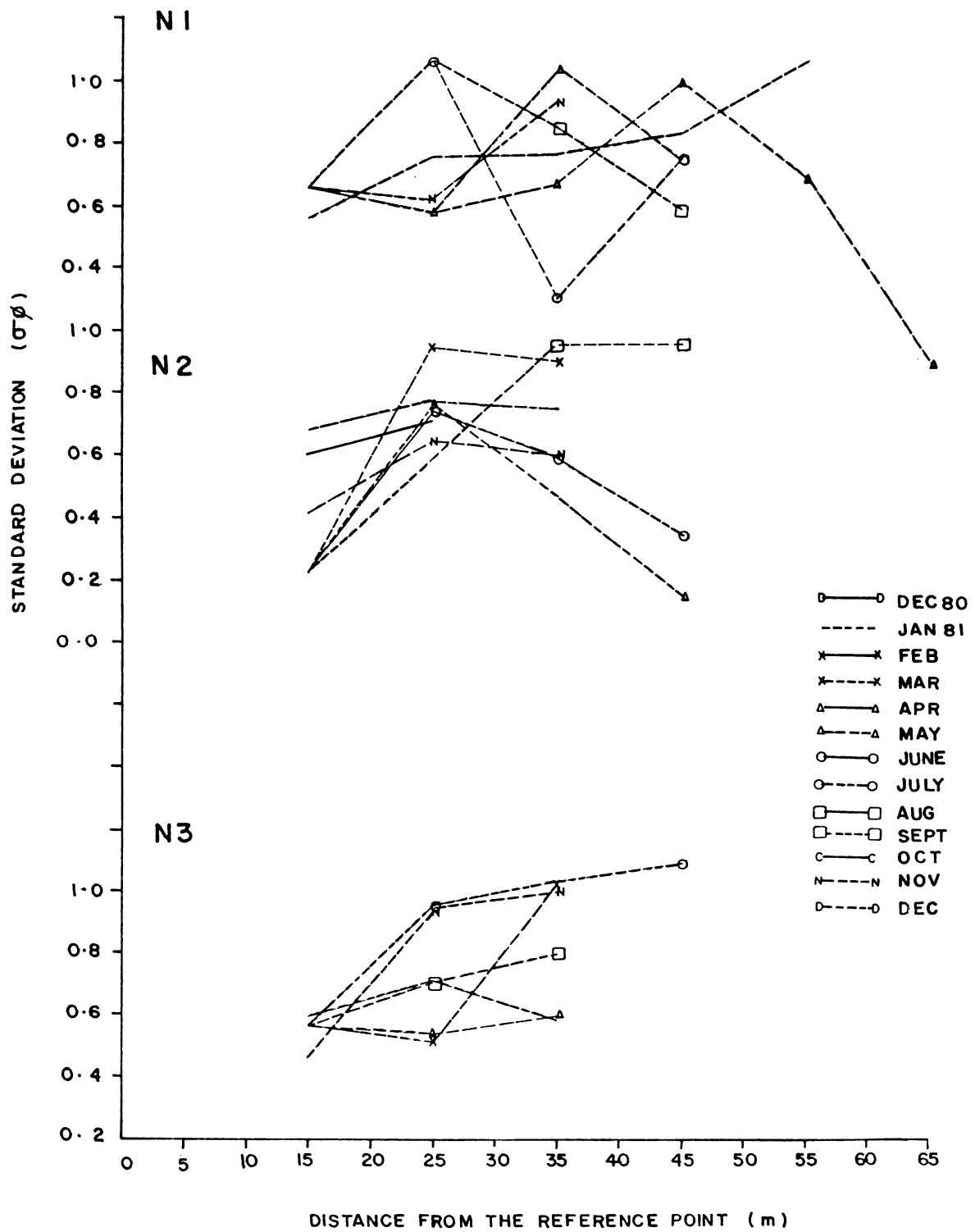


FIG. 3.2 a Monthly variation of standard deviation of grain size along profiles at Narakkal zone .

In general, the beach sediments at Narakkal zone belong to medium ($1 - 2 \phi$) to very fine sand ($3 - 4 \phi$) and are of well to poorly sorted class.

Zone - Malipuram

The variations of grain size distribution show that at M1 (Fig.3.1b), the mean grain size in the backshore initially decreases slightly and then increases towards the berm crest (25 m from R.P) reaching a value of 2.2ϕ (fine sand) at the berm crest. In the upper foreshore, the grain size decreases to 2.7ϕ , while in the lower foreshore it again increases (2.2ϕ) and then decreases to 3.0ϕ at MLW (60 m). During March and May, however, the mean grain size continuously increases towards MLW. The sediments in the backshore and foreshore remain in the fine sand class. Beyond MLW, grain size varies between fine sand and silt. The finest material 5.5ϕ (silt) occurs during May beyond MLW. During most of the period, the material beyond MLW is within the very fine sand limits.

At M2, the mean grain size decreases slightly from backshore (2.3ϕ) to the berm crest (2.7ϕ) at 15 m. In the foreshore region, the distribution shows temporal variations of grain size. In this region, the coarsest material (2.2ϕ) occurs during March and finest material (5.3ϕ) occurs during

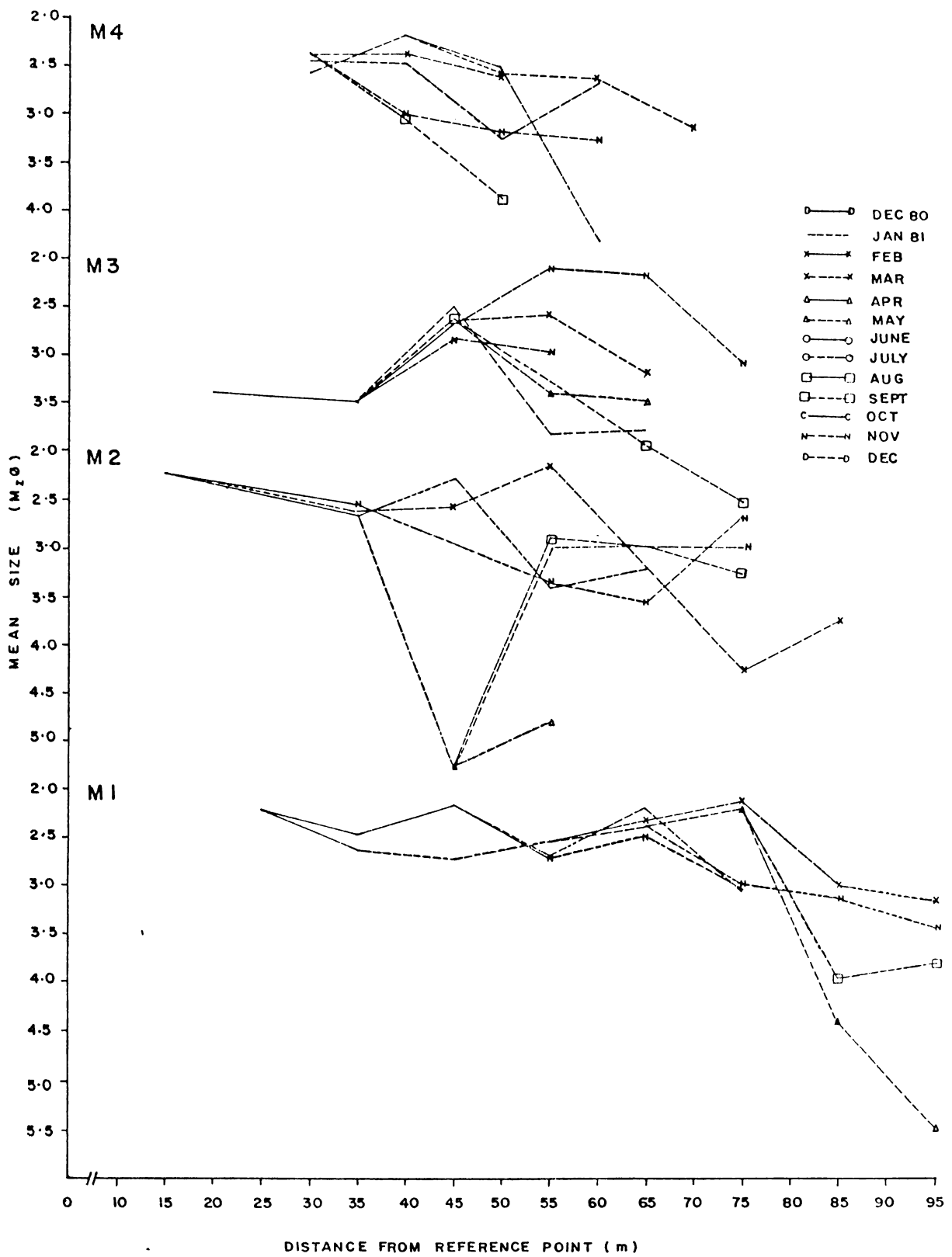


FIG. 3.1b Monthly variation of mean grain size distribution along profiles at Malipuram zone .

May, July and September. Beyond MLW (55 m), the grain size varies between 2.5 - 4.2 ϕ (fine to very fine sand) with silt occurring during March.

The mean grain size at M3 shows an increase in the upper foreshore from 3.5 ϕ to 2.8 ϕ and then decreases towards the lower foreshore from 2.5 ϕ to 4.0 ϕ . During November, however, the grain size continues to increase in the foreshore region attaining the maximum value (2.2 ϕ) near MLW. Beyond MLW, the mean grain size decreases and attains the lowest size of 4.5 ϕ during September.

At M4, the mean grain size increases in the upper foreshore reaching the value 2.3 ϕ and then decreases towards MLW (40 m). But during September and November, the grain size shows a decreasing trend in the foreshore. Thus the sediments are composed of fine to very fine sand in the foreshore and fine sand to silt beyond MLW.

The variation of standard deviation, at M1 (Fig.3.2b), shows that in the foreshore, sorting varies between very well to moderately sorted, though most of time it is in the moderately sorted class. Beyond MLW, the sorting varies from very well to poorly sorted class. At M2, the material in the foreshore belongs to moderately sorted to poorly sorted class and beyond MLW it is essentially in the poorly sorted class. At M3, in the upper foreshore, material is moderately

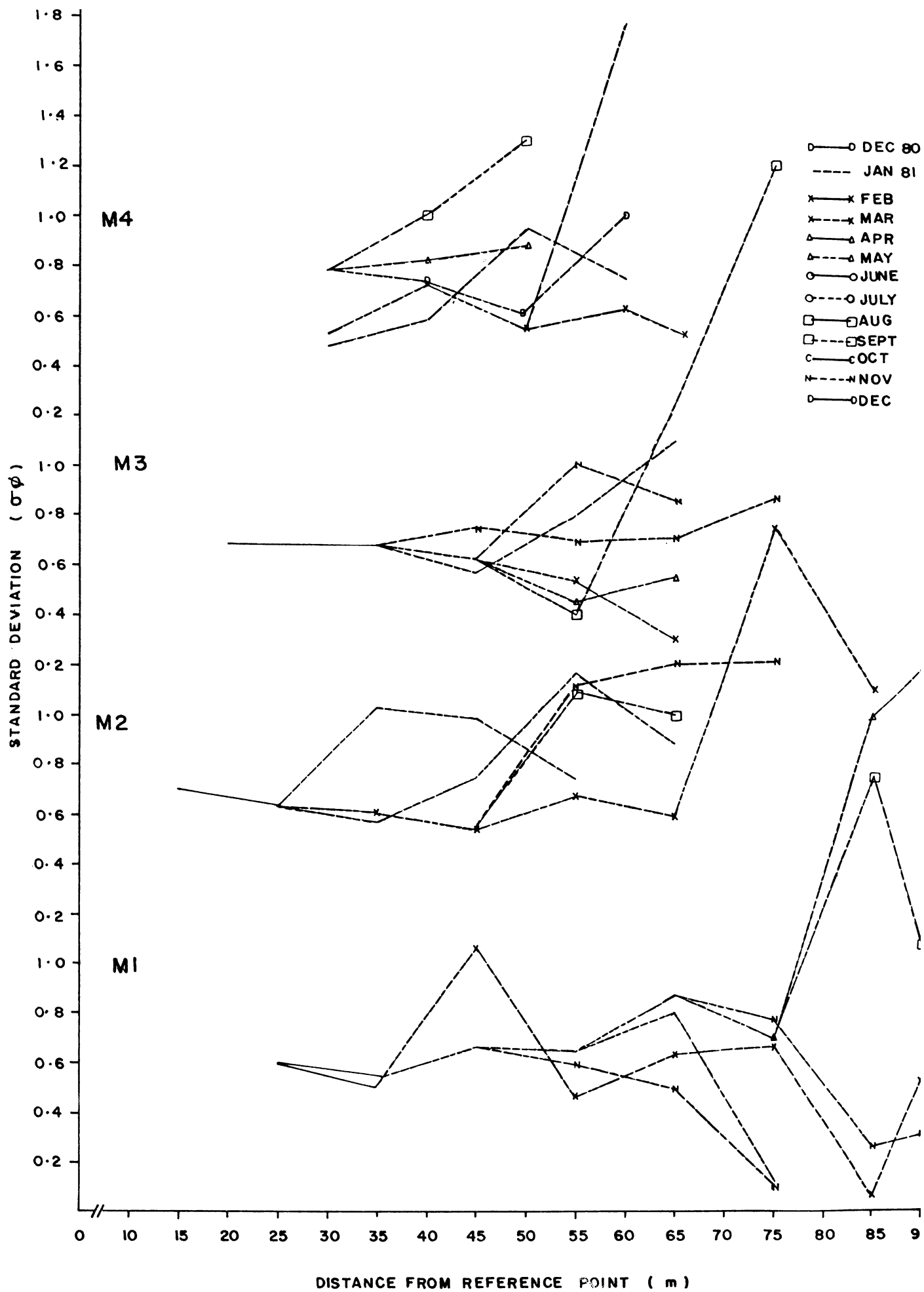


FIG. 3-2 b Monthly variation of standard deviation of grain size along profiles

sorted while in the lower foreshore it is between well sorted to moderately sorted class. Beyond MLW, it varies from very well sorted to poorly sorted class. Sediments at M4 belong to moderately sorted class, except during September when they are poorly sorted. Beyond MLW, they belong to moderately sorted to poorly sorted class.

In general, sediment in the Malipuram zone belongs to the fine sand to silt with sorting ranging from well sorted to poorly sorted class.

Zone - Fort Cochin

The mean grain size distribution at F1 (Fig.3.1c) shows that in the upper foreshore the sediment remains in the fine sand class ($2 - 3 \phi$) while the mean grain size decreases towards the MLW (80 m). However, during July and September, the mean grain size shows slight increasing trend towards MLW. Beyond MLW, the material remains coarser (2.2ϕ) during May. The coarsest (2.1ϕ ; fine sand) and finest (3.9ϕ ; very fine sand) materials occur at MLW during July and November respectively.

At F2, the mean grain size shows decreasing trend, with least temporal variation, between berm crest and mid-foreshore. In this region, the material remains in the fine sand class limit. From mid-foreshore, the grain size increases to 1.7ϕ , except during January and November, and

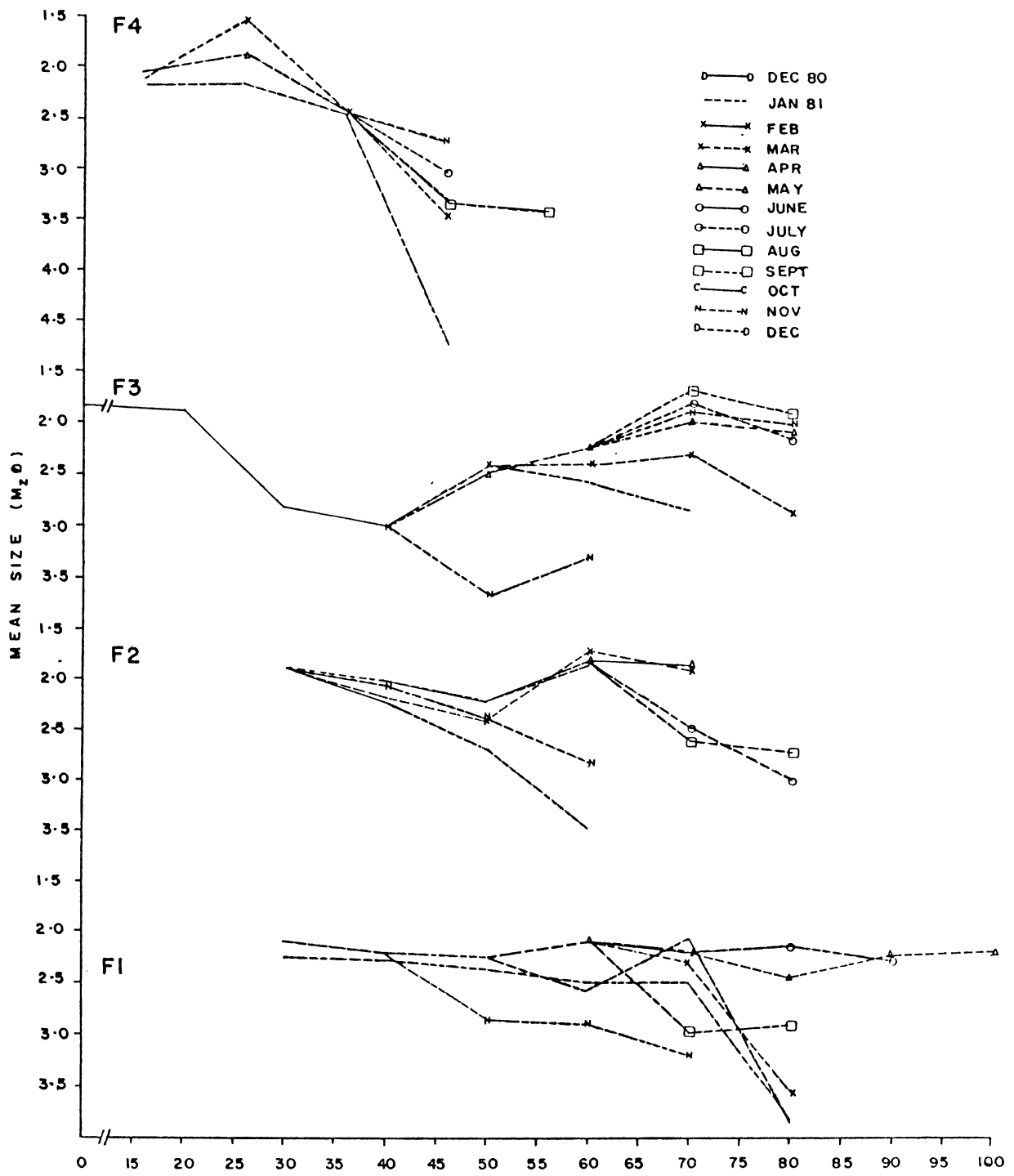


FIG.3.1c Monthly variation of mean grain size distribution along profiles at Fort Cochin zone .

then decreases to MLW (70 m). The maximum temporal variation of the grain size occurs at lower foreshore (60 m from R.P) where the coarsest material (1.8 ϕ) occurs during March and finest material (3.5 ϕ) occurs during January.

The mean grain size at F3 shows a decrease from backshore to berm where the sediments are in the medium to very fine sand limits. From berm crest (60 m) to the lower foreshore, the mean grain size increases, except during January and November. From lower foreshore to MLW (100 m), the mean grain size once again decreases. The material in the lower foreshore remains mostly in the medium to fine sand class.

At F4, the mean grain size increases from R.P to the step (at 25 m) and then decreases rapidly towards MLW (50 m). The coarsest material occurs at the step during March (1.55 ϕ ; medium sand) and finest material occurs close to MLW during November (4.7 ϕ ; silt). At the mid-foreshore, the temporal variation of grain size from fine sand to silt occurs close to MLW.

The variation of the standard deviation at F1 (Fig.3.2c) shows that the material remains in the moderately sorted class between backshore and mid-foreshore, whereas in the lower foreshore upto MLW (80 m), the sorting varies between

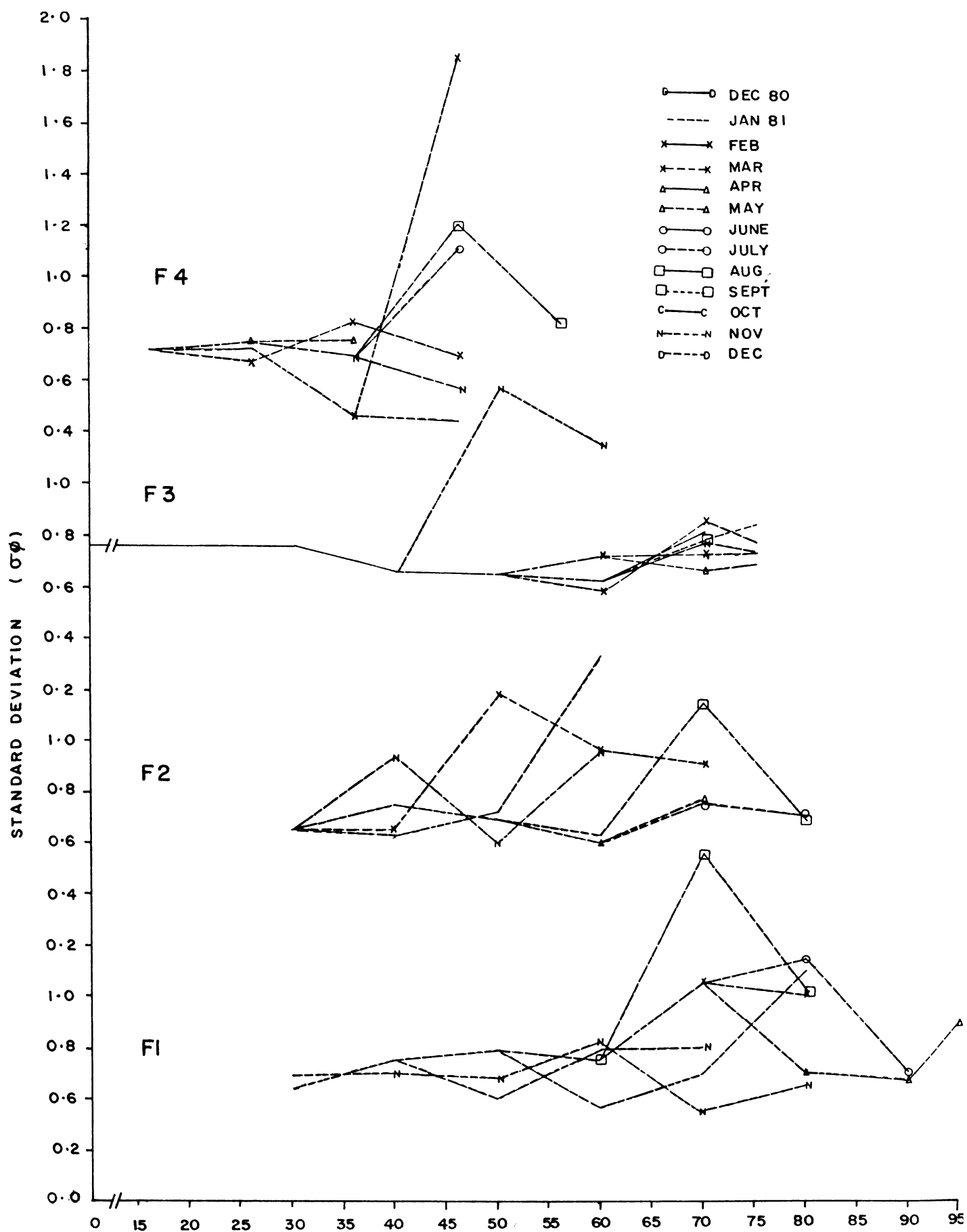


FIG. 3.2c Monthly variation of standard deviation of grain size along profiles at Fort Cochin zone .

moderately to poorly sorted class. In general, the material remains in the moderately sorted class. At F2, standard deviation values show temporal variations right from the berm crest to MLW. The material remains in the moderately sorted to poorly sorted class. The material at F3 remains in the moderately sorted class all through the beach, except during November when poorly sorted material occurs at the upper foreshore. At F4 the sediments are in the moderately sorted class, except during July, September and November when poorly sorted material prevails at the lower foreshore.

In general, the sediment in the Fort Cochin zone is within the medium to fine sand class with moderate sorting.

Zone - Anthakaranazhi

The mean grain size distribution at A1 (Fig.3.1d) shows a decreasing trend in the upper foreshore. The maximum temporal variation of the grain size occurs near MLW (40 - 50 m). The coarsest material belonging to medium sand class (1.3 ϕ) occurs beyond MLW, whereas the finest material (very fine sand) occurs above MLW during December.

At A2, mean grain size shows a decreasing trend from berm crest to upper foreshore, varying from medium sand to fine sand, except during October when fine sand also occurs. From mid-foreshore to MLW, the material is in the fine sand class limit.

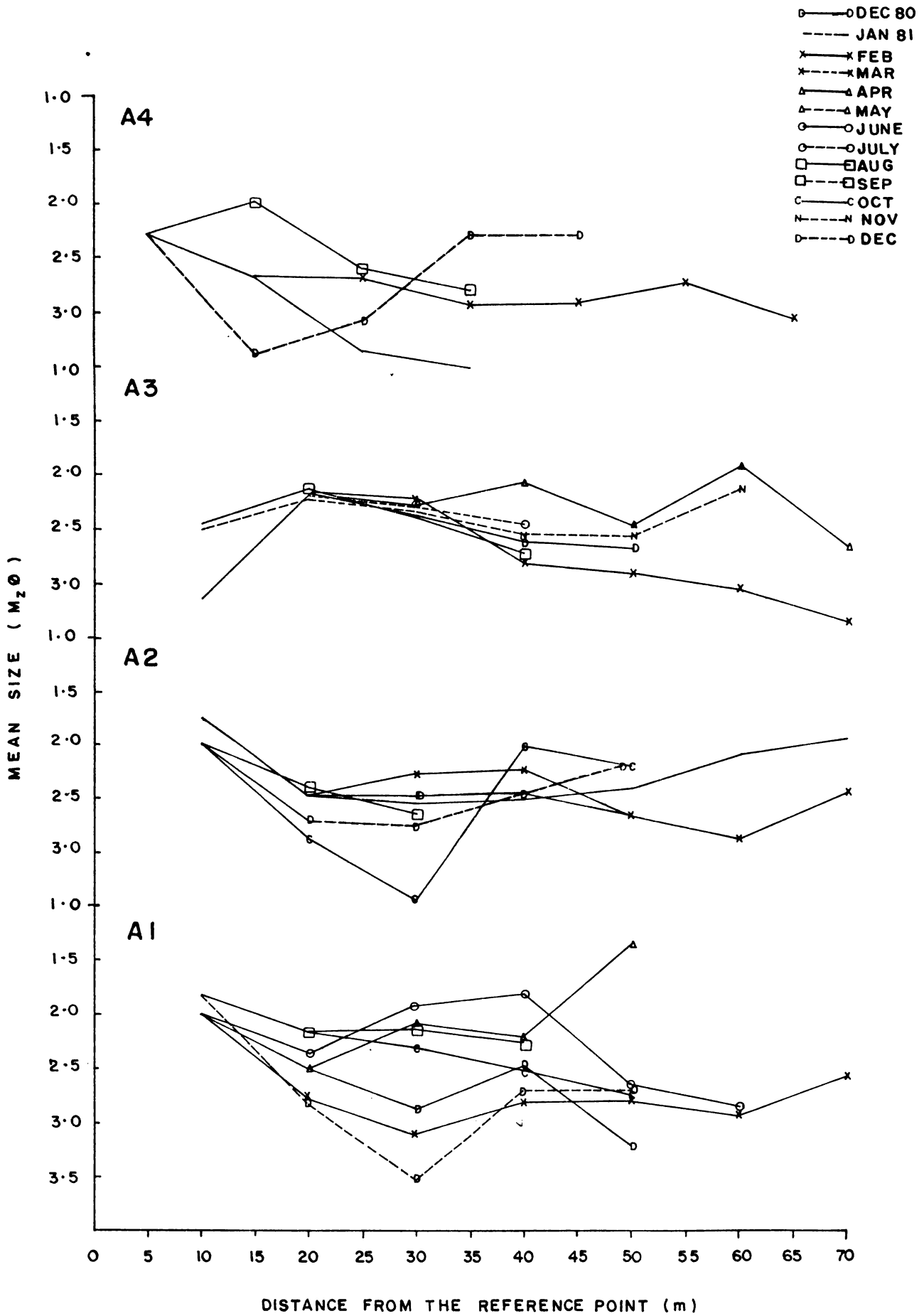


FIG 3.1d Monthly variation of mean grain size distribution along profiles at Anthakaranazhi zone .

The mean grain size at A3, increases from backshore to berm crest and decreases towards MLW (50 m). The temporal variation of grain size is the least in the lower foreshore. Beyond MLW, the temporal variation of grain size becomes more, with the coarsest material (1.9 ϕ ; medium sand) occurring during April, and the finest material (3.4 ϕ ; very fine sand) during February.

At A4, the mean grain size shows greater temporal variation along the entire beach. The coarsest material occurs at the upper foreshore (2.0 ϕ ; medium sand) during August whereas finest material occurs at MLW (3.5 ϕ ; very fine sand) during December. In general, the material remains in the fine to very fine sand class.

The standard deviation of the grain size shows that at A1 (Fig.3.2d) the sediments are in the moderately sorted class upto the lower foreshore. Beyond the MLW the sorting become poor during April and December. At A2 and A3, the material remains in the moderately sorted class except during December, when the sorting becomes poor. At A4, the material always remains in the moderately sorted class.

In general, in the Anthakaranazhi zone, the material is of the fine sand class with moderate sorting.

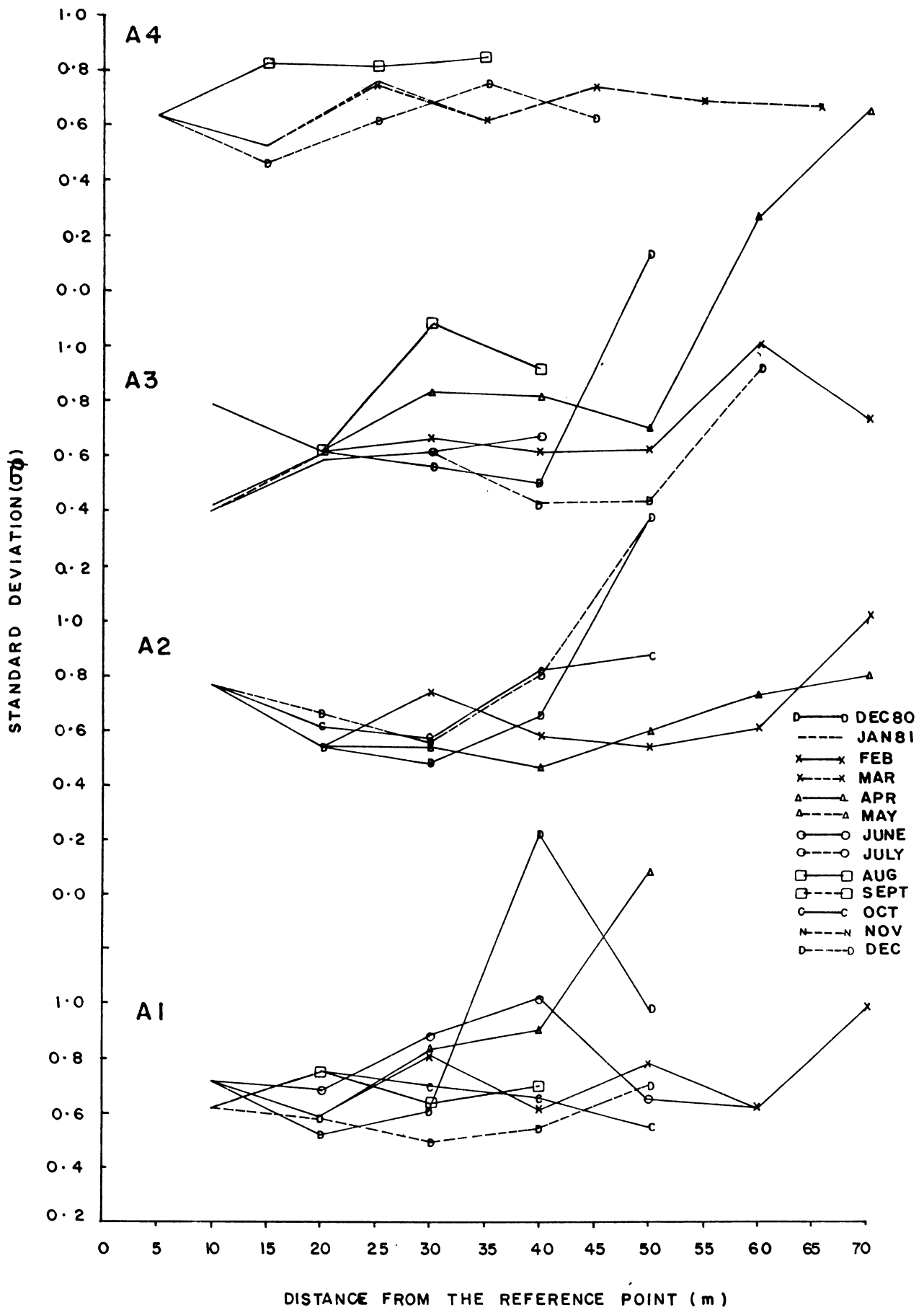


FIG. 3.2 d Monthly variation of standard deviation of grain size along profiles at Anthakaranazhi zone .

The results of the grain size analysis of the beach material of the four zones can be summarized as:

- (1) In any given zone, the sediment distribution does not show any spatial variation.
- (2) The variations are significant between the zones, for example the sediments of Fort Cochin beach are significantly different from those of Narakkal and Malipuram.
- (3) The variations are less conspicuous at Anthakaranazhi zone as compared to those of Fort Cochin zone.
- (4) The beaches at Narakkal and Malipuram exhibit higher concentration of very fine sediments in the silt or clay limits.

CHAPTER 4 : WAVE REFRACTION

4.1. Materials and methods

4.2. Results

4.2.1. Deep water wave climate

4.2.2. Refraction function

4.2.3. Nearshore wave amplification

4.2.4. Direction function

4.2.5. Breaker characteristics

All nearshore processes including beach morphological changes are caused principally by the wave forcing in the surf zone. The changes in geometric form of beaches and their constituent sediments occurring during the period of study have been discussed in the foregoing Chapters. An analysis of the prevailing nearshore wave climate is presented in this Chapter.

Waves have been found to provide necessary energy for the movement of water and attendant sediments within the nearshore zone. They govern the evolution of beaches which act as buffer zones for the impinging wave energy. The shape and size of these deposits, in turn, give rise to changes in the incoming wave energy through changes in the nature of wave breaking. When one considers the changes of this dynamic zone over a long time-scale, the dominating effect of waves in deciding the orientation of this near-elastic and energy absorbing zone becomes evident.

In order to understand the shallow water wave climate, knowledge of the nature of propagation of waves into the shallow region is essential. As the deep water waves approach the coast,

a change in the wave height occurs because of changes in their velocity of propagation. This is known as the shoaling effect. Since the phase velocity is a function of depth in shallow water, when the wave front propagates over the bottom of variable bathymetry, the wave front bends and tries to get aligned to the bottom contours. This is known as the refraction of water waves. Refraction causes convergence and divergence of wave energy along the wave crest. As the wave form finally approach the shore, the wave energy gets dissipated through shoaling, refraction, percolation and breaking. Much of this energy loss occurs due to the frictional effects. A knowledge of the wave field in deep water is a pre-requisite to study the nearshore wave climate.

The wave condition in deep water can be defined by data pertaining to wave field on monthly basis. This data, coupled with the effect of wave refraction over the shallow continental shelves, will provide the required input for the study of processes of sediment motion in the nearshore zone.

4.1. Materials and methods

The deep water wave climate was obtained by statistically analysing the data available in IDWR's on the visual observation reported by ships of opportunity in a 3° square comprising the area under study for the period

1974 - 1980. The frequency percentage of occurrence of wave height, period and direction of approach are presented in the form of rose diagrams and table. Deep water waves propagating shoreward from directions 220° to 300° TN with periods varying from 6 sec to 14 sec are likely to influence the nearshore regions of the coast under study.

Wave refraction diagrams for the above periods and directions of wave approach have been constructed for unit deep water wave height following the method of Arthur et al. (1952) making use of the latest hydrographic chart No.220, published by Naval Hydrographic Office, Dehra Dun. The refraction and direction functions have been calculated at 20 locations, fixed arbitrarily, along the stretch of the coast from Azhikode to Anthakaranazhi (Fig.1.5). These functions provide an index for the relative amplification or reduction of wave heights as the waves approach the coast. The refraction functions have been calculated using the formula (Pierson et al., 1955)

The ratio of shallow water(H) and deep water(H_o) wave heights has been computed following Bretschneider (1966 b)

$$\frac{H}{H_o} = \left[\frac{L_o}{L} \right]^{1/2} \left[\frac{b_o/b}{1 + \frac{4\pi d/L_o}{\sinh \frac{4\pi d}{L_o}}} \right]^{1/2}$$

In the above relations, b_o and b are the distances of separation of wave rays, C_o and C are wave crest speeds, L_o and L are the wave lengths in deep and shallow waters respectively and d is the shallow water depth. When the waves break farther away due to caustics or instabilities, construction of refraction diagrams have been discontinued at those depths. This might give rise to some under estimation of the available wave energy at the final break point.

The height, direction of approach and orientation of breakers with respect to the shoreline have also been presented on a monthly basis.

4.2. Results

4.2.1. Deep water wave climate

A detailed examination of the Table 4.1 and the wave roses (Fig.4.1) indicates that the general direction of

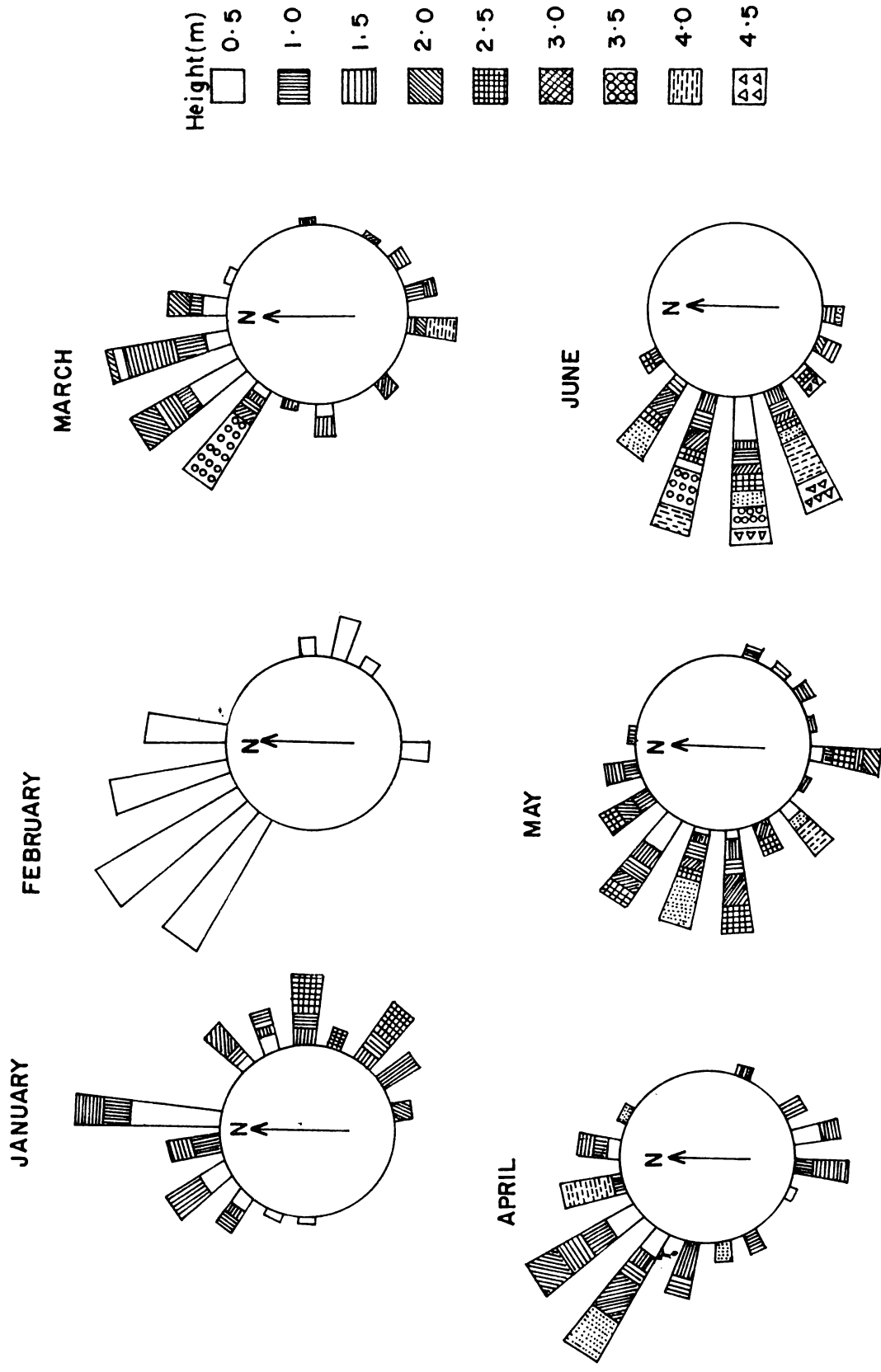


FIG. 4-1 Monthly wave roses showing heights and direction of approach off Cochin .

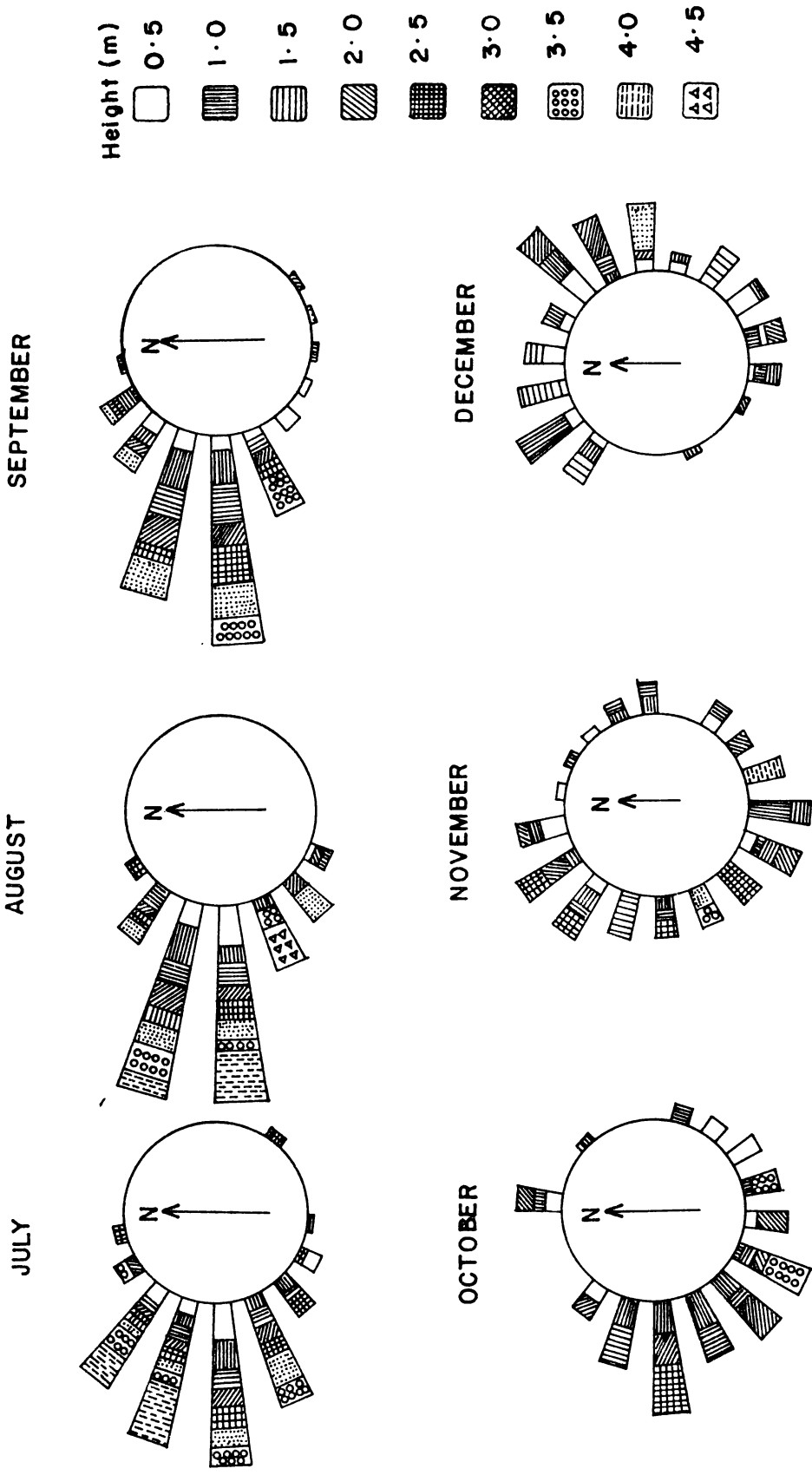


FIG . 4-1 Monthly wave roses showing heights and direction of approach off Cochjin .
(continued)

Table 4.1. Monthly percentage frequency of swell periods
off Cochin

Month	Period (sec.)									
	5	6	7	8	9	10	11	12	13	14
January	43.4	19.7	5.3	2.6	1.3	11.8	2.6	2.6	4.0	6.6
February	53.3	19.5	3.9	3.9	5.2	1.3	-	2.6	6.5	3.9
March	23.3	30.0	6.7	15.0	5.0	3.3	5.0	8.3	-	3.3
April	44.8	20.9	13.4	14.9	1.5	3.0	1.5	-	-	-
May	28.9	23.1	14.4	12.5	1.9	2.9	4.8	3.9	2.9	4.8
June	18.7	28.0	13.1	14.0	5.6	14.9	-	-	1.9	3.7
July	23.7	19.5	19.5	16.1	7.1	5.9	0.9	0.9	2.5	3.4
August	12.4	24.0	23.3	16.3	7.0	7.8	5.4	1.6	1.6	0.8
September	24.8	23.0	20.4	7.1	4.4	6.2	-	1.8	5.3	7.1
October	36.5	22.2	12.7	9.5	9.5	6.4	-	-	-	3.2
November	39.0	12.9	12.9	9.1	2.6	3.9	2.6	1.3	1.3	14.3
December	59.4	21.7	4.4	5.8	-	2.9	-	-	2.9	2.9

approach of deep water waves during January, February and March is from NNW to NW ($300^{\circ} - 350^{\circ}\text{TN}$). During April, a gradual shift in deep water wave direction towards the southern quadrant takes place. During the period May to October, the waves approach from $260^{\circ} - 290^{\circ}\text{TN}$ with increased consistency. During November, a change in direction of approach of waves is indicated and the waves approach mostly from $300^{\circ} - 350^{\circ}\text{TN}$. This feature continues till the end of March.

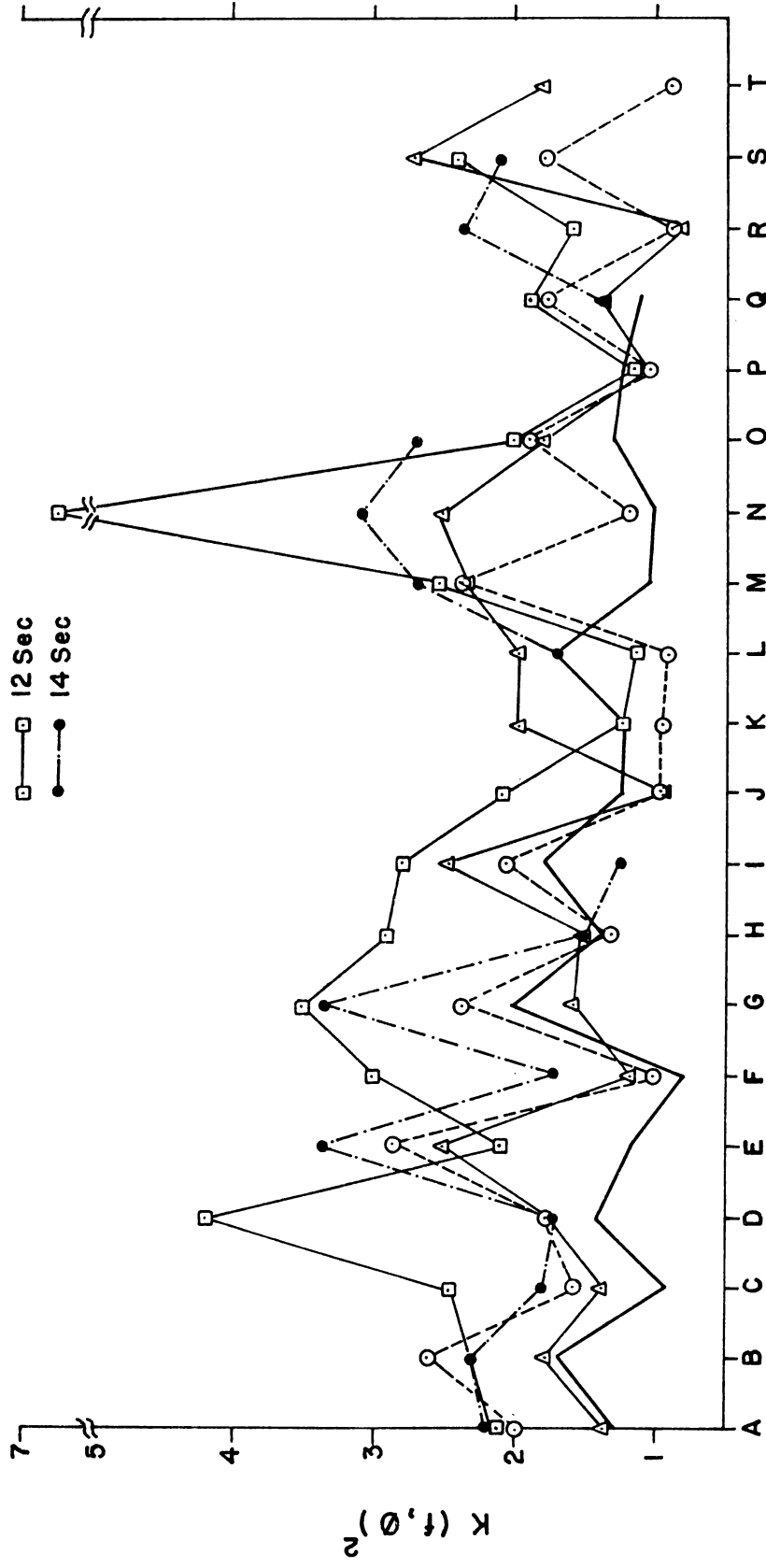
During December to February, the wave heights are generally less than 2 m. By March/April, the waves attain heights as much as 3 to 4 m indicating a growing phase. Between May and September, the wave heights vary from 2 - 3 m and show a further decrease to 1 m by October. During November, a slight increase is seen in the wave height.

4.2.2. Refraction function

The refraction functions for the different directions of approach calculated at all the twenty locations (A to T) are presented in Fig.4.2 a-d. Waves approaching from 220°TN (Fig.4.2a) show convergence and divergence of energy in a similar manner for all periods except for 12 sec, which give rise to convergence at locations C, D and H and divergence at E. For waves approaching the coast from 240° , all periods cause convergence and divergence of energy at

DIRECTION 220° TN

- 6 Sec
- 8 Sec
- △---△ 10 Sec
- 12 Sec
- 14 Sec

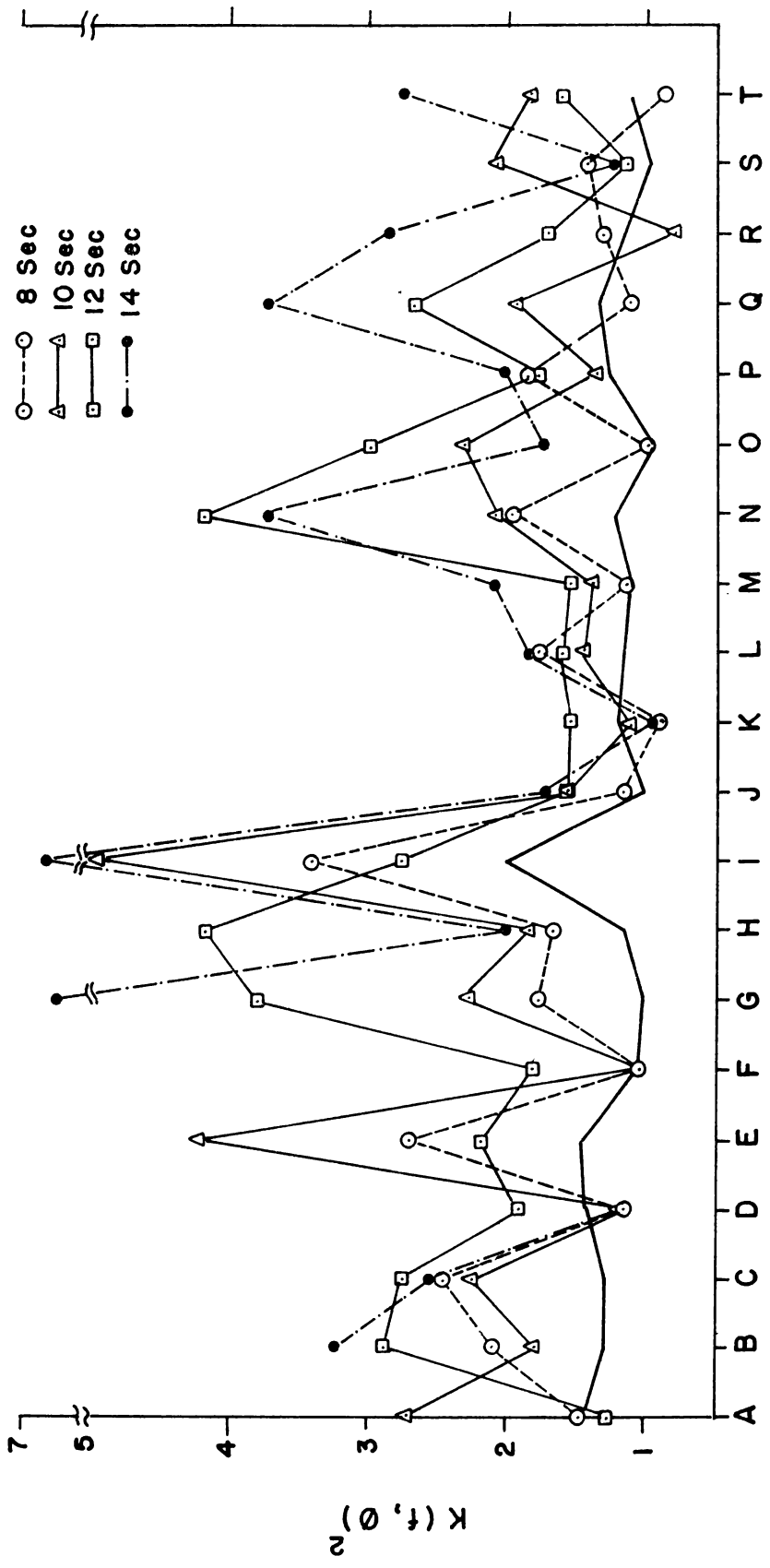


LOCATIONS

FIG. 4.2 a Variation of refraction function along locations A-T for wave approaching from 220° TN

DIRECTION 240° TN

- 6 Sec
- 8 Sec
- △ 10 Sec
- 12 Sec
- 14 Sec



LOCATIONS

FIG. 4-2b Variation of refraction function along locations A-T for wave approaching from 240° TN

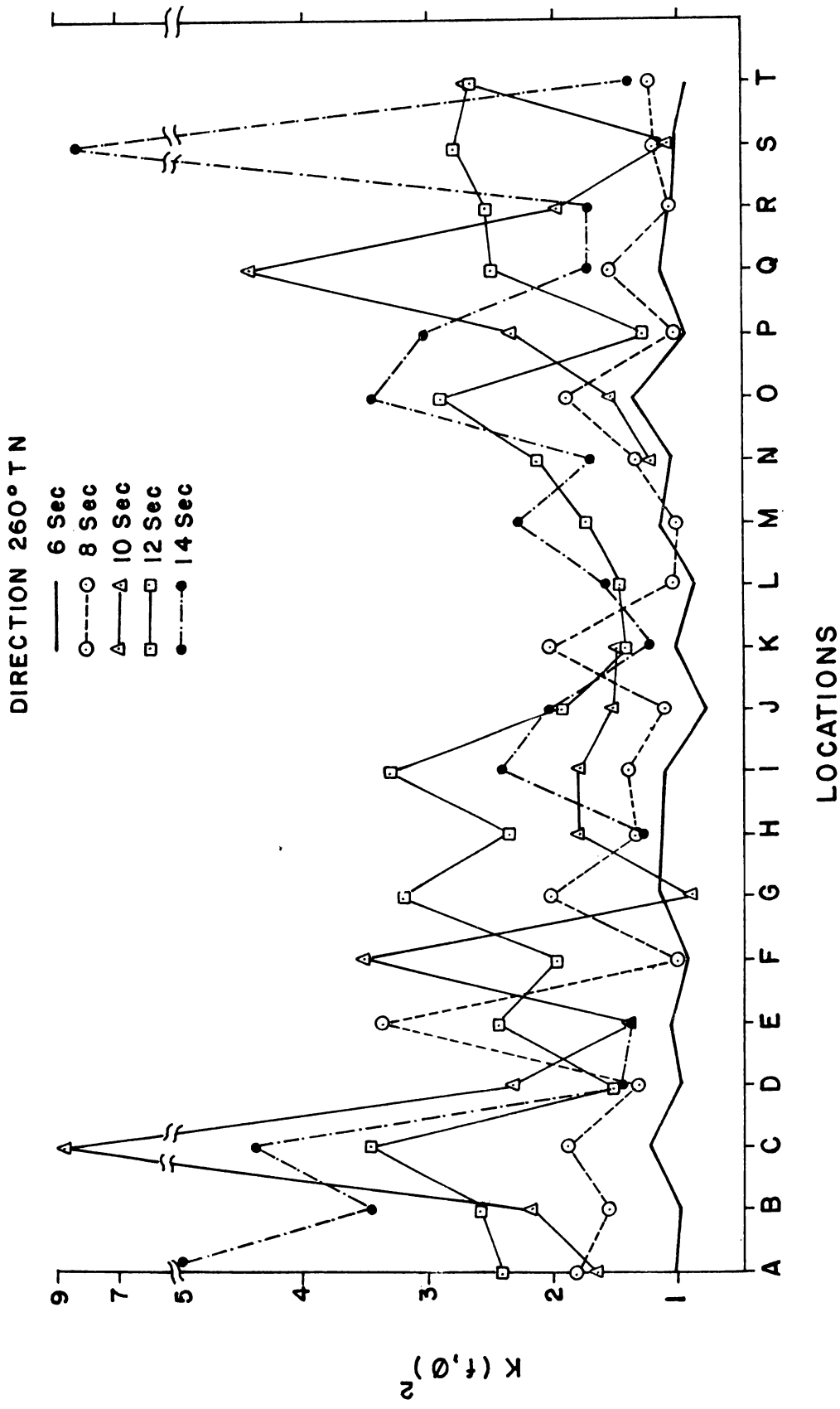


FIG. 4'2c Variation of refraction function along locations A - T for wave approaching from 260° TN

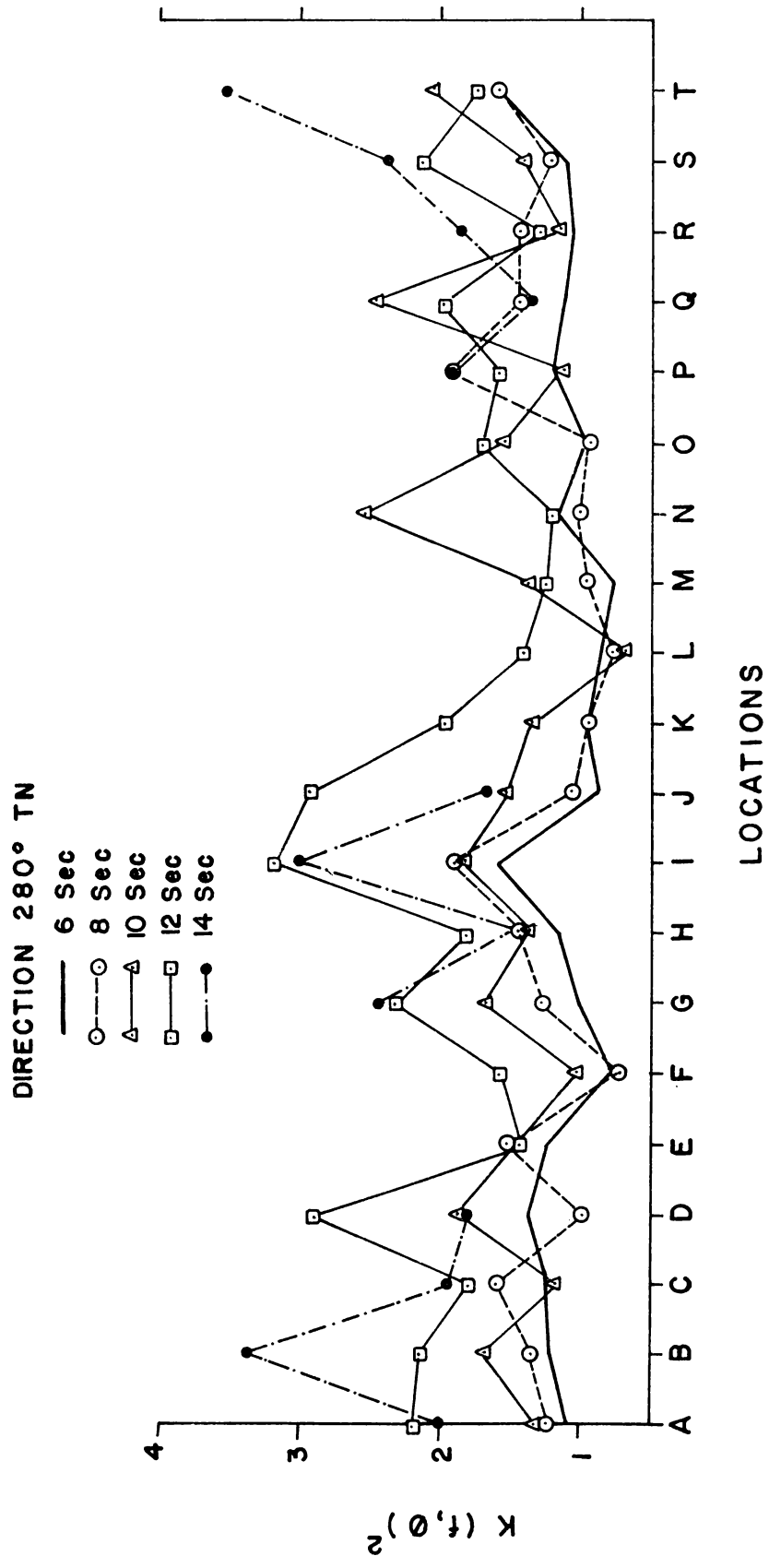
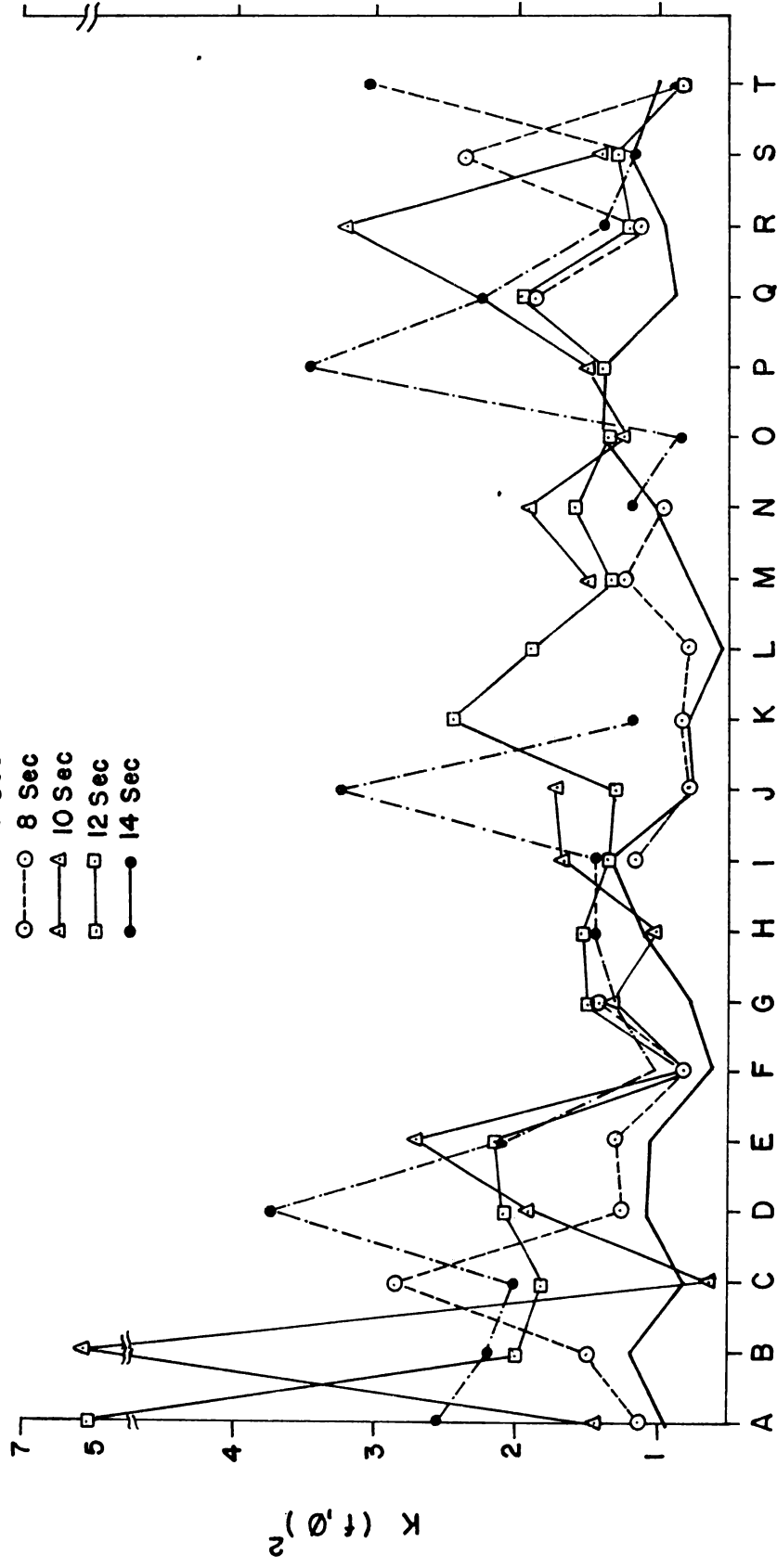


FIG. 4.2d Variation of refraction function along locations A-T for wave approaching from 280° TN

DIRECTION 300°TN

- 6 Sec
- 8 Sec
- △ 10 Sec
- 12 Sec
- 14 Sec



LOCATIONS

FIG. 4-2e Variation of refraction function along locations A-T for wave approaching from 300°TN

same locations (Fig.4.2b). Waves of all period produce strong divergence between locations J and M while strong divergence is caused by waves of 10 and 14 sec at I and by 14 sec waves at G. Waves approaching the coast from 260° (Fig.4.2c) produce stronger convergence on the northern and southern locations while comparatively lower values are encountered along the locations in the middle zone. The refraction functions have comparatively lower values at all locations for all periods when the wave approach is from 280° TN (Fig.4.2d). When the wave approach is from 300° TN (Fig.4.2e), strong convergences are produced by 10 sec and 14 sec waves.

In general, the distribution of refraction function shows wave energy concentration at the extremes of the area of study for waves approaching from 260° , 280° and 300° TN. For waves from 240° , the wave height amplification takes place between location H and L. When waves approach from 260° , which is a near normal direction of approach, the refraction functions present alternating highs and lows. The refraction functions show higher values for waves approaching the coast from southern quadrant than for those approaching from northern quadrant with a general increase in the value with period.

4.2.3. Nearshore wave amplification

Table 4.2 gives the wave height at 2 m contour for unit deep water height for different periods and directions

Table 4.2. Values of $\sqrt{K} = (H/H_0)$ at 2 m isobath for waves of different periods and directions of approach

Direction 220°TN

Locations	Period (sec.)				
	6	8	10	12	14
A	1.15	1.41	1.17	1.46	1.48
B	1.31	1.61	1.51	1.53	1.52
C	0.96	1.26	1.18	1.57	1.34
D	1.19	1.33	1.33	2.05	1.32
E	1.08	1.69	1.58	1.46	1.84
F	0.89	1.01	1.09	1.73	1.32
G	1.43	1.54	1.26	1.87	1.84
H	1.18	1.14	1.25	1.70	1.23
I	1.35	1.43	1.58	1.67	1.13
J	1.12	0.98	0.96	1.45	
K	1.10	0.98	1.42	1.12	
L	1.31	0.96	1.41	1.07	1.31
M	1.03	1.55	1.54	1.60	1.64
N	1.01	1.09	1.59	2.45	1.77
O	1.15	1.38	1.35	1.42	1.65
P	1.11	1.03	1.10	1.08	2.11
Q	1.05	1.34	1.18	1.38	1.22
R		0.93	0.91	1.29	1.55
S		1.34	1.66	1.57	1.46
T		0.95	1.35		

Table 4.2 Continued.

Locations	Direction 240°TN				
	Period (sec.)				
	6	8	10	12	14
A	1.21	1.22	1.66	1.14	
B	1.15	1.45	1.35	1.71	1.80
C	1.15	1.57	1.51	1.66	1.66
D	1.21	1.08	1.11	1.38	1.12
E	1.22	1.65	2.06	1.48	
F	1.04	1.03	1.02	1.35	
G	1.02	1.34	1.52	1.96	2.47
H	1.08	1.29	1.37	2.05	1.41
I	1.43	1.85	2.26	1.66	2.53
J	1.01	1.08	1.25	1.25	1.32
K	1.10	0.96	1.09	1.25	0.99
L	1.08	1.34	1.22	1.28	1.37
M	1.06	1.07	1.18	1.25	1.46
N	1.22	1.40	1.45	2.05	1.94
O	0.98	0.99	1.52	1.73	1.32
P	1.14	1.36	1.17	1.33	1.43
Q	1.16	1.06	1.41	1.64	1.94
R	1.08	1.15	0.90	1.31	1.69
S	0.99	1.19	1.46	1.08	1.12
T	1.05	0.95	1.37	1.27	1.67

Table 4.2 Continued.

Locations	Direction 260°TN				
	Period (sec.)				
	6	8	10	12	14
A	1.03	1.36	1.30	1.56	2.33
B	1.01	1.26	1.47	1.62	1.86
C	1.14	1.38	2.98	1.87	2.11
D	1.01	1.16	1.54	1.25	1.25
E	1.05	1.85	1.17	1.57	1.18
F	0.96	1.01	1.89	1.42	
G	1.09	1.43	0.96	1.80	
H	1.08	1.14	1.37	1.55	1.16
I	1.06	1.19	1.35	1.84	1.56
J	0.89	1.07	1.25	1.39	1.44
K	1.02	1.43	1.23	1.19	1.12
L	0.95	1.03		1.23	1.28
M	1.08	1.01		1.32	1.52
N	1.04	1.16	1.12	1.46	1.31
O	1.18	1.38	1.25	1.71	1.86
P	0.97	1.02	1.54	1.14	1.75
Q	1.08	1.26	2.11	1.58	1.32
R	1.01	1.04	1.41	1.60	1.32
S	1.04	1.11	1.04	1.67	2.95
T	0.96	1.11	1.66	1.64	1.19

Table 4.2 Continued

Locations	Direction 280°TN				
	Period (sec.)				
	6	8	10	12	14
A	1.05	1.12	1.16	1.48	1.43
B	1.11	1.16	1.30	1.46	1.84
C	1.11	1.26	1.09	1.33	1.40
D	1.17	0.99	1.37	1.71	1.34
E	1.11	1.23	1.22	1.20	
F	0.88	0.86	1.02	1.25	
G	1.01	1.14	1.30	1.53	1.56
H	1.08	1.19	1.17	1.35	1.22
I	1.26	1.37	1.37	1.79	1.74
J	0.95	1.03	1.24	1.71	1.29
K	0.99	0.98	1.16	1.41	
L	0.92	0.88	0.84	1.18	
M	0.88	0.99	1.17	1.12	
N	1.08	1.01	1.60	1.11	
O	0.98	0.98	1.25	1.31	
P	1.10	1.39	1.07	1.26	1.37
Q	1.06	1.19	1.57	1.41	1.16
R	1.03	1.19	1.11	1.15	1.36
S	1.06	1.11	1.19	1.46	1.55
T	1.26	1.26	1.45	1.32	1.88

Table 4.2 Continued.

Locations	Direction 300°TN				
	Period (sec.)				
	6	8	10	12	14
A	0.98	1.07	1.21	2.29	1.60
B	1.10	1.23	2.36	1.42	1.49
C	0.91	1.69	0.81	1.35	1.43
D	1.05	1.12	1.39	1.45	1.94
E	1.03	1.14	1.66	1.46	1.46
F	0.79	0.91	0.90	0.89	1.01
G	0.88	1.19	1.15	1.23	1.15
H	1.06		1.01	1.25	1.22
I	1.16	1.08	1.30	1.16	1.20
J	0.86	0.88	1.32	1.15	1.80
K	0.84	0.91		1.57	1.09
L	0.75	0.89		1.38	
M	0.89	1.12	1.23	1.16	
N	1.01	0.99	1.39	1.45	1.09
O	1.07		0.87	1.16	0.93
P	1.07		1.23	1.18	1.86
Q	0.94	1.37	1.51	1.57	1.49
R	0.97	1.07	1.80	1.10	1.18
S	1.10	1.55	1.19	1.15	1.09
T	0.99	0.89	0.89	0.93	1.75

of approach. Waves of periods 6 and 8 sec approaching from 280° and 300° TN, show reduction in wave height at 2 m contour between locations F and M. For all other wave periods and directions of approach, amplification of deep water wave height is indicated. In general, the amplifications in wave height is more for waves approaching from 220° , 240° and 260° compared to waves approaching from 280° and 300° along many parts of the shore under study. It is also seen that for some locations, the wave heights have been amplified 2 to 3 times the deep water wave height. But these waves experiencing greater amplification might result in breaking before reaching 2 m isobath through instabilities or caustics. Following the limiting wave height $H_b = 0.83d$ (Longuet-Higgins, 1972), the maximum height of the waves at 2 m isobath could be only 1.66 m. Thus waves exceeding this limit would collapse prior to reaching the shore and subsequently expend the energy over a wide nearshore zone through spilling or multiple breakers. For 6 and 8 sec period waves, the nearshore wave heights are less than the limiting wave height of 1.66 m at 2 m isobath. For higher periods, the wave height exceeds this optimum value at most of the locations.

4.2.4. Direction function

The angle θ made by the wave ray with the normal to the 2 m isobath gives an idea about the direction of longshore

currents generated due to oblique approach of waves to the shoreline. Angle measured towards north and south of the normal to the 2 m depth contour are indicated in Table 4.3 with negative(-) and positive(+) signs respectively. Zero indicates normal approach.

Comparatively larger angles are indicated for 6 sec period waves approaching from both the northern and southern quadrants. Waves approaching from 260° , which is a near-normal approach, shows smaller angles. In general, there is a decrease in the direction function with increasing periods.

4.2.5. Breaker characteristics

Breaker heights, periods and the angles of breaking observed at all the locations along the four zones are presented in Table 4.4 a-d. These observations at N1, N2 and N3 along the Narakkal zone indicate breaker heights of 0.2 to 0.3 m except during southwest monsoon period when practically negligible or calm conditions prevail at N2 and N3. The predominant breaker periods are found to be 8 to 12 sec in this zone. The breaker heights observed along Malipuram zone varied from 0.1 to 0.2 m. During southwest monsoon period, calm conditions prevail along this zone. Along the Fort Cochin zone, during southwest monsoon season more or less calm conditions prevailed at F2, F3 and F4. Along the Anthakaranazh

Table 4.3. Direction function (θ) for different periods and directions of approach along locations A to T

Period 6 sec.					
Locations	Direction (degrees TN)				
	220	240	260	280	300
A	15	2	-8	-20	-29
B	20	-4	-7	23	30
C	-20	-7	-4	21	-32
D	-21	-6	2	21	30
E	-21	10	1	-16	-21
F	-21	7	-1	-11	-23
G	14	2	8	24	30
H	-17	-4	7	22	32
I	-22	11	-3	22	32
J	-24	14	-4	-8	-24
K	-23	-10	1	13	24
L	23	13	0	-10	-18
M	21	7	3	-18	25
N	-25	-12	-2	17	26
O	26	14	0	-15	24
P	-25	-13	0	13	-24
Q	-25	13	1	-12	-22
R		13	-1	-13	20
S		-15	3	11	20
T		-14	-1	11	-27

Table 4.3. Continued.

Period 8 sec.					
Locations	Direction (degrees TN)				
	220	240	260	280	300
A	7	0	-12	-19	-22
B	15	3	- 8	20	27
C	-15	2	8	19	26
D	12	- 5	- 5	-16	-25
E	19	8	7	12	19
F	-12	- 5	- 3	- 6	-21
G	10	2	12	23	28
H	-14	0	-11	22	27
I	23	7	8	20	-24
J	-14	-15	- 3	-12	- 9
K	-15	- 9	2	-10	13
L	-19	7	- 1	- 2	-11
M	13	- 3	- 6	12	21
N	-17	6	6	9	-22
O	17	- 7	2	-10	-18
P	-18	7	- 4	8	21
Q	19	-11	1	- 8	17
R	-14	5	- 1	-11	-19
S	20	9	- 2	- 9	-14
T	-14	- 6	4	15	-21

Table 4.3. Continued.

Period 10 sec.					
Locations	Direction (degrees TN)				
	220	240	260	280	300
A	10	0	-11	-19	-22
B	9	9	8	15	19
C	- 9	-11	6	-16	
D	13	7	2	13	18
E	15	- 3	- 3	- 8	17
F	- 8	11	1	-18	
G	1	-14	-30	19	7
H	- 9	7	9	-16	-36
I	6	- 5	-17	13	26
J	- 6	-30	-35	- 1	41
K	13	4	- 4	- 1	-22
L	-13	0	- 4	- 1	-15
M	8	22	- 7	11	30
N	-11	4	-11	11	25
O	12	-15	7	-11	
P	-15	8	4	- 8	30
Q	14	-16	3	5	19
R	-10		- 4	-10	26
S	13	6	0	6	20
T	-12	-10	1	10	

Table 4.3. Continued.

Period 12 sec.					
Locations	Direction (degrees N)				
	220	240	260	280	300
A	5	1	-12	-10	-29
B	8	- 4	4	-11	-15
C	12	- 7	2	- 9	-14
D	11	5	- 1	7	11
E	-15	- 8	1	- 2	9
F	7	5	1	1	-18
G	4	1	11	17	21
H	- 9	2	- 3	-13	18
I	-17	-11	2	8	- 9
J	-20	-10	- 9	7	0
K	-10	8	- 4	- 1	5
L	- 9	- 8	4	1	- 4
M	9	6	3	- 7	- 8
N	11	5	3	- 8	10
O	14	- 8	0	5	- 7
P	-14	7	- 1	- 4	11
Q	15	-11	2	2	8
R	-13	- 8	3	- 6	- 5
S	14	9	2	4	10
T		5	- 1	- 7	10

Table 4.3. Continued.

Period 14 sec.					
Locations	Direction (degrees TN)				
	220	240	260	280	300
A	3	0	- 5	-13	-25
B	13	- 3	- 5	11	18
C	-18	- 5	5	-11	-12
D	12	5	- 1	- 6	13
E	-18	7	- 2	4	- 7
F	-18	- 2	1	8	- 7
G	5	- 3	-15	17	26
H	-11	3	- 5	-12	26
I	-18	- 9	2	6	-11
J	-23	13	-12	- 2	2
K	-13	- 6	- 6	5	- 2
L	11	- 8	4	- 1	- 2
M	6	2	3	- 7	-12
N	10	3	- 4	- 7	10
O	-12	5	3	- 6	-10
P	13	- 7	0	3	8
Q	-14	7	- 4	- 1	- 6
R	18	- 6	1	3	- 6
S	-11	7	3	5	-10
T		4	0	8	11

+ angle measured towards south

- angle measured towards north

Table 4.4a. Observed breaker characteristics at Narakkal

Month	LOCATION N1				LOCATION N2				LOCATION N3			
	Height (cm)	Period (sec)	Angle (deg)	Breaker	Height (cm)	Period (sec)	Angle (deg)	Breaker	Height (cm)	Period (sec)	Angle (deg)	Breaker
Nov. 1980	30	10	15		30	10	20		50	10	20	
Dec.	20	10	10		20	10	10		20	10	10	
Jan. 1981	20	10	-15		20	11	-15		20	10	-15	
Feb.	20	8	-5		20	8	-5		20	8		
Mar.	40	8	-10		40	8	-10		35	8	-15	
Apr.	20	12	-10		20	12	-10					
May	0				0				0			
Jun.	20	8	10		0				0			
Jul.	20	12	-5		20	12	-5		20	12	-5	
Aug.	10	15			10	15			10	15		
Sep.	20	9	-10		20	9	-10		20	8	-5	
Oct.	15	10	-10		20	10	-10		10	10	-10	
Nov.	35	10	5		35	10	-5		40	10	5	
Dec.	10	10	-12		10	10	-10		10	10	-10	
Jan. 1982	30	10	-10		30	10	-10		30	10	-10	
Feb.	45	8	-10		45	8	-10		40	8	-10	

+ waves from south

- waves from north

Table 4.4b. Observed breaker characteristics at Malipuram

Month	LOCATION M1			LOCATION M2			LOCATION M3			LOCATION M4		
	Breaker	Height (cm)	Angle (deg)									
Oct. 1980		10		13	- 5	10	13	- 5	10	13	- 5	
Nov.	10	13	15	13	15	15	13	12	15	13	10	10
Dec.	10	12	10	12	12	10	13	13	10	13	10	10
Jan. 1981	15	11	-10	10	-12	10	10	-10	10	11	-10	
Feb.	10	10	-10	9	-10	10	10	-15	15	9	-10	
Mar.	15	9	- 5	9	- 7	15	10	- 5	20	10	- 5	
Apr.	10	11	- 5	0	0	0	10	-12	10	0	- 5	
May	0	0		0	10	10	10	10	10	0		
Jun.	0	0		0	10	10	10		10	10		
Jul.	0	0		0	0	0	15	- 5	15	15	- 5	
Aug.	10	10	- 5	15	- 5	10	8	10	20	8	10	
Sep.	20	8	-10	8	- 5	10	11	- 5	10	11	10	
Oct.	30	11	-10	11	- 5	20	13	-10	15	12	-10	
Nov.	25	12	-10	13	-10	15	11	-10	10	12	-10	
Dec.	10	11	- 5	11	-15	10	11	-10	10	11	- 5	
Jan. 1982	15	11	- 5	10	- 5	15	10	-10	15	10	- 5	
Feb.	15	9	-10	9	-10	20	9	-15	20	9	-12	

+ waves from south

- waves from north

Table 4.4c. Observed breaker characteristics at Fort Cochin

Month	LOCATION F1		LOCATION F2		LOCATION F3		LOCATION F4		
	Breaker	Breaker	Breaker	Breaker	Breaker	Breaker	Breaker	Breaker	
	Height (cm)	Period (sec)	Angle (deg)	Height (cm)	Period (sec)	Angle (deg)	Height (cm)	Period (sec)	Angle (deg)
Nov. 1980	75	10	- 5	80	10	-10	65	10	-10
Dec.	65	10	- 8	65	10	-10	45	10	- 8
Jan. 1981	95	9	- 5	80	9	-15	85	10	-15
Feb.	75	10	-10	55	10	-10	35	10	-10
Mar.	45	9	-15	45	9	-10	20	9	-15
Apr.	65	10	-10	100	10	- 5	90	10	-15
May	65	8,9	-10	70	9	-10	40	8,9	- 5
Jun.	25	6,7	- 5	0			10	6	- 5
Jul.	30	5,6	-10	0			10	6	-10
Aug.	30	7	-10	0			0		
Sep.	50	8	-10	50	7,8	-10	40	8	-15
Oct.	45	8	-15	45	8	-10	0		
Nov.	20	8,10	-15	25	8,10	-10	20	8	-10
Dec.	65	9	-10	50	9	-10	50	9	- 8
Jan. 1982	80	10	- 5	75	10	- 5	55	9	-10
Feb.	80	10	-10	70	10	-10	45	10	-10

+ waves from south

- waves from north

Table 4.4d. Observed breaker characteristics at Anthakaranazhi

Month	LOCATION A1			LOCATION A2			LOCATION A3			LOCATION A4		
	Breaker	Angle (deg)	Height (cm)									
Nov. 1980	10	0	85	10	0	85	10	-5	85	10	-5	85
Dec.	10	-5	85	10	-5	85	10	-5	90	10	-5	90
Jan. 1981	10	0	40	10	-5	55	10	0	55	10	0	55
Feb.	10	0	80	10	0	80	10	0	80	10	0	80
Mar.	9	-12	100	9	-10	100	9	-15	80	9	-10	80
Apr.	10,11	0	125	10	0	120	10	-5	125	10	-5	125
May	8	10	150	8	10	150	8	10	150	8	-5	150
Jun.	5,6	-5	210	5,6	-5	225	5,6	-5	250	5,6	-5	250
Jul.	6,7	-5	235	6,7	-5	225	5,7	10	225	6,7	10	225
Aug.	7	-10	80	7	-10	80	7	5	80	7	10	80
Sep.	8	-5	160	8	-5	175	8	0	175	8	-5	175
Oct.	10	-5	50	10	-5	40	10	-5	40	10	-5	40
Nov.	10	-5	100	10	-5	100	10	-5	100	10	-5	100
Dec.	11	-5	125	11	-5	100	11	-5	100	11	-5	100
Jan. 1982	10	-5	50	10	-5	55	10	-5	60	10	-5	60
Feb.	8,10	-5	75	8,10	0	70	10	0	70	8,10	0	70

+ waves from south

- waves from north

zone, the breaker height varied from 0.40 m during non-monsoon months to 2.5 m during southwest monsoon season. The breaker angles showed much lesser values along this zone compared to other zones.

CHAPTER 5 : NEARSHORE CIRCULATION

	<u>Page</u>
5.1. Materials and methods	65
5.2. Results	66
5.2.1. Cellular circulation	66
5.2.2. Bottom orbital velocity	68
5.2.3. Observed longshore currents	70

The observed sediment characteristics and their temporal changes during the period of observation have been presented in Chapter 3. The wave forcing which causes sediment movement has been analysed in the light of nearshore wave climate and presented in Chapter 4. Before analysing the movement of these sediments in the surf zone, the flow pattern induced by the incoming wave field along this stretch of the coast is described in this Chapter.

Waves arriving from the offshore areas transport momentum from offshore sources to the nearshore areas. When waves attain a height comparable to water depth at any point in shallow zone, they break forming a surf zone where forces needed to resist the incoming flux of momentum are established. Two types of forces could be distinguished associated with waves. They are the wave set-up and bottom shear. The former evolves as a change in the time average of water surface elevation while the latter is the drag felt by a steady current over the bottom. When the waves break

at an angle to the shoreline a steady alongshore current may be induced which would balance the bottom shear force. If this bottom shear force is sufficiently strong and if sea bottom behaves similar to a movable bed, water will erode the sediment off the bottom and transport them to calmer areas for subsequent deposition. This causes a change in the structural configuration. In these cases, it is the sediment that receives the momentum. Once a particle is entrained by the shear force, the vertical distance to which the sediment would get elevated depends upon the lift force originating from the rotational behaviour of the grains of sediments, the size of the vortex and rate of dissipation of energy in the turbulent portion of the boundary layer. Subsequent dispersal of the sediment is related to the impinging fluid forces.

Within the surf zone, the swash and backwash transfer the sediments up and down the beach face, more so, in a zig-zag manner and alongshore. These flows are very translatory in character and hence, make any extrapolation for the entire stretch of the beach very difficult.

Realising the complexities in describing the flow field in the surf zone with a sufficient degree of accuracy, several researchers obtained different quantitative measures of field

of motion in relation to the breaker characteristics (Galvin, 1972). For example, several of the theories proposed for longshore currents are based on the concept of radiation stress (Longuet-Higgins, 1970a and 1970b; Thornton, 1971). The observed cellular circulations have been found to depend on the longshore gradients in wave set-up as demonstrated by Bowen (1969b). These longshore variations in wave height and wave set-up could be due to wave refraction in shallow waters or the interaction of incoming swell waves with edge waves. This was theoretically and experimentally examined by Bowen and Inman (1969) and the incoming swells have been found to generate standing edge waves with periods equivalent to those of the incoming swell waves. This interaction results in alternate high and low breakers giving rise to regular circulation cells. The importance of topographically forced circulations have been demonstrated by Sonu (1972) and tested through numerical models by Noda (1974). The above studies, experimental or theoretical, have brought out the importance of topography and radiation stresses in the realistic derivation of the complicated field of motion within the surf zone.

In this Chapter an attempt is made to describe the inferred wave induced nearshore circulation.

5.1. Materials and methods

The wave height in the nearshore zone along the stretch under study from a depth of 25 m has been computed from wave refraction diagrams following Bretschneider (1966b) and using the formula

$$H = H_0 \left[\frac{L_0}{L} \right]^{1/2} \left[\frac{b_0/b}{1 + \frac{4\pi d/L_0}{\sinh \frac{4\pi d}{L_0}}} \right]^{1/2}$$

From these wave heights, the orbital velocities associated with the waves close to the lower boundary-layer of the fluid column have been calculated using the relation (Lamb, 1945)

$$U_{\max} = \frac{\pi H}{T} \frac{1}{\sinh \frac{2\pi d}{L}}$$

where U_{\max} is the maximum horizontal component of the orbital velocity, H and L are the wave height and wave length at water depth d , and T is the wave period. These values, which are significant in many ways, especially in the initiation of the movement of sediment grains of a given

size, have been plotted and isolines drawn separately for swell waves approaching the shore from 240, 260, 280 and 300°TN with periods varying from 6 to 12 sec.

The magnitude and direction of longshore currents were measured during field observations by noting the time required for buoyant floats released into the surf zone to cover a specified distance along the coast (about 50 m). This is repeated thrice and the average value is considered as representative of the magnitude of the longshore current.

5.2. Results

5.2.1. Cellular circulation

The wave induced flow field within the surf zone and beyond in the nearshore regions is shown in Fig.5.1 a-e. These flows derived from the energy available at 2 m isobath are deduced from the convergence and divergence of waves as obtained from the refraction diagrams and reflect the nature of the field of motion due to the energy flux across the shore. This will help in understanding the up and down movement of water with its attendant sediments from the region of wave breaking to the beach face.

The distance of 2 m isobath from mean low water varies widely in the area. This gives rise to considerable variations

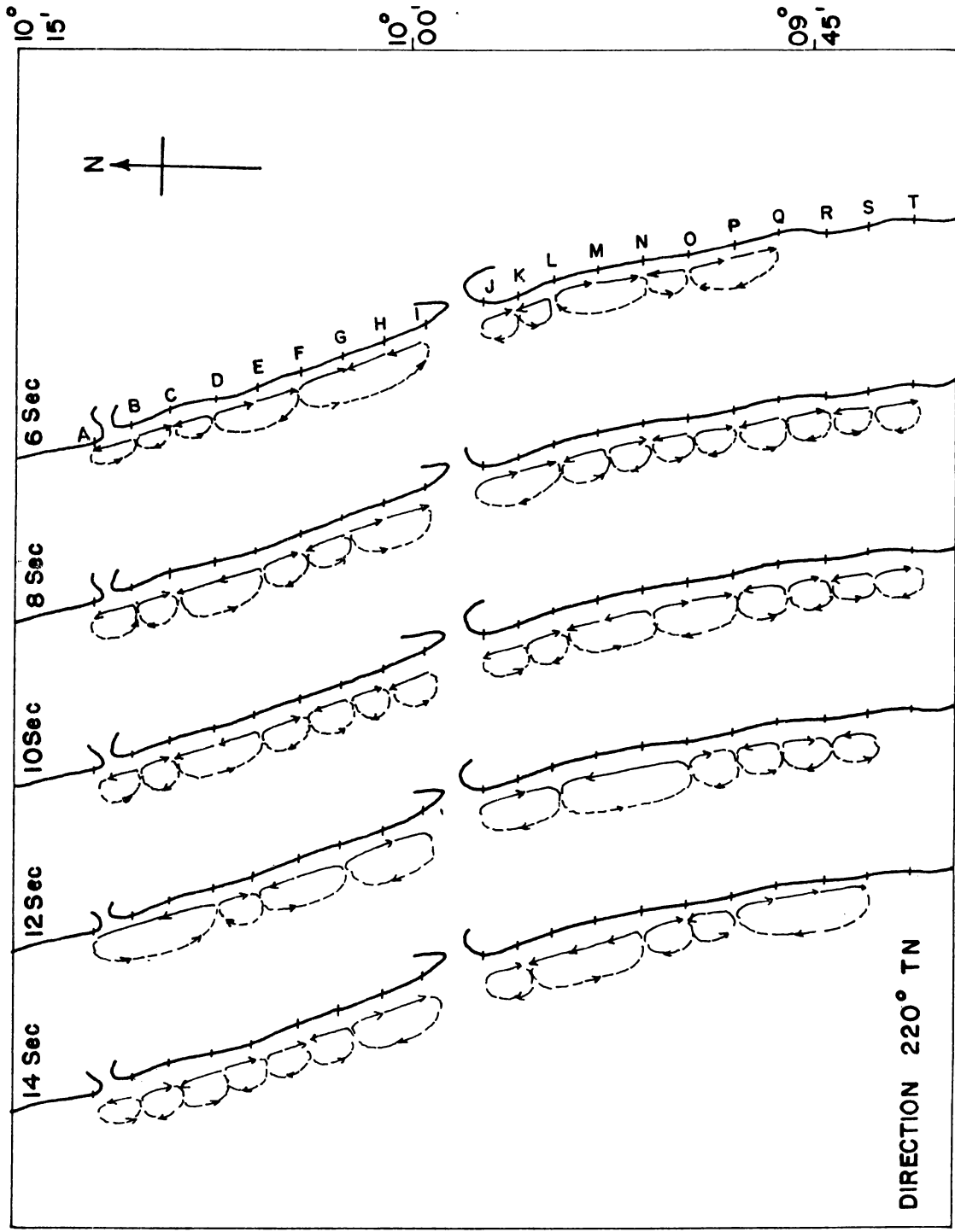


FIG. 5.1 a Cellular circulation associated with wave convergence and divergence

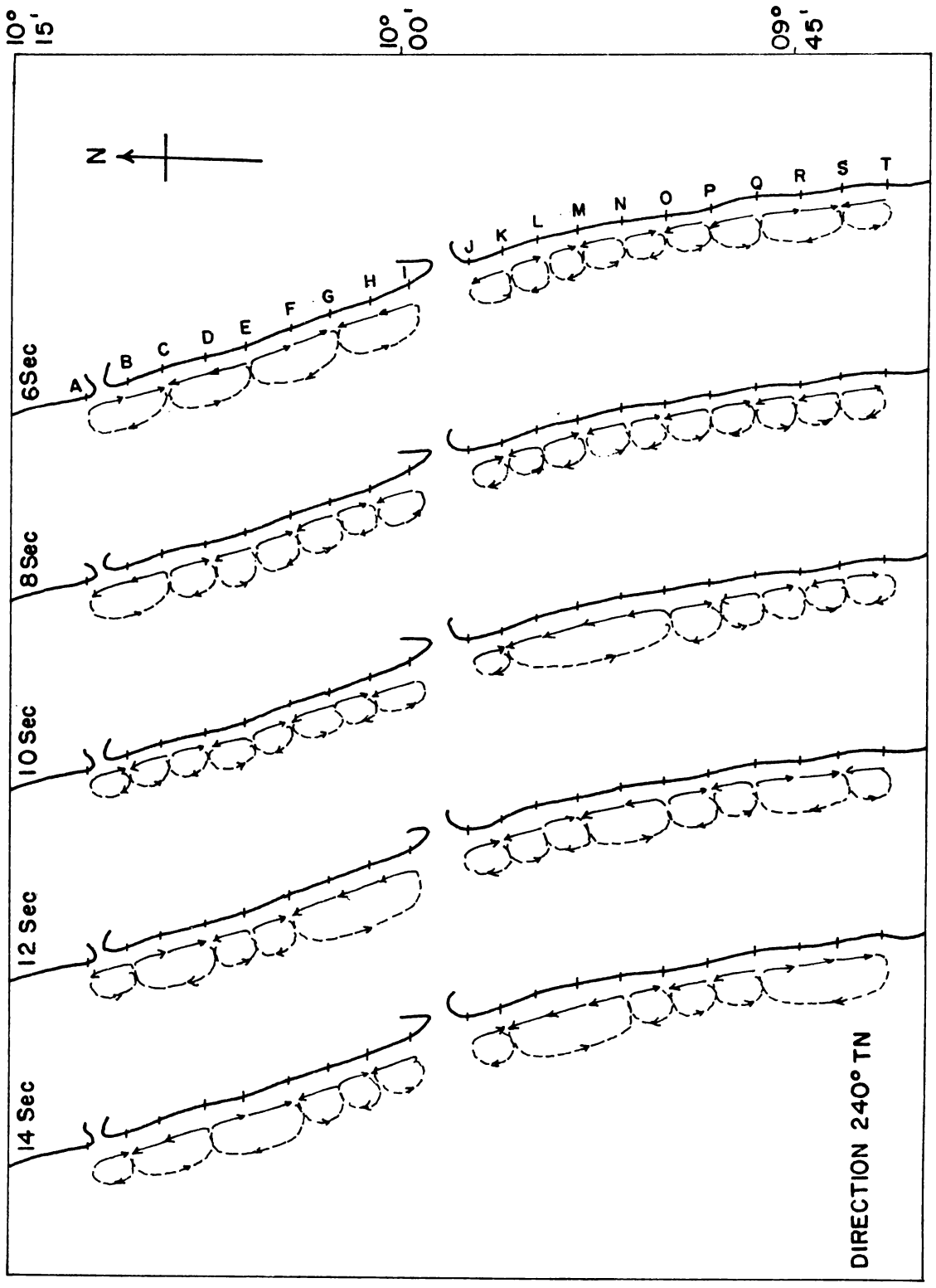


FIG. 5.1b Cellular circulation associated with wave convergence and divergence .

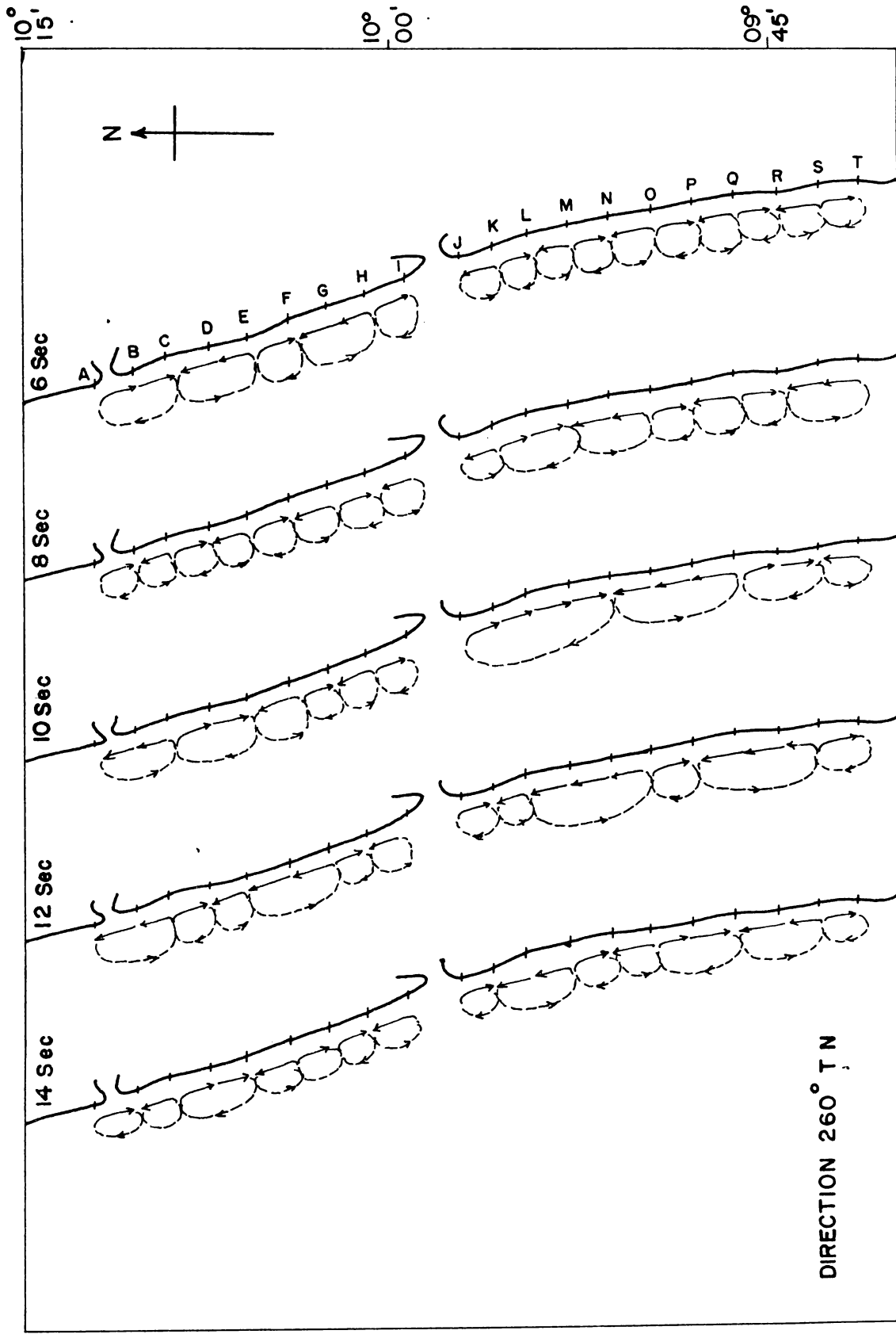


FIG. 5.1c Cellular circulation associated with wave convergence and divergence .

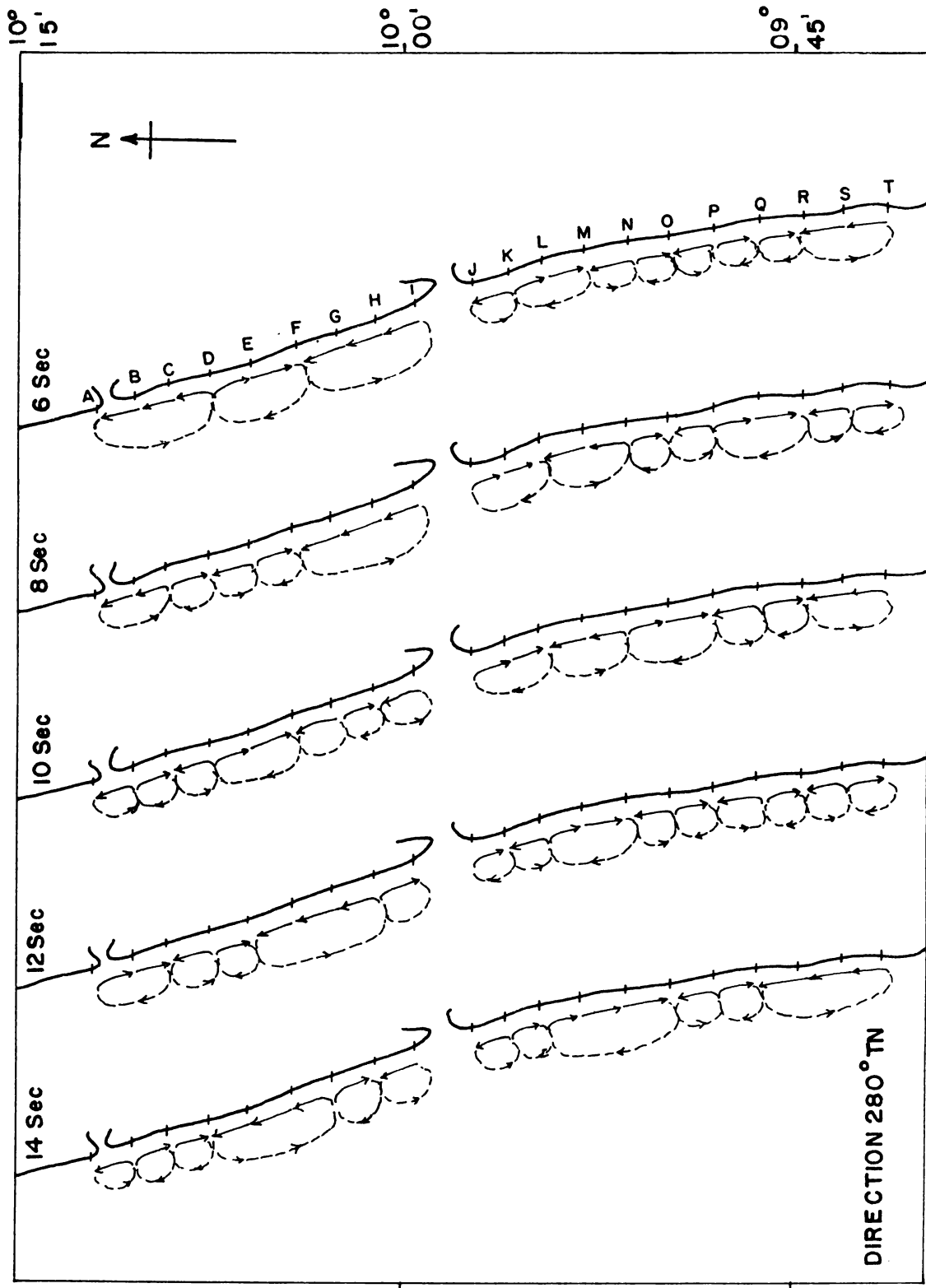


FIG. 5-1d Cellular circulation associated with wave convergence and divergence .

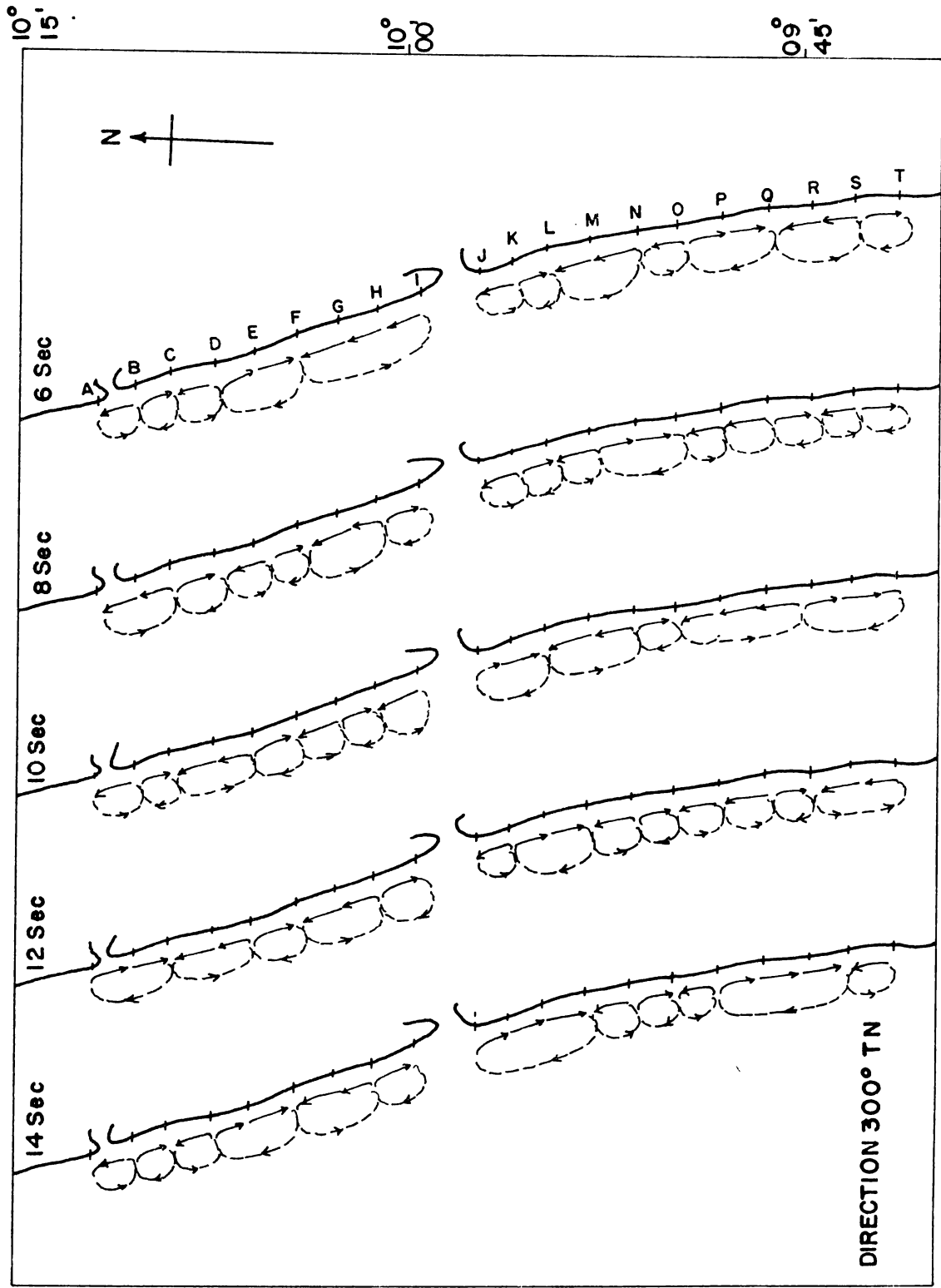


FIG. 5.1e Cellular circulation associated with wave convergence and divergence .

in the width of surf zone assuming that all the incoming waves break at this isobath. The flows deduced from the available energy fluxes at this isobath indicate irregular and non-uniform motion. The flows are directed from the regions of wave convergence to regions of wave divergence. In general, these flows present nearly closed cellular flows, clockwise or anti-clockwise, with large variations in space and time.

The flows associated with waves of 6 sec period approaching the coast from 220°TN indicate larger circulation cells (Fig.5.1a). As the wave period increases from 6 to 10 sec the cells become larger in size and lesser in number. For 12 and 14 sec waves, the cells occupy comparatively larger areas in both northern and southern stretches of the coast.

For waves approaching the coast from 240°TN (Fig.5.1b), larger cells are obtained at the northern stretch of the coast when the wave periods are 6, 12 and 14 sec, while smaller cells appear along the southern stretch (for almost all wave periods) except between K-N (for 10 and 14 sec waves) and between Q-T (for 14 sec waves).

Waves from 260° and 280°TN (Fig.5.1 c and d) generally generate larger cells for most of the periods. This feature is more conspicuous in the southern part for 10 and 12 sec waves (approaching from 260°) and in the northern part for

6 sec waves (approaching from 280°TN). There is a clockwise circulation off Vypeen and anti-clockwise circulation off Fort Cochin associated with 6, 8 and 10 sec waves approaching the coast from 260°TN , while the circulation reverses in its direction when the wave approach changes to 280°TN with periods 12 and 14 sec.

Waves approaching from 300°TN with periods 6 and 12 sec also produce large cells along the northern stretch. Waves of 10 and 14 sec period, produce large cells at the southern stretch (Fig.5.1e). For 14 sec waves, there is anti-clockwise flows off Vypeen and clockwise flow off Fort Cochin.

In general, one notices the flow within this narrow zone to be consisting of cellular flow pattern, both clockwise and anti-clockwise. These cells exhibit significant variations in space and time.

5.2.2. Bottom orbital velocity

The flow pattern presented in Fig.5.2 a-d is based on the computed, instantaneous U_{\max} values and indicates the maximum orbital velocities of the fluid particles inside the bottom boundary-layer of the fluid column from the shore to distances where the water depths are 25 m. The distribution of the J_{\max} values beyond 2 m isobath and upto 25 m provides information

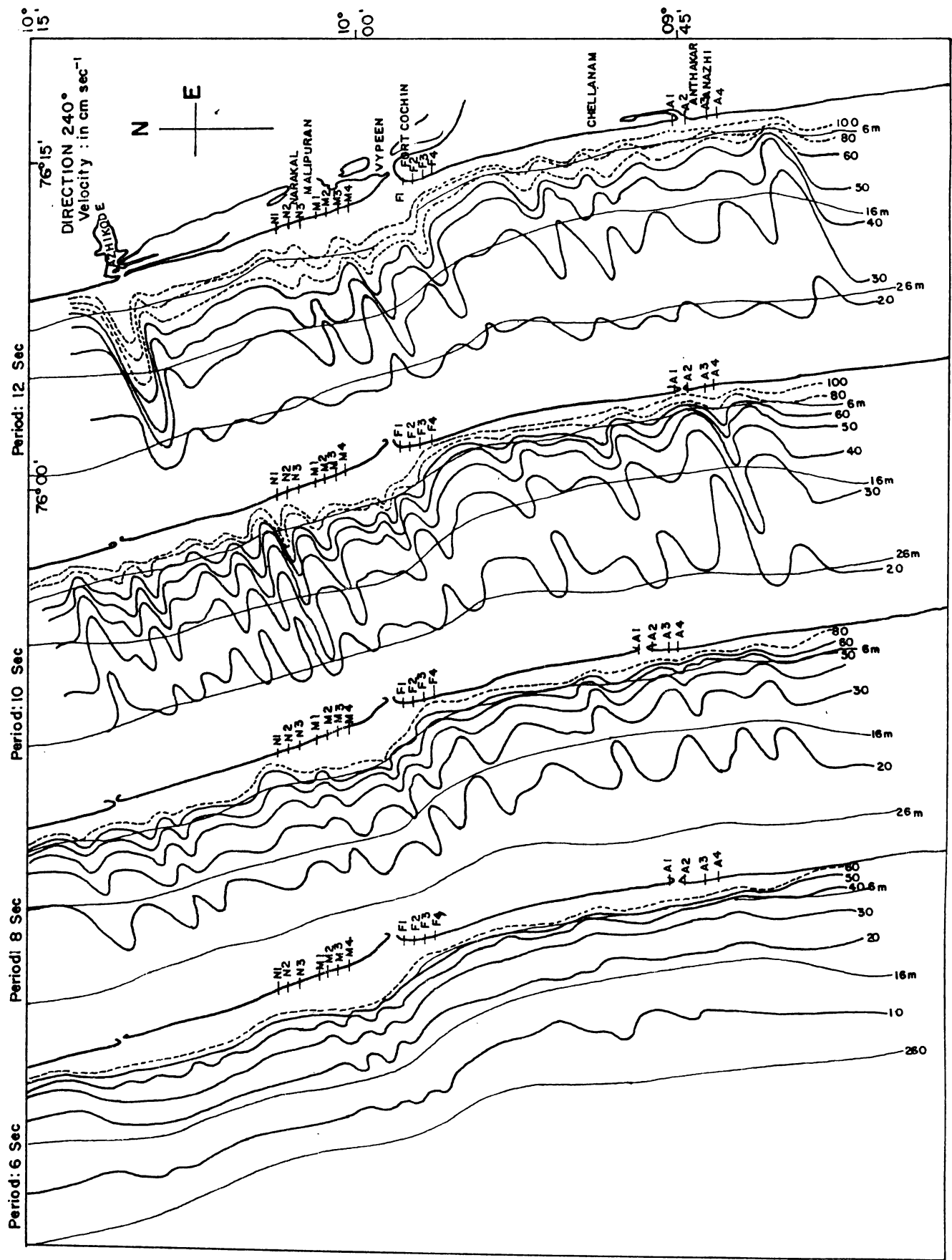


FIG. 5.2 a Distribution of bottom orbital velocity in the near shore zone .

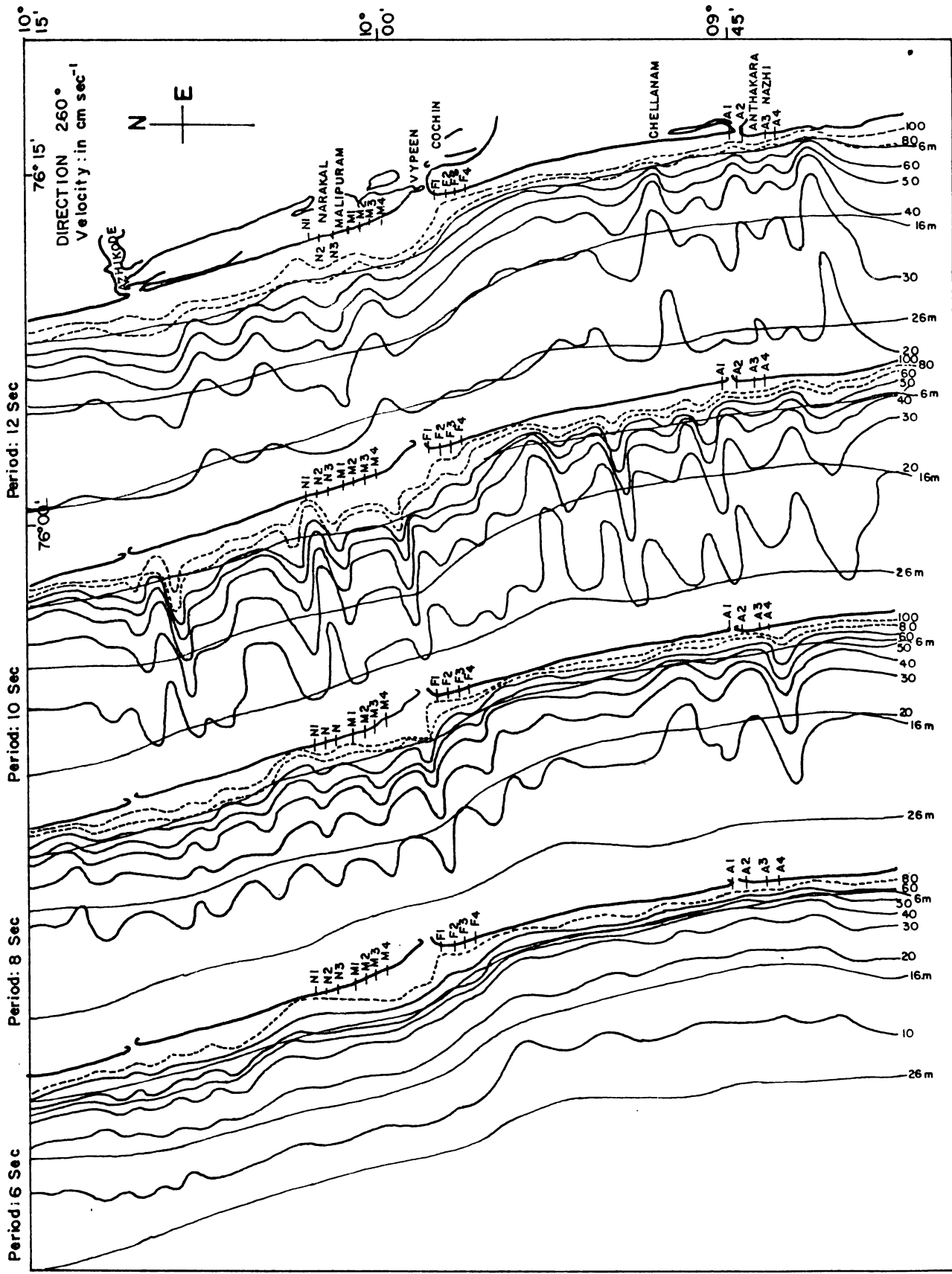


FIG. 5.2 b Distribution of bottom orbital velocity in the near shore zone .

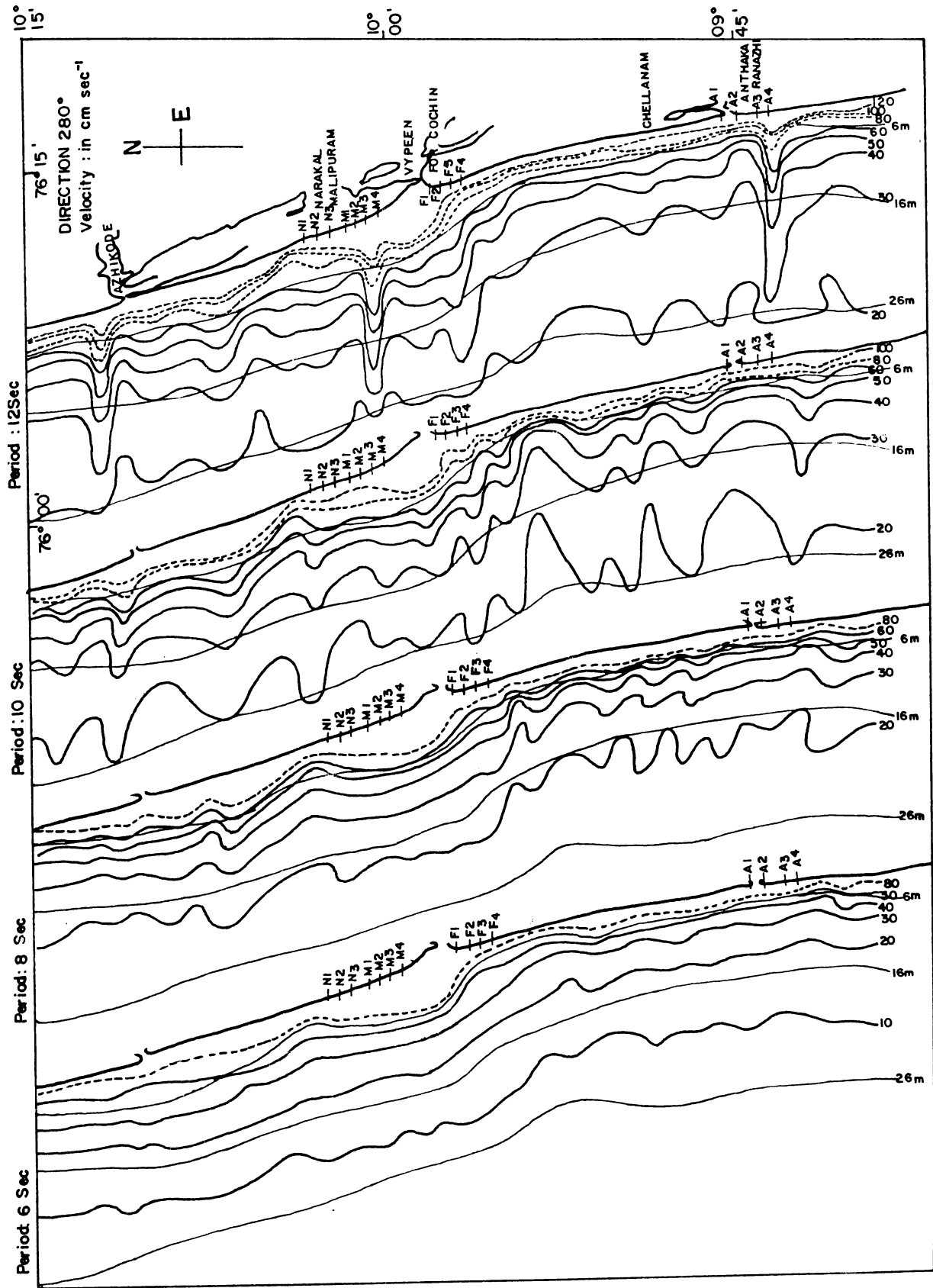


FIG. 5.2c Distribution of bottom orbital velocity in the near shore zone .

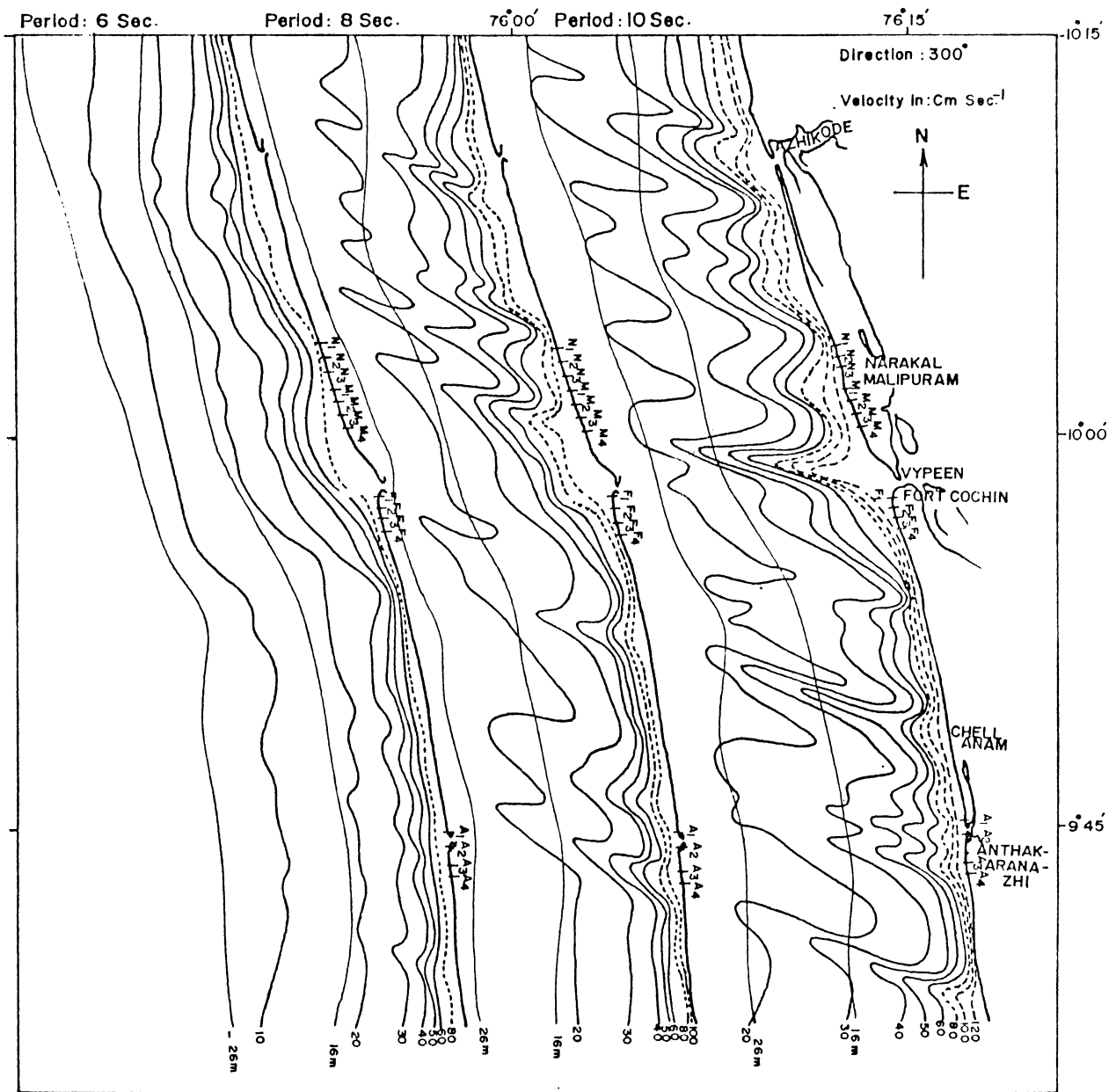


FIG.5.2d Distribution of bottom orbital velocity in the near shore zone .

on the ability of these flows in bringing the bottom sediments into suspension and transporting them by mean flows. These values are valid in the immediate vicinity of the bottom boundary-layer of the fluid column over which the oscillating wave motion occurs.

In general, one finds an increase in U_{\max} values in a shoreward direction and with increasing wave period. The flows appear to be directed more or less parallel to the isobaths in the offshore region especially for waves of lower periods. With an increase in wave period, one observes irregular and meandering flows with widely varying lateral shear. The flows present maximum meandering for waves of 10 sec period for all the deep water directions considered here. In addition, when waves approach from extreme northerly directions (280° and 300°), the axis of the large scale and conspicuous meanders have been observed to make considerable angle with the shoreline (Fig. 5.2 c and d) indicating relatively stronger flows. Considering the lateral shears, one notices flows with clockwise and anti-clockwise rotational tendency. These may give rise to variations in the pressure distributions and would contribute substantially to the non-uniform flows. Broadly, one realises such differential flows on either sides of the Cochin harbour entrance channel.

5.2.3. Observed longshore currents

The longshore currents observed during the field surveys from November 1980 to February 1982 at Narakkal, Malipuram, Fort Cochin and Anthakaranazhi zones along the stretch of the coast under study are presented in Table 5.1.

During most of the months, the longshore currents are directed towards south at Narakkal zone. A reversal in its direction is observed during November and December, 1980. The magnitude of these currents vary from 5 to 13 sec^{-1} . Converging flows have been observed between N1 and N2 during June 1981 and between N2 and N3 during August 1981. In the Malipuram zone, southerly currents are observed during most of the period except during November and December 1980 and April, 1981. Rip currents have been observed between M2 and M3 during October and November, 1981. The magnitude of the longshore currents generally vary between 5 and 12 cm sec^{-1} . In Fort Cochin zone, longshore currents are directed towards south at most of the locations during the period of study. Rip currents have been observed between F2 and F3 during November, 1981. The magnitude of these currents varied from 5 to 50 cm sec^{-1} . At Anthakaranazhi also, the longshore currents are directed towards south. Northerly currents are observed during November and December 1980, January and May 1981, and January 1982. During June to July, southerly currents have

Table 5.1. Observed longshore current (mean) speed and direction

Month	LONGSHORE CURRENT (cm s ⁻¹)															
	NARAKKAL				MALIPURAM				FORT COCHIN				ANTHAKARANAZHI			
	N1	N2	N3	M1	M2	M3	M4	F1	F2	F3	F4	A1	A2	A3	A4	
Oct. 1980				2 S	2 S	2 S	2 S									
Nov.	2 N	6 N	2 N	6 N	11 N	12 N	4 N	52 S	22 S	26 S	18 S	3 S	3 S	2 S	2 S	
Dec.	13 N	7 N	5 N	8 S	4 S	4 S	4 S	24 S	51 S	14 S	4 S	7 N	7 N	8 N	6 N	
Jan. 1981	8 S	10 S	6 S	8 S	3 S	3 S	3 S	23 S	17 S	17 S	4 S	4 N	4 N	5 N	5 N	
Feb.	4 S	4 S	4 S	13 S	4 S	4 S	4 S	22 S	22 S	18 S	4 S	3 S	3 S	2 S	3 S	
Mar.	7 S	12 S	12 S	3 S	3 S	3 S	3 S	18 S	18 S	13 S	8 S	13 S	14 S	9 S	8 S	
Apr.	8 S	4 S	4 S	4 N	4 N	3 N	3 N	13 S	19 S	17 S	4 S	4 S	4 S	3 S	3 S	
May	4 S	4 S	4 S	3 S	3 S	3 S	3 S	18 S	29 S	19 S	6 N	8 N	5 N	12 N	12 N	
Jun.	6 S	12 N	4 N	2 S	2 S	3 S	3 S	53 S	18 S	16 N	16 N	18 S	14 S	13 N	14 N	
Jul.	3 S	7 S	7 N	2 S	2 S	2 S	3 S	53 S	53 S	18 S	18 S	14 N	43 S	12 N	12 N	
Aug.	6 S	4 S	3 N	3 S	7 S	6 S	6 S	52 S	52 S	18 S	4 S	44 S	44 S	9 S	9 S	
Sep.	11 S	7 S	4 S	4 S	6 N	3 N	4 N	50 S	50 S	19 S	19 S	54 S	44 S	4 S	41 S	
Oct.	8 S	8 S	4 S	12 S	4 N	4 S	4 N	14 S	7 S	12 S	9 S	5 S	5 S	4 S	4 S	
Nov.	3 N	4 N	3 N	13 S	4 N	4 N	3 N	14 S	22 S	4 N	4 N	21 S	7 S	4 S	3 S	
Dec.	4 N	4 N	3 N	16 S	4 S	4 S	4 S	13 S	13 S	3 S	3 S	8 S	4 S	3 S	8 S	
Jan. 1982	5 S	5 S	5 S	8 S	7 S	4 S	3 S	50 S	8 S	4 S	4 S	4 N	4 N	8 N	8 N	
Feb.	6 S	4 S	3 S	12 S	7 S	6 S	4 S	14 S	7 S	8 S	4 S	3 N	3 N	3 S	4 S	

Seasonal opening between A1 and A2 remained open from June 1981 to September 1981.

been observed at A2 and northerly currents at A3 and A4. The magnitude of these currents vary between 5 and 40 cm sec⁻¹ along this zone.

CHAPTER 6 : SEDIMENT TRANSPORT

	<u>Page</u>
6.1. Materials and methods	7
6.2. Results	7
6.2.1. Alongshore component of wave energy	7
6.2.2. Littoral sediment drift	78

The nature of wave induced currents and the associated circulation of water in the nearshore environs have been described in Chapter 5. In this chapter an attempt is made to compute quantitatively the sediment transport within the surf zone along the stretch of the coast under study.

The sediment movement along any section of shore is generally governed by the forces associated with the incoming waves and the availability of sediments within the area. Broadly, the rate and direction of littoral movement of sediment could be considered as a function dependent on the alongshore component of wave energy, and the physical characteristics of the available sediments such as shape, size, specific gravity etc. This transport, which is one of the most important processes in the nearshore environment, is a prime tool for coastal zone development and management.

It is known that, in the wave breaking zone, the non-linearity associated with the motion of fluid increases making the computations or prediction of sediment transport extremely difficult. Moreover, in this zone the rate and

volume of sediment transport is most intense and the variations in the transport mode and quantities are also high. However, in the littoral zone analytical or empirical approximations for sediment transport can be made by extrapolating the wave induced flows outside this area based on linear approximations.

The sediment load in reality consists of particles of different sizes and also exhibits variations in space and time. The mobility of these sediments depend on the sensitivity of the coastline to the littoral sediment flux. The nature of these sediment has its own effect on the forces available within the environment. For example, sediments in very fine size limits such as muds, as encountered along this coast, would increase the natural cohesion and help in stabilizing the sand substrates by curtailing the percolation and reducing the lift forces induced by the pressure differences across the sediment-water interface.

Thus, in general, in the littoral zone, one needs to infer the dynamics of the sediment movement from the wave field and the mean flow characteristics within the surf zone for advective transport in addition to zig-zag motion on the beach face associated with the swash and backwash caused by waves of translation.

Many investigations have been carried out on this important aspect of the coastal zone. These studies based on field and laboratory experiments have (lead) to the development of the empirical formulae following the relationship between the wave forces and the transport of sediment (Krumbein, 1944; Savelle, 1950; Eaton, 1951; Galvin, 1972 and Komar, 1976). The available formulae for sediment transport have been compiled and discussed extensively, detailing their merits and demerits by Horikawa (1978).

6.1. Materials and methods

The wave data, presented in Chapter 4, for this region has been utilized for the computations on sediment transport. The alongshore component of the available wave energy at 2 m isobath is computed, following Johnson and Eagleson (1966) and using the formula

$$E = \frac{\gamma H_0^2 C_0}{16} \sin \theta \cos \theta$$

for waves approaching from deep water direction of $220^\circ - 300^\circ$ TN with periods from 6 - 14 sec. Further, it has been assumed that these only waves occur on any day in any particular month. In the above equation γ is the specific weight of seawater, H_0 is the deep water wave height,

C_0 is the deep water wave velocity and Θ the angle which the wave ray makes with the shore-normal as obtained from the wave refraction diagrams (Table 4.2). The alongshore components of wave energy (kg-m m^{-1} of the wave) calculated at all the locations B to T (Fig.1.5) are presented in Table 6.1. When H_0 exceeds 2 m and the wave further gets amplified due to refraction during its shoreward propagation, a limiting wave height of 2 m only was considered to prevail at or close to 2 m depth contour for the simple reason $H_b = 0.83d$ (Longuett-Higgins, 1972).

The probable littoral sediment drift $Q(\text{m}^3)$ within the surf zone has been evaluated using the empirical relation (Inman and Bagnold, 1963).

$$Q = 210.7 E$$

where E is expressed in 10^6 kg-m.m^{-1} of the wave.

6.2. Results

6.2.1. Alongshore component of wave energy

The monthly deep water wave conditions (Chapter 4) coupled with the refraction analysis provided the desired input data for studies on sediment movement following the above relationship. The available longshore component of the wave energy potential (Table 6.1) indicates considerable

Table 6.1. Alongshore component of wave energy E (kg-m.m⁻¹ of wave) per day

Locations	Month											
	Feb.	Mar.	Apr.	May	Jun.	Jul.	Aug.	Sep.	Oct.	Nov.	Dec.	
B	2479.68	8475.84	20545.90	5063.04	9694.08	5011.20	6799.68	12553.92	6013.44	768.96	16692.48	
C	2116.80	8484.48	21997.44	5028.48	5944.32	4484.16	6013.44	2401.92	5901.12	17.28	11370.24	
D	2090.88	10532.16	19198.08	2860.64	4717.44	2816.64	3533.76	1321.92	5520.96	- 267.84	10860.48	
E	777.60	5702.40	17288.64	4354.56	3611.52	2064.96	2496.96	1105.92	5676.48	-1356.48	8553.60	
F	1572.48	7620.48	19742.40	2384.64	4510.08	1909.44	2471.04	1581.12	4268.16	- 864.07	9028.80	
G	2903.04	10100.16	19224.00	7205.76	9218.88	7810.56	7426.24	7266.24	7577.28	2669.76	10860.48	
H	2885.76	10307.52	26040.96	5235.84	6542.12	5149.44	6713.28	4207.68	5762.88	466.56	11275.20	
I	1961.28	8441.28	20252.16	2773.44	4060.80	1235.52	1736.64	2574.72	6030.72	-1753.92	11370.24	
J	717.12	3144.96	3758.40	3611.52	-1304.64	-3127.68	-1218.24	-2998.08	-1200.96	-2427.84	8873.28	
K	924.48	2522.88	10454.47	-1252.80	- 673.92	527.04	- 751.68	-1399.68	3274.56	-1598.40	9460.80	
L	665.28	3283.20	11335.68	-2289.60	-1546.56	-1235.52	-2177.28	-1183.68	- 164.16	-2090.88	7551.36	
M	1848.96	5495.04	14627.52	2548.80	9564.48	2980.80	3957.12	2712.96	4276.80	- 259.20	9607.68	
N	1589.76	6419.52	15621.12	2626.56	5106.24	2462.40	3525.12	2522.88	4034.88	- 665.28	9892.80	
O	1658.88	6039.36	16104.96	2237.76	2462.40	967.68	2752.08	1105.92	4026.24	-2039.04	1034.08	
P	1641.60	6480.00	17418.24	846.72	2246.40	466.56	2021.76	656.64	4760.64	-1779.84	9469.44	
Q	1356.48	5711.04	13582.08	267.84	423.36	- 397.44	293.76	3620.16	2583.36	-4173.12	8873.28	
R	1416.96	4743.36	16588.80	1391.04	2410.56	699.84	2116.80	751.68	5883.84	-1477.44	8069.76	
S	1460.16	5097.60	12173.76	803.52	1969.92	259.20	1736.64	155.52	4717.44	- 388.80	8069.76	
T	1883.52	6143.04	18316.80	1140.48	3283.20	2047.68	3585.60	1598.40	5590.08	- 86.40	10152.00	

+ southerly
- northerly

variations from month to month at each of the nineteen locations. In general, the entire stretch of the shore experiences two energy maxima - one during April and the other during December. On an average, the longshore component of wave energy shows a southerly (down coast) component during all the months except November, when the direction reverses to northerly (up coast) at almost all locations. Also at locations J, K and L, the longshore wave energy shows northerly component during May to September.

6.2.2. Littoral sediment drift

The quantity of littoral sediments subjected to alongshore drift shows large variations (table 6.2). North of Cochin harbour entrance channel, for both the seasons (rough and fair weather), the magnitude of the drift decreases in a southerly direction (from B to E) and increases towards G. South of G, the drift values show a decreasing trend towards I. In this stretch the littoral drift values are higher during rough weather season than the fair weather season. The maximum sediment drift values occur at B and G, which is $2.07 \text{ m}^3/\text{m}$ per day and $2.11 \text{ m}^3/\text{m}$ per day respectively during rough weather season and $1.45 \text{ m}^3/\text{m}$ per day and $1.44 \text{ m}^3/\text{m}$ per day respectively during fair weather season. The lowest drift value (0.81) occurs at E during fair weather season. This low value is marginally more (1.09) during rough weather season.

Table 6.2. Computed littoral drift ($\text{m}^3 \cdot \text{m}^{-1}$ per day) during rough and fair weather seasons.

Locations	Littoral drift ($\text{m}^3 \cdot \text{m}^{-1}$ per day)			
	April-September (rough weather season)	Average for rough weather season	October-March (fair weather season)	Average for fair weather season
B	2.07		1.45	
C	1.61	1.53 $\text{m}^3 \cdot \text{m}^{-1}$ per day	1.18	1.15 $\text{m}^3 \cdot \text{m}^{-1}$ per day
D	1.21		1.01	
E	1.09		0.81	
F	1.14		0.91	
G	2.11		1.44	
H	1.89		1.29	
I	1.15		1.10	
Cochin harbour entrance channel				
J	-0.04		0.38	
K	0.24		0.61	
L	0.10		0.39	
M	1.28	0.70 $\text{m}^3 \cdot \text{m}^{-1}$ per day	0.88	0.73 $\text{m}^3 \cdot \text{m}^{-1}$ per day
N	1.12		0.89	
O	0.90		0.84	
P	0.83		0.87	
Q	0.62		0.60	
R	0.84		0.78	
S	0.60		0.80	
T	1.05		1.00	

South of Cochin harbour entrance channel, littoral drift magnitudes are much less compared to the northern side of the channel and also show irregular trend. The lowest value of drift along this section occurs at J which shows a northerly component ($-0.04 \text{ m}^3/\text{m}$ per day) during rough weather season and a southerly component ($0.38 \text{ m}^3/\text{m}$ per day) during fair weather season.

The overall littoral drift along the stretch under study is southerly. North of Cochin harbour entrance channel, the drift values are high compared to the values on the southern side.

CHAPTER 7 : SYNTHESIS

The observed geometric changes of the beaches at various locations from Azhikode to Anthakaranazhi along the central part of the Kerala coast, the distribution of sediments of these beaches, the available wave energy potential, the wave induced flows and the computed littoral drift from the mean wave climates have been presented in Chapters 2-6. This chapter attempts to understand the extent to which the beaches zone responds to the time-varying functions in the process of maintaining near-equilibrium conditions involving movement of their constituent sediments, largely within the surf zone and to a lesser extent beyond the surf zone.

The beaches of the west coast, in general, can be divided into two categories - those bordering the mainland and interspersed by rocky promontories or headlands on the northern half of the coast and those bordering the barrier islands backed by extensive lagoonal systems on the southern half. While the width of the continental shelf adjacent to this coast shows a widening from south to north, the sediment distribution in the nearshore sea bottom has been found to be in the limits of silty-clays or clayey-silts with marginal

differences in their depths of occurrence. The entire coast is directly exposed to seasonally changing winds - the monsoons (Fig.1.3). These winds present spatial differences in their times of onset and magnitudes. The associated wave climate (Fig.4.1) exhibits similar changes as their intensities and the spectral ranges depend mostly on the available fetches and their proximity to the coast. These waves, in the form of swells on their shoreward propagation, though expend part of their energy through refraction and bottom friction, give rise to movement of sedimentary material in the nearshore littoral zone. The movement of the loose and unconsolidate material (Chapter 3) within the surf zone in turn gives rise to changes in the shape and size of the beach zone which acts as an energy absorbing media. These changes in the littoral zone lead to intense erosion or accretion on the beaches depending upon the availability of sediments for transportation. In the absence of adequate sediment supplies from either offshore or mainland, directly or indirectly through other agencies, certain regions experience irreversible transformations leading to recession of shoreline.

For example, along the central regions of the Kerala coast, i.e., in the vicinity of Cochin harbour (Fig.1.5), the prograding nature of the shoreline of the

barrier (Vypeen island) and the recession of the shore on the southern side (Chellanam island) can probably be considered as the result of the developmental activities for the purposes of trade and navigation. The increased problem of maintenance of the approach channel to the harbour, probably accentuated the movement of sedimentary material - an understanding of which would help better monitoring and management of such large scale activities involving considerable financial implications.

This study aims to understand the sediment transport along this stretch of the coast considering the increased problem of beach erosion (described in Chapter 1, section 1.9) in spite of attempts made to prevent or reduce erosion through construction of artificial shore protection structures such as seawalls and groins.

As seen in Chapter 2, the beaches investigated along all the four zones have experienced erosion and accretion of varying magnitudes at all the locations. The beaches within Narakkal and Anthakaranazhi zones, in general, indicated near-cyclic behaviour, undergoing similar patterns of accretion and erosion within each of the zones (Fig. 2.4a and d). However, the responses of Narakkal zone differed from those of Anthakaranazhi. Beaches of Malipuram and Fort Cochin zones

showed wide range of variation with varying lags and leads in the times of occurrence of accretion or erosion (Fig.2.4 b and c). The observed intra- and inter-variability points to the fact that the changes are probably the result of differential wave activity in the dynamic shore zone and the variable flows present close to the shore.

An examination of the wave climate of this coast (Fig.4.1) shows that waves approaching the coast with deep water directions of 220°TN to 300°TN and with periods varying from 6 sec to 14 sec, contribute significantly in the complex littoral movement of sediments along this coast. These waves as they propagate over the shelf, and after experiencing refraction to variable degrees, indicate divergence of wave energy followed on either sides by convergence along the coast (Fig.4.2 a-e). These converging and diverging zones of wave energy have been found to shift along the shore with changes in the wave period. Under the influence of the alternating converging and diverging zones, the observed erosion and deposition of sediments on these beaches are not continuous over sufficiently longer time scales but are likely to exhibit greater variability. This is more so in the Malipuram and Fort Cochin zones, as the refraction functions show greater variation in the convergence and divergence pattern at location H to K, for different wave periods and directions of approach. This may be the reason

for the observed differential response of beaches, specially within Malipuram and Fort Cochin zones.

The changes observed in the sediment characteristics of these beaches (Chapter 3) show that, excepting the beaches in Fort Cochin zone, all the beaches in the remaining three zones are composed of sediments finer than fine sands. The fine size of the sediments together with the morphological variations due to varying hydraulic forces reflect on the low wave energies prevailing in this environment.

In the light of the direct exposure of this coast to the southwest monsoon wind and wave climates (Fig.4.1), one expects higher wave energy and coarser sediments along the shoreline. The wave records at a location, about 200 km north of this area (i.e., Mangalore) have also indicated an increase in the wave activity (wave height exceeding 3.5 m; Dattatri, 1973) preceding the southwest monsoon. The computed energies along this coast are of the order of 10^4 kg m.m^{-1} per day during the onset of southwest monsoon (Table 6.1). So one would naturally expect erosion of beaches under the influence of these high monsoonal waves. But the observed fine to very fine sediments of these beaches and their irregular responses to incoming wave energy - by way of accretion of beaches at Narakkal and Malipuram zones during southwest monsoon period - thus, present an anomaly. A plausible

explanation for this anomaly, along this stretch of the coast, could probably be sought from a feature which absorbs most of this available wave energy. The energy absorbing media appears to be only the loose and unconsolidated sediments, with varying thickness, in the silty-clay and clayey-silt size limits, of the nearshore and innershelf areas.

When a progressive gravity wave propagates into shallow waters, much of the energy loss occurs through bottom percolation, free surface dissipation and bottom or boundary-layer friction. Energy losses caused by percolation are negligible on muddy coasts since clays are highly impermeable. Bottom friction is a measure of viscous dissipation in the bottom boundary-layer. Within this boundary-layer, the frictional and inertial forces are of non-negligible magnitudes, while outside the boundary-layer only forces due to inertia predominate. In the case of laminar motion, under oscillating flows associated with wave motion, the thickness of the boundary-layer (δ) has been found to be governed by the local viscosity and the frequency of harmonic motion (Longuet-Higgins, 1953). For turbulent motion, under oscillatory flows, this thickness is a function of the rate of vortex generation. When the bottom is rough or uneven the thickness of the bottom boundary-layer has been shown to increase much faster compared to a smooth bottom (Telki and Anderson, 1970). The maximum thickness of the

boundary-layer has been found to occur immediately following the maximum horizontal velocity in the bottom layer.

In the present case, the presence of calm and muddy water in patches off Narakkal and Malipuram affect the kinematic viscosity of the waters. During the monsoon season, the thickness of the boundary-layer shows an order of magnitude difference for a wave of given period (Table 7.1) in contrast to calm weather season. The boundary layer acts as a source of vorticity which gets diffused into the interior of the fluid and alters the viscosity of the fluid (Longuett-Higgins, 1953). This gives rise to asymmetric or skewed velocity distribution. An examination of the distribution of U_{max} values (Fig. 5.2 a-d) indicates such asymmetry in the flow field. The lateral shear in the immediate vicinity of the thick bottom boundary-layer helps in providing the necessary lift forces for sediment entrainment which in turn increases the viscosity. The increase in apparent viscosity helps in reducing the wave energy in addition to the drag forces exerted by the loose and unconsolidated bottom sediments.

In a study carried out under similar environmental conditions along the coast of Surinam, South America, Wells (1977) has reported the modifications occurring in the

Table 7.1. Thickness of bottom boundary-layer (δ in cm) for different wave periods and kinematic viscosities (ν) where $\delta = 5\left(\frac{2\nu}{\omega}\right)^{1/2}$; ω is the radiant frequency.

Kinematic viscosity ($\text{cm}^2/\text{sec.}$)	Period (sec)				
	6	8	10	12	14
0.001	0.22	0.25	0.28	0.31	0.33
0.01	0.69	0.80	0.90	0.98	1.06
0.10	2.19	2.52	2.82	3.09	3.34
1.00	6.91	7.98	8.92	9.77	10.56
10.00	21.85	25.23	28.21	30.90	33.38
100.00	69.10	79.79	89.21	97.72	105.56
450.00	146.59	169.26	189.23	207.30	223.91

form of incoming waves as they propagate over a fluid-mud boundary. This observation showed that the characteristics of the changed wave forms are similar to those of solitary waves. He also explained the steady decrease of wave height upto the shoreline, through wave energy dissipation within the bottom boundary-layer.

Thus, the presence of mud patches and the wide and shallow nearshore area immediately north of Cochin entrance channel (Fig.1.5) offer maximum resistance and provide maximum shelter on the leeside i.e., to the beaches in the Malipuram and Narakkal zone, from the high waves of southwest monsoon season, as could be inferred from the observed wave heights in this zone (Table 4.4 a and b). The attenuation in wave energy, probably, helps in the accretion of beaches on the leeside of this zone during the southwest monsoon season.

The occurrence of the areas of increased sediments in suspension along the coast, during southwest monsoon season, in patches indicates that the source of these sediments lies in the vicinity of the coast or probably on the advective transport from offshore. Along this part of the Kerala coast, only very fine sediments in suspended form enter the nearshore zone from land sources as the coarser grained sediments get trapped within the lagoons. The shoreward advective transport could be either the upwelled water or the net shoreward compo-

of bottom water in response to seaward flows of the light (fresh) surface water during the rough weather season. The wave induced particle motion alongwith the wind and wave set-up, may also contribute indirectly to this shoreward advective transport.

The beaches at Anthakaranazhi zone, are the only beaches which responded to the monsoonal wave activity similar to the mainland sandy beaches. The morphological changes of beaches in this zone indicated close dependence on the prevailing wave climate off this coast and experience erosion during the period of increased wave energy associated with the monsoonal wave climate.

The sediment transport in the littoral zone is predicted based on linear approximation of wave-induced flows outside this area, and extrapolating the phenomena in the surf zone (Chapter 6). Coming to the surf zone, two distinct modes of transport - one parallel to the beach and the other perpendicular to the beach - could be distinguished. The net movement of the sedimentary material depends largely on the intensity of wave breaking and the angle at which this breaking occurs.

The accumulation or depletion of material at different zones can be analysed on the basis of the littoral cell and

sediment budget concept suggested by Inman and Frautschy (1966). A littoral cell is defined as a coastal segment that contains complete sedimentation cycle including sources, transport path and sinks. The area between river Periyar to Cochin harbour entrance channel (Fig.1.5) can be considered as one littoral cell - the Vypeen littoral cell - and the area south of this can be considered as Chellanam littoral cell. River Periyar is the principal natural source supplying sediments, however small their quantity be, to the Vypeen cell where as the opening to Cochin harbour (south of Vypeen island) seems to provide some sediment to the adjoining beaches.

The computed littoral sediment transport for the rough and fair weather seasons (Table 6.2) indicates a net southerly transport within the surf zone along both the littoral cells. However, when waves approach from extreme deep water direction of 220° TN, the transport could be considerable giving rise to a net northerly drift. Sediments introduced to Vypeen littoral cell get transported towards south by the incident waves. This transport within the surf zone would occur in the form of meanders or cellular circulation (Fig.5.1 a-e) depending upon the direction of deep water wave approach. When the waves approach is near-normal, the transport occurs through cellular flows. But when the waves make large angle with the shore, the sediment transport will be predominantly by meandering flows.

When the sediment reaches the southern most point of the Vypeen littoral cell, the Cochin harbour entrance channel provides an obstruction for further southerly transport. The strong flows associated with the flood and ebb currents, through the channel, act in a way similar to that of a dynamic barrier for these sediments, preventing any by-passing of sediments from the Vypeen littoral cell to Chellanam cell. The most obvious effect of the channel is to impound material in the nearshore area on its northern side. This causes increase in width of the beaches and seaward extension of the shoal area (e.g., Malipuram zone).

Detailed examination of the bathymetric charts shows a progression of shoreline north of Cochin with flat inshore bottom contours (Fig.1.5). This feature indicates depositional nature of the stretch of the shore north of Cochin harbour entrance channel. The progression of the shore corresponds roughly to location G to I. The net southerly drift estimated, indicates that the growth of shoreline near Vypeen takes place at the expense of the sediment that should have by-passed the estuarine mouth in the absence of the channel. Moreover, part of the finer sedimentary particles entering the channel through the backwater system may be carried further offshore by the strong ebb current which is a permanent loss to the littoral cell. The nearshore area of

Vypeen represents the final sediment sink for most of the sediment transport in this littoral cell.

In the Chellanam littoral cell, south of Cochin, inadequate supply of sediments from north causes erosion of existing material on the beach. This erosion could be clearly noticed at Fort Cochin zone (Chapter 2). Hence, the bathymetry exhibits steep slopes (Fig.1.5) indicating recession of shoreline in the Chellanam littoral cell.

As the sandy sediments in the shore zone are limited to a depth of only 1 - 2 m along most parts of this stretch and the beaches being low, the computed wave energy values (Chapter 6) reflect only the potential of available energy for sediment drift. Moreover, the backwater system extending over the study area traps the otherwise available sand size sediments and depletes the barrier beaches. With inadequate supply of sediment from north, the littoral flows associated with the wave activity are likely to be undersaturated and give rise to erosion of the existing material in the beach zone. Hence along these barrier beaches, the material eroded along any given stretch would be available at locations either south or north of the area of intense erosion.

This study indicates clearly that the sediment movement along the beaches bordering these barrier beaches is not a continuous process but is confined to more or less

closed cells within which the sediments get recirculated. The location of these cells show considerable spatial variations and contribute to changes in beach morphology in addition to modifying the incoming wave field. The erosion of the beaches has necessitated the construction of seawalls for shore protection. These alongshore structures have not been found to be effective for the simple reason that the shore stability along this stretch is mostly governed by variations in the alongshore transport of material and inadequate supply from main land sources.

REFERENCES

- ACHUTHAPANICKER, G. (1971).
Coastal protection works at Chellanam and Vypeen,
Proc. of the Sym. on Coastal Erosion and Protection
KERI, Peechi, : 10.1 - 10.11.
- ANANTHA KRISHNAN, R., PARTHASARATHY, B. AND PATHAN, J.M. (197
Meteorology of Kerala, in: Contribution to Marine
Sciences Dedicated to C.V. Kurian, edited by
G.S. Sharma, A. Mohandas and A. Antony, pp 60-125.
- ANTONY, M.K. (1976).
Wave refraction off Calangute Beach, Goa, with
special reference to sediment transport and rip
currents, Indian J. Mar. Sci., 5(2): 1-8.
- ARANUVACHAPUN, S. AND JOHNSON, J.A. (1979).
Beach profiles at Gorleston and Great Yarmouth,
Coastal Eng., 2: 201-213.
- ARTHUR, R.S., MUNK, W.H. AND ISSACS, J.D. (1952).
The direct construction of wave rays,
Trans. Am. Geophys. Union, 33: 855-865.
- AUBREY, D.G., INMAN, D.L. AND NORDSTORM, C.E. (1976).
Beach profiles at Torrey Pines, California,
Proc. 15th Int. Conf. on Coastal Eng.,
Amer. Soc. Civil Eng., : 1297-1311.
- AUBREY, D.G. (1978).
Statistical and Dynamical Prediction of Changes
in Natural Sand Beaches, Ph.D. dissertation,
Scripps Inst. Oceanogr., San Diego, Calif., 194 pp.

- AUBREY, D.G. (1979).
Seasonal patterns of onshore/offshore sediment movement, J. Geophys. Res., 84: 6347-6354.
- BOWEN, A.J. (1969b).
Rip currents, 1: Theoretical investigations, J. Geophys. Res., 74: 5467-5478.
- BOWEN, A.J. AND INMAN, D.L. (1969).
Rip currents, 2: Laboratory and field observations, J. Geophys. Res., 74: 5479-5488.
- BRETSCHNEIDER, C.L. (1966b).
Wave generation by wind, deep and shallow water, in: Estuary and Coastal Hydrodynamics, edited by A.f. Ippen, Mc Graw Hill, New York, pp 133-196.
- BRISTOW, R.C. (1938).
History of Mud Banks 1 and 2, Cochin Govt. Press, Ernakulam, 55 pp.
- CLARKE, D.J., ELIOT, I.G. AND FREW, J.R. (1984).
Variation in subaerial beach sediment volume on a small sandy beach over a monthly lunar tidal cycle, Mar. Geol., 58: 319-344.
- DAS, P.K., HARIHARAN, V. AND VARADACHARI, V.V.R. (1966).
Some studies on wave refraction in relation to beach erosion along the Kerala coast, Proc. of Indian Acc. of Sci., 64(3): 192-202.
- DATTATRI, J. (1973).
Waves off Mangalore Harbour-west coast of India, Journal of the Waterways, Harbours and Coastal Engineering Division, ASCE, 99: 39-58.

- DORA, Y.L., DAMODARAN, R. AND JOSANTO, V. (1968).
Texture of the Narakkal mud bank sediments,
Bull. Dept. Mar. biol. Oceanogr. Univ., Kerala,
4: 1-10.
- EATON, R.O. (1951).
Littoral processes on sandy coasts, Proc. 1st Conf. Coastal Engr. Council Wave Res. Univ. California, Berkely, Calif.,: 140-154.
- EMERY, K.O. (1961).
A simple method of measuring beach profiles,
Limnology and Oceanography, 6: 90-92.
- FOLK, R.L. AND WARD, W.C. (1957).
Brazos River Bar: A study in the significance of grain size parameters, J. Sed. Petrol., 27(1): 3-26.
- GALVIN, C.J. (1972).
A gross longshore transport rate formula,
Proc. 13th Coastal Eng. Conf., 2: 953-969.
- GOLE, C.V. AND TARAPORE, S.Z. (1966).
Radio-active tracer studies at Cochin harbour,
Proc. of Inter Nat. Indian Ocean Expedition, Expedition Newsletter, 4(2): 28.
- GOPINATHAN, C.K. AND QASIM, S.Z. (1974).
Mudbanks of Kerala - Their formation and characteristics, Indian J. Mar. Sci., 3(4): 105-114.
- GOUVEIA, A.D., JOSEPH, P.S. AND KURUP, P.G. (1976).
Wave refraction in relation to beach stability along the coast from Cape Ramas to Karwar, Mahasagar - Bull. Natn. Inst. Oceanogr., 9(1 and 2): 11-18.

HMSO (1975).

West Coast of India Pilot, 10th edition,
London.

HORIKAWA, K. (1978).

Coastal Engineering: An Introduction to Ocean
Engineering, University of Tokyo Press, 402 pp.

INMAN, D.L. AND BAGNOLD, R.A. (1963).

Beach and nearshore processes, 2, Littoral
processes, in: The Sea, Vol.3, edited by
M.N. Hill, Interscience, New York, pp 529-553.

INMAN, D.L. AND FRAUSTSCHY, J.D. (1966).

Littoral processes and the development of shoreline,
Coastal Engineers, Santa Barbara Speciality Conf.,
ASCE,: 511-536.

JACOB, P.G. AND QASIM, S.Z. (1974).

Mud of a mud bank in Kerala, Southwest Coast of
India, Indian J. Mar. Sci., 3(4): 115-119.

JOHNSON, J.W. AND EAGLESON, P.S. (1966).

Coastal Processes, in: Estuary and Coastline
Hydrodynamics, edited by A.T. Ippen, Mc Graw Hill,
New York, pp 404-492.

KNMI (1952).

Indian Ocean Oceanographic and Meteorological Data,
Pub. No.135, Koninkuk Nederlands Meteorologisch
Institute, De Blit.

KOMAR, P.D. (1976).

Beach Processes and Sedimentation, Prentice-Hall Inc.,
Englewood Cliffs, New Jersey, 429 pp.

KRISHNAN, M.S. (1968).

Geology of India and Burma, 5th edition,
Higgins Bothams, 536 pp.

- KRUMBEIN, W.C. (1944).
Shore currents and sand movement on a model beach,
Tech. Mem. No.7, U.S. Army Beach Erosion Board,
Washington.
- KRUMBEIN, W.C. AND PETTIJOHN, F.J. (1938).
Manual of Sedimentary Petrography,
Appleton-Century-Crofts Inc., New York, 549 pp.
- KURIAN, C.V. (1967).
Studies on the benthos of the south west coast of
India, Proc. Sym. Indian Ocean. Bull. NISI, 38(2):
649-656.
- KURUP, P.G. (1972).
Littoral currents in relation to the mud bank
formation along the coast of Kerala, Mahasagar -
Bull. Natn. Inst. Oceanogr., 5(3): 158-162.
- KURUP, P.G. AND VARADACHARI, V.V.R. (1975).
Flocculation of mud in mud bank at Purakad,
Kerala coast, Indian J. Mar. Sci., 4(2): 21-24.
- KURUP, P.G. (1977).
Studies on the physical aspects of the mudbanks
along the Kerala coast with special reference to
Purakad mudbank, Bull. Dept. Mar. Sci. Univ. Cochin,
8: 1-72.
- LAMB, H. (1945).
Hydrodynamics, Dover Publications, New York, 738 pp.
- LONGUETT-HIGGINS, M.S. (1953).
Mass transport in water waves, Phil. Trans. Royal
Soc. London, 245, 245(903): 535-581.

LONGUETT-HIGGINS, M.S. (1970a).

Longshore currents generated by obliquely incident sea waves, 1. J. Geophys. Res., 75: 6778-6789.

LONGUETT-HIGGINS, M.S. (1970b).

Longshore currents generated by obliquely incident sea waves, 2, J. Geophys. Res., 75: 6790-6801.

LONGUETT-HIGGINS, M.S. (1972).

Recent progress in the study of longshore currents, In: Waves on Beaches and Resulting Sediment Transport, edited by R.E. Meyer, Academic Press, New York, pp 203-248.

MAC PHERSON, H. AND KURUP, P.G. (1981).

Wave damping at Kerala Mudbanks, Indian J. Mar. Sci., 10(1): 154-160.

MANOHAR, M. (1960).

Sediment movement at Indian Ports, Proc. of 7th Conf. on Coastal Eng., 1: 342-374.

MATTIAT, B., PETERS, J. AND Ec KHARD, F.J. (1973).

Results of petrographical analyses on sediments from the Indian Pakistan continental margin (Arabian sea), Meteor. Forschungsergebnisse, 14: 1-50.

Mc Cormick, J.M. AND SALVADORI, M.G. (1968).

Numerical Methods in FORTRAN, Prentice-Hall of India Private Limited, New Delhi, 324 pp.

MONI, N.S. AND NAMBIAR, K.K.N. (1965).

Study of artificial nourishment at Purakad coastal area, Kerala, Thirty fifth Annual Research Session Session of CBIP, India.

- MONI, N.S. (1970).
Study of mudbanks along the southwest coast of India, Proc. of the 12th Coastal Eng. Conf., Washington, D.C., 2: 739-750.
- MONI, N.S. (1971).
Study of mudbanks along the southwest coast of India, Proc. of the Sym. on Coastal Erosion and Protection, KERI, Peechi, : 8.1-8.8.
- MONI, N.S. (1972).
Systematic study of coastal erosion and defence work in the south west coast of India, Proc. of the 13th Coastal Eng. Conf., Washington, D.C., : 1427-1450.
- MONI, N.S. (1980).
Coastal erosion in Kerala - Some aspects, Proc. of Seminar on Geology and Geomorphology of Kerala, GSI Special Publication, 5: 87-90.
- MURTY, C.S. (1977).
Studies on the physical aspects of the shoreline dynamics at some selected places along the west coast of India, Ph.D. Thesis, University of Kerala, 149 pp.
- MURTY, C.G., SASTRY, J.S. AND VARADACHARI, V.V.R. (1980).
Shoreline deformation in relation to shore protection structures along Kerala coast, Indian J. Mar. Sci., 9(2): 77-81.
- MURTY, C.S. AND VARADACHARI, V.V.R. (1980).
Topographic changes of the beach at Valiathura, Kerala, Indian J. Mar. Sci., 9(1): 31-34.

- MURTY, C.S., VEERAYYA, M. AND VARADACHARI, V.V.R. (1982).
Morphological changes of the beaches of Goa,
Indian J. Mar. Sci., 11(1): 35-42.
- NAIR, R.R. AND MURTY, P.S.N. (1968).
Clay mineralogy of the mudbanks of Cochin,
Curr. Sci., 37(20): 589-590.
- NAIR, R.R. AND PYLEE, A. (1968).
Size distribution and carbonate content of the
sediments of the western shelf of India,
Proc. Sym. Indian Ocean Bull. NISI, 38(1):
411-420.
- NAIR, R.R., VARMA, P.U., PYLEE, A.A. AND VARADACHARI, V.V.R.
(1972).
Studies on sediment transport in Mopla Bay harbour,
Cannanore, using fluorescent tracers, J. Indian
Geophys. Union, 10(1-4): 193-197.
- NODA, E.K. (1974).
Wave induced nearshore circulation, J. Geophys. Res.
79: 4097-4106.
- PIERSON, W.J., NEUMAN, G. AND JAMES, R.W. (1965).
Practical Method for Observing and Forecasting
Ocean Waves, H.O. Pub. No.603, U.S. Navy
Hydrographic Office, 284 pp.
- PRABHAKAR Rao, G. (1968).
Sediments of the nearshore regions off Neendakara-
Kayamkulam coast and Ashtamudi and Vatta Estuaries,
Kerala, India, Proc. Sym. Indian Ocean Bull. NISI,
38(1): 513-551.

- PRASANNA KUMAR, S., SHENOI, S.S.C. AND KURUP, P.G. (1983).
Littoral drift along shoreline between Munamban and Anthakaranazhi, Kerala coast, Indian J. Mar. Sci., 12(4): 209-212.
- RAVINDRAN, T.A., KHALID, M.M. AND MONI, N.S. (1971).
Study of shoreline changes of selected reaches of Kerala, Proc. of the Sym. on Coastal Erosion and Protection, KERI, Peechi,: 9.1 - 9.7.
- REDDY, M.P.M. (1970).
A systematic study of wave conditions and sediment transport near Mormugao harbour, Mahasagar - Bull. Natn. Inst. Oceanogr., 3(1): 27-44.
- REDDY, M.P.M. AND VARADACHARI, V.V.R. (1972).
Sediment movement in relation to wave refraction along the west coast of India, J. Indian Geophys. Union, 10(1-4): 169-191.
- SASTRY, J.S. AND D'SOUZA, R.S. (1973).
Littoral drift in the environs of Tarapur Atomic Power Station, J. Inst. Engrs. (India), 53: 170-176
- SAVILLE, T. (1950).
Model study of sand transport along an infinitely long, straight beach, Trans. Am. Geophys. Union, 33(4): 555-565.
- SCHOTT, W. (1968).
Recent sedimentation in the Indian ocean. First results of Meteor. Indian Ocean Expedition 1964-'65 Proc. Sym. Indian Ocean Bull. NISI, 1(38): 224-227.
- SHENOI, S.S.C. AND PRASANNA KUMAR, S. (1982).
Littoral processes along shoreline from Azhikode to Anthakaranazhi on the Kerala coast, Indian J. Mar. Sci., 11(3): 201-207.

- SHENOI, S.S.C. (1984).
Studies on the Littoral Processes in Relation to Stability of Beaches Around Cochin, Ph.D. Thesis, University of Cochin, 145 pp.
- SONU, C.J. (1972).
Field observation of nearshore circulation and meandering currents, J. Geophys. Res., 77: 3232-3247.
- SRIVASTAVA, P.S., NAIR, D.K. AND KARTHA, K.R.R. (1968).
Monthly wave characteristics of the Arabian sea, Indian J. Met. Geophys., 19(3): 329-330.
- SUNDARA RAMAM, K.V., VARKEY, M.J., VIJAYARAJAN, P.K., JOHN, V.C. AND JOSEPH, M.X. (1974).
Waves in coastal waters off Mangalore, Part 1: Distribution of wave characteristics, Indian J. Met. Geophys., 25: 453-460.
- TELKI, P.G. AND ANDERSON, M.W. (1970).
Bottom boundary shear stresses on a model beach, Proc. 12th Conf. on Coastal Eng., Washington, D.C.,: 269-288.
- THORNTON, E.B. (1970).
Variations of longshore current across the surf zone, Proc. 12th Conf. Coastal Eng., Washington, D.C.,: 291-308.
- VARKEY, M.J., KESAVADAS, V., SWAMY, G.N., JOSEPH, P.S. AND SASTRY, J.S. (1982).
Wave (swell) Atlas for Arabian sea and Bay of Bengal, Nat. Inst. Oceanogr. India, 385 pp.
- VARMA, P.U. AND KURUP, P.G. (1969).
Formation of Chakara (Mudbank) on the Kerala coast, Curr. Sci., 38(23): 559-560.

- VARMA, P.U. AND VARADACHARI, V.V.R. (1977).
Stability of the coastline from Manakkodam to
Thottappally along the Kerala coast,
Proc. of the Indian Acc. of Sci., 85(4): 191-198.
- VEERAYYA, M. (1972).
Textural characteristics of Calangute Beach Sediment
Goa coast, Indian J. Mar. Sci., 1(2): 28-44.
- VEERAYYA, M. AND VARADACHARI, V.V.R. (1975).
Depositional environment of coastal sediments of
Calangute, Goa, Sedimentary Geology, 14: 63-74.
- VEERAYYA, M., MURTY, C.S. AND VARADACHARI, V.V.R. (1981).
Sediment distribution in the offshore regions of
Goa, Indian J. Mar. Sci., 10(4): 332-336.
- WELLS, J.T. (1977).
Shallow-water waves and fluid-mud dynamics,
Coast of Surinam, South America, Ph.D. Thesis,
Louisiana State University, 99 pp.
- WINANT, C.D., INMAN, D.L. AND NORDSTROM, C.E. (1975).
Description of seasonal beach changes using empirical
eigen functions, J. Geophys. Res., 80(15): 1979-1986.

APPENDIX

Empirical Eigen Function technique - also known as principal component analysis, empirical orthogonal function analysis, eigen analysis or factor analysis - is a powerful tool for the analysis and interpretation of morphological variability of beaches. The EEF analysis is an offshoot of the classical eigen value problem which arises when one tries to solve an ordinary differential equation subjected to specific boundary conditions. A solution to the differential equation with boundary conditions exists only for certain values of parameter which satisfy the equation. These specific values are eigen values and the equation that must be satisfied is the eigen vector equation. For a system of linear equations the eigen value problem takes the form

$$(A - \lambda I) X = 0$$

where A is matrix of coefficients of simultaneous equation, λ is the eigen value and I is the identity matrix.

The beach profile data obtained at each of the locations (Fig.1.5) is set into a data matrix H with each of the matrix containing a time series for the beach

elevation/depression at particular stations along the profile and each column containing the beach profile at a particular time. The variability of data matrix H could be explained in terms of a few simple functions, which are the eigen functions of the matrix H . This is achieved by normalising and decomposing H into a product of three matrices using singular value decomposition (SVD) technique

$$X_{m \times n} = \frac{H}{(m \times n)^{1/2}} = U_{m \times r} \Gamma_{r \times r} V_{r \times n}^T \quad (1)$$

where m and n are number of rows and columns of the data matrix respectively, and T is the transpose of the matrix. The column vectors of U and V matrices are orthogonal

$$\text{i.e., } U^T U = I, \quad V^T V = I$$

and Γ is a diagonal matrix with diagonal elements called the singular values of H , and $r [r \leq \min(m, n)]$ is the rank of the matrix H . U , Γ and V satisfying equation (1) are obtained in the following manner.

Pre-multiplying equation (1) by X^T and post-multiplying by V

$$X^T X V = V \Gamma U^T U \Gamma V^T V$$

$$B V = V \Gamma^2 = V \lambda$$

where $\lambda = \Gamma^2$ is a diagonal matrix with diagonal element

$$\lambda_i = \gamma_i^2$$

$$\text{Then } (B - \lambda I) V = 0 \quad (2)$$

which is a matrix eigen value problem to obtain matrix V, where $B = X^T X$. Similarly the matrix U can be obtained by post-multiplying (1) by $X^T U$

$$X X^T U = U \Gamma V^T V \Gamma U^T U$$

$$A U = U \Gamma^2 = U \lambda$$

$$\text{i.e., } (A - \lambda I) U = 0 \quad (3)$$

which is again matrix eigen value problem to obtain U where $A = X X^T$. Value of λ is obtained by solving the characteristic equation of (2), i.e., $|B - \lambda I| = 0$, and its substitution in equation (2) leads to the system of equations which are solved following the standard Gaussian elimination method (Mc Cormick and Salvadori, 1968) to obtain values of V. Knowing V and λ , U can be obtained from equation (3).

One can thus represent the matrix in the form

$$X = H / (\text{m} \times \text{n})^{1/2} = U \Gamma V^T$$

$$H = h_{ij} = (\text{m} \times \text{n})^{1/2} \left[\lambda_1^{1/2} U_1 V_1^T + \lambda_2^{1/2} U_2 V_2^T + \lambda_3^{1/2} U_3 V_3^T + \dots + \lambda_r^{1/2} U_r V_r^T \right]$$

$$h_{(x,t)} = \sum_{i=1}^r a_i U_i(x) V_i(t)$$

and $a_i = (\lambda_i n_x n_t)^{1/2}$ is the normalisation factor.

Generally the magnitude of the eigen values reduces rapidly from its highest value and only a few factors are sufficient for the close representation of the data matrix. The ratio between the sum of the squares of the elements (i.e., variance) of the factor model and that of the data matrix is considered as the measure of closeness of the model data.

$$\text{Measure of closeness} = \frac{\sum_{i=1}^K \lambda_i}{\sum_{i=1}^Y \lambda_i}$$

where K is the number of factors and r is the rank of the data matrix.

Since the eigen functions are data derived, the structure of the function is defined by actual data set and does not assume a priori functional form. The functions are orthogonal, and each function represents a certain amount of mean square value of the data. The eigen function associated with the largest eigen value represents the data best in the least square sense, while the second function (in rank) describes the residual mean square data best in the least square sense. Thus a large number of data variables can be efficiently represented by a few empirical functions which describe most of the mean square value of the data.